

THE ROLE OF MATH-BTB FAMILY PROTEINS TaMAB2 AND AtBPM1 IN PLANT DEVELOPMENT AND STRESS RESPONSE

Škiljaica, Andreja

Doctoral thesis / Disertacija

2022

Degree Grantor / Ustanova koja je dodijelila akademski / stručni stupanj: **University of Zagreb, Faculty of Science / Sveučilište u Zagrebu, Prirodoslovno-matematički fakultet**

Permanent link / Trajna poveznica: <https://um.nsk.hr/um:nbn:hr:217:744869>

Rights / Prava: [In copyright](#)/[Zaštićeno autorskim pravom.](#)

Download date / Datum preuzimanja: **2025-01-27**



Repository / Repozitorij:

[Repository of the Faculty of Science - University of Zagreb](#)





University of Zagreb

Faculty of Science
Department of Biology

Andreja Škiljaica

**THE ROLE OF MATH-BTB FAMILY
PROTEINS TaMAB2 AND AtBPM1 IN
PLANT DEVELOPMENT AND STRESS
RESPONSE**

DOCTORAL DISSERTATION

Zagreb, 2022



University of Zagreb

Faculty of Science
Department of Biology

Andreja Škiljaica

**THE ROLE OF MATH-BTB FAMILY
PROTEINS TaMAB2 AND AtBPM1 IN
PLANT DEVELOPMENT AND STRESS
RESPONSE**

DOCTORAL DISSERTATION

Supervisor:
Dr. Nataša Bauer, Assoc. Prof.

Zagreb, 2022



Sveučilište u Zagrebu

Prirodoslovno-matematički fakultet
Biološki odsjek

Andreja Škiljaica

ULOGA PROTEINA TaMAB2 I AtBPM1 IZ PORODICE MATH-BTB U BILJNOM RAZVOJU I ODGOVORU NA STRES

DOKTORSKI RAD

Mentor:
Izv. prof. dr. sc. Nataša Bauer

Zagreb, 2022

This doctoral thesis was prepared in the Division of Molecular Biology, Department of Biology, Faculty of Science, University of Zagreb under the supervision of Dr. Nataša Bauer, Assoc. Prof. The thesis was prepared as part of the University postgraduate program of Biology at the Department of Biology, Faculty of Science, University of Zagreb.

Ovaj je doktorski rad izrađen u Zavodu za molekularnu biologiju Biološkog odsjeka Prirodoslovno-matematičkog fakulteta Sveučilišta u Zagrebu, pod vodstvom dr. sc. Nataše Bauer, izv. prof., u sklopu Sveučilišnog poslijediplomskog doktorskog studija Biologije pri Biološkom odsjeku Prirodoslovno-matematičkog fakulteta Sveučilišta u Zagrebu.

INFORMATION ABOUT SUPERVISOR

Dr. Nataša Bauer. Assoc. Prof. graduated in molecular biology in 1996 from the Department of Biology, Faculty of Science, University of Zagreb. At the same institution, she obtained an M.A. degree in molecular biology in 2002, and completed her PhD in 2006 under supervision of Dr. Sibila Jelaska Prof. Emer. and Dr. Hrvoje Fulgosi, PhD.

From 1996 to 2009, she worked as a research assistant in the group of Dr. Sibila Jelaska Prof. Emer. at the Division of Molecular Biology, Department of Biology, Faculty of Science, University of Zagreb. From 2009 to 2017, she was Assistant Professor at the same institution and in 2017 she became Associate Professor, which remains her current position in the Division. She teaches three classes in undergraduate and graduate molecular biology programs, Animal and Plant Cell Culture, Genetic Engineering in Biotechnology, and Plant Engineering.

To date, Nataša Bauer co-authored 28 scientific peer-review articles and two book chapters. According to Google Scholar, by February 2022, her works have been cited 539 times, with h-index 13. The focus of her academic study and research are the fields of plant molecular biology and biotechnology, plant development and stress response. She mentored two PhD studies, 19 master's studies and is currently supervising one PhD study.

Since 2018, Nataša Bauer is the Technical Editor In-Chief in *Acta Botanica Croatica*, an international journal of botany published by Department of Biology, Faculty of Science, University of Zagreb.

ZAHVALE

Hvala mojoj mentorici, profesorici Nataši Bauer, što me naučila većini eksperimentalnih metoda korištenih pri izradi ovog rada. Hvala i na svim korisnim komentarima i sugestijama tijekom pisanja ove disertacije.

Zahvaljujem profesorici Dunji Leljak-Levanić na mnogim korisnim savjetima tijekom posljednjih nekoliko godina rada, a i tijekom diplomskog studija.

Zahvalna sam svojim kolegicama iz laboratorija, Mateji Jagić, Tamari Vuk i Mirti Tokić, na razmjeni znanja i vještina, ali i prijateljskoj, kolegijalnoj i prije svega veseloj radnoj atmosferi.

Hvala Luciji Markulin na savjetima o provedi metode RT-qPCR te analize stabilnosti referentnih gena, i na svim šalama.

Zahvalna sam Vedrani Vičić Bočkor na tehničkim savjetima u vezi izvedbe eseja Duolink PLA.

Hvala Josipu Skeji na savjetima u vezi analize filogenije. Hvala Ana-Mariji Boljkovac na pripremi medija i kemikalija te održavanju laboratorija. Hvala svim drugim zaposlenicima Zavoda za molekularnu biologiju, koji su mi uskočili u pomoć u raznim prilikama, bilo radi posudbe materijala i uređaja, ili pak korisnim savjetom.

Zahvaljujem Luciji Horvat s Instituta Ruđer Bošković na analizi preparata konfokalnim mikroskopom.

Zahvalna sam studenticama i studentima s kojima sam imala priliku surađivati u sklopu laboratorijskih stručnih praksi i diplomskih radova – ta su mi iskustva bila izuzetno poučna.

Zahvaljujem svojim roditeljima, Mariji i Zvonku Škiljaici, i cijeloj svojoj obitelji, na bezuvjetnoj podršci tijekom mog obrazovnog puta. I na kraju, posebno hvala Nikolini, na koju se uvijek mogu osloniti.

THE ROLE OF MATH-BTB FAMILY PROTEINS TaMAB2 AND AtBPM1 IN PLANT DEVELOPMENT AND STRESS RESPONSE

ANDREJA ŠKILJAICA

Division of Molecular Biology, Faculty of Science, Horvatovac 102a, 10000 Zagreb

MATH-BTB proteins are substrate-specific adaptors of CUL3-based E3 ligases, promoting ubiquitination and proteasomal degradation of target proteins. In this work, MATH-BTB proteins of wheat *Triticum aestivum* (TaMAB) and *Arabidopsis thaliana* (AtBPM) were phylogenetically analyzed. Forty-six putative *TaMAB* genes retrieved from EnsemblPlants database clustered in the grasses-specific expanded clade of MATH-BTB proteins. AtBPM proteins characteristically clustered in the smaller core clade. Two members, wheat TaMAB2 and *Arabidopsis* AtBPM1, were functionally analyzed. Overexpression of TaMAB2 in *Arabidopsis* affected epidermal cell length, indicating involvement in cytoskeletal regulation. TaMAB2 colocalized with ubiquitin, indicating possible involvement in the Cul3-E3 ligase complex. To assess whether environmental conditions affect *AtBPM* genes and AtBPM1 protein, *Arabidopsis* wild type plants and transgenic plants overexpressing AtBPM1 were exposed to osmotic and salt stress, different levels of light exposure and elevated temperature. Downstream analyses revealed perturbations of *AtBPM* genes and AtBPM1 protein on a transcriptional, post-transcriptional and post-translational level in different experimental conditions, indicating complex environment-dependent regulation.

(118 pages, 16 figures, 5 tables, 135 references, original in: English)

Keywords: *Arabidopsis*, drought, heat stress, MATH-BTB, protein stability, wheat

Supervisor: Dr. Nataša Bauer, Assoc. Prof.

Reviewers: Dr. Nenad Malenica, Assist. Prof.

Dr. Marin Ježić, Assist. Prof.

Dr. Pascal Genschik, PhD

PROŠIRENI SAŽETAK

Obitelj MATH-BTB sastoji se od proteina koji sadrže dvije domene, MATH (Meprin and TRAF Homology) i BTB (Broad-complex, Tramtrack, and Bric-à-brac). U genomima gotovo svih eukariota, velik broj gena sadrži funkcionalni slijed koji kodira ili domenu MATH ili domenu BTB uz barem jednu drugu domenu. Proteini koji sadrže domenu BTB svrstani su u dvije glavne skupine: oni koji sudjeluju u proteinskim interakcijama posredovanim domenom BTB i oni koji vežu DNA kako bi regulirali transkripciju (Stogios i sur., 2005). Svi dosad istraženi proteini koji sadrže domenu MATH uključeni su u regulaciju obrade proteina (Zapata i sur., 2007). Proteini iz podskupine MATH-BTB, koji sadrže i MATH i BTB domenu, opisani su kao adapteri kompleksa ubikvitin ligaze E3 zasnovane na proteinu Cullin 3 (CUL3). Ovaj tip ligaze E3 (u daljnjem tekstu: ligaza CUL3-E3) sudjeluje u proteasomskoj razgradnji ciljnih proteina. Kompleks ligaze CUL3-E3 čini protein osovine CUL3 koji s jedne strane veže protein RING-BOX1 (RBX1) i preko njega ubikvitin ligazu E2, a s druge strane veže domenu BTB proteina adaptera. Protein adapter svojom domenom MATH veže ciljni protein, i time ga dovodi u neposrednu blizinu ligaze E2 koja ga obilježava poliubikvitinskim lancem i time ga usmjerava u razgradnju na proteasomu 26S (Chen i sur., 2013, Gingerich i sur., 2005, Juranić i sur., 2012, Stogios i sur., 2005., između ostalih). Najranije opisan životinjski protein iz obitelji MATH-BTB je protein MATERNAL EFFECT LETHAL-26 (MEL-26) iz oblića *Caenorhabditis elegans*. MEL-26 je adapter ligaze E3 koji posreduje u razgradnji proteina MEI-1, proteina iz skupine katanina s ulogom cijepanja mikrotubula. Ovaj proces odvija se nakon mejoze i ključan je za sastavljanje mitotičkog vretena (Pintard i sur., 2004). Proteini MATH-BTB široko su zastupljeni i u biljkama, no detaljno je proučeno samo nekoliko članova. Filogenetička analiza gena *MATH-BTB* u dvosupnici talijinom uročnjaku (*Arabidopsis thaliana* (L.) Heynh) i jednosupnici riži (*Oryza sativa* L.) pokazala je da geni *MATH-BTB* grupiraju u dvije skupine: manju, evolucijski očuvaniju osnovnu skupinu i veću, proširenu skupinu (Gingerich i sur., 2005). Uključivanje više kopnenih biljnih vrsta u filogenetičku analizu potvrdilo je razdvajanje biljnih gena *MATH-BTB* u dvije skupine, uz dodatno grupiranje gena iz proširene skupine u pet manjih podskupina, nazvanih E1 do E5 (Gingerich i sur., 2007; Juranić i Dresselhaus, 2014). Dok genom uročnjaka kodira samo šest gena *MATH-BTB* (*AtBPM1-6*), koji grupiraju u osnovnu skupinu (Gingerich i sur. 2005; 2007; Juranić i Dresselhaus, 2014), evoluciju trava (porodica Poaceae) obilježila je velika ekspanzija gena *MATH-BTB*, koji specifično grupiraju u proširenu skupinu (Gingerich i sur., 2007; Juranić i Dresselhaus, 2014).

Do sada je opisano nekoliko biljnih proteina MATH-BTB. Jedan od njih je protein ZmMAB1 kukuruza (*Zea mays* L.), protein iz proširene skupine eksprimiran u muškom i ženskom gametofitu (Juranić i sur., 2012). Istraživanje mutanata sa smanjenom ekspresijom gena *ZmMAB1* pokazalo je da protein ZmMAB1 ima ulogu u pozicioniranju jezgara tijekom prijelaza iz mitoze u mejozu u muškom i ženskom gametofitu, kao i u formiranju i funkciji diobenog vretena tijekom mejoze (Juranić i sur., 2012). Proučena su i dva gena *MATH-BTB* pšenice (*Triticum aestivum* L.). Dok je *TaMAB1* eksprimiran isključivo u jajnim stanicama pšenice, *TaMAB2* je eksprimiran u zigoti i u dvostaničnom proembriju (Leljak-Levanić i sur., 2013). Prekomjerna ekspresija rekombinantnog proteina TaMAB2 obilježenog zelenim fluorescentnim proteinom (eng. *green fluorescent protein*, GFP) u stanicama duhana BY2, rezultirala je lokalizacijom proteina TaMAB2 u jezgri i oko nje (Leljak-Levanić i sur., 2013).

Obitelj proteina MATH-BTB uročnjaka (nadalje BPM) detaljnije je proučena. Djelujući kao adapteri ligaza CUL3-E3 specifični za vezanje supstrata, proteini BPM posreduju u razgradnji različitih transkripcijskih faktora, te stoga djeluju kao regulatori različitih razvojnih procesa i odgovora na stres. Primjerice, proteini BPM povezani su s regulacijom odgovora na hormon abscizinsku kiselinu (ABA), ključnog mehanizma odgovora biljke na biotski i abiotski stres. Proteini BPM potiču razgradnju transkripcijskog faktora ATHB6 iz obitelji leucinskih zatvarača (eng. *homeodomain-leucine zipper*; HD-ZIP), koji koči signalni put hormona ABA (Himmelbach i sur., 2002). Proteini BPM, potičući njegovu razgradnju, promoviraju signalni put hormona ABA (Lechner i sur., 2011). Nadalje, proteini BPM3 i BPM5 potiču razgradnju protein fosfataza tipa 2C (PP2C), negativnih regulatora signalnog puta hormona ABA, čime reguliraju količinu raspoloživih proteina PP2C tijekom odgovora na stres (Julian i sur., 2019). Proteini BPM uključeni su i u regulaciju cvjetanja, potičući razgradnju transkripcijskog faktora MYB56 iz porodice R2R3-MYB, koji smanjuje ekspresiju gena *FLOWERING LOCUS T (FT)*, ključnog aktivatora cvatnje u uročnjaku (Chen i sur., 2015). Proteini BPM također su povezani s reakcijom na etilen i to putem interakcije s transkripcijskim faktorima iz obitelji *Apetala2/ethylene response factor (AP2/ERF)*. Primjerice, proteini BPM destabiliziraju transkripcijski faktor WRINKLED 1 (WRI1) te tako utječu na metabolizam masnih kiselina i razvoj sjemena u uročnjaku (Chen i sur., 2013). Nedavno je još jedan član obitelji AP2/ERF povezan s proteinima BPM, krovni transkripcijski faktor DEHYDRATION-RESPONSIVE ELEMENT BINDING 2A (DREB2A) uključen u odgovor na sušu i toplinski stres u uročnjaku. DREB2A potiče ekspresiju mnogih gena osjetljivih na sušu i

toplinski stres, a i ekspresija gena *DREB2A* inducirana je stresom (Sakuma i sur., 2006a; 2006b). Proteini BPM stupaju u interakciju s *DREB2A* i potiču njegovu razgradnju putem aktivnosti CUL3-E3 ligaze, čime reguliraju količinu raspoloživog proteina *DREB2A* u uvjetima stresa (Morimoto i sur., 2017).

Prvi cilj ovog rada bila je filogenetička analiza proteina MATH-BTB pšenice i uročnjaka. Radi dobivanja uvida u evolucijsku povijest proteina pšenice iz obitelji MATH-BTB, temeljem aminokiselinske sekvence proteina TaMAB2 pretražen je genom pšenice u bazi podataka Ensembl Plants. Ovom pretragom dobivena je lista od 46 gena *MATH-BTB*, anotiranih kao *TaMAB1-46* u skladu s nomenklaturom predloženom za gene *TaMAB1-2* (*Triticum aestivum* MATH-BTB; Leljak-Levanić et al., 2013). Aminokiselinske sekvence proteina TaMAB pretražene su u bazi podataka NCBI radi provjere prisutnosti evolucijski očuvanih domena MATH i BTB, prema bazama Protein family (Pfam) i Conserved Domains (CD). Za svih 46 proteina predviđeno je postojanje barem jedne domene MATH i jedne domene BTB, dok protein TaMAB46 sadrži po dvije kopije domena MATH i BTB. Ovaj rezultat ukazuje na veliku ekspanziju gena *MATH-BTB* pšenice, što je u skladu s postojećim podacima o ekspanziji obitelji *MATH-BTB* u drugim vrstama trava, kao što su riža, kukuruz, *Sorghum bicolor* i *Brachypodium distachion* (Gingerich i sur., 2007; Juranić i Dresselhaus, 2014). Iz baze Ensembl Plants preuzeti su podaci o postojanju varijanti alternativnog prekrajanja RNA (eng. *splicing variants*) i broju egzona u kodirajućoj regiji. Dok većina gena *TaMAB* kodira za jednu RNA, četiri gena *TaMAB* kodiraju po dvije alternativne varijante prekrajanja. Najveći broj gena *TaMAB* sadrži jedan ili dva egzona, dok manji broj gena sadrži tri, četiri, pet ili, u jednom slučaju, osam egzona u kodirajućoj regiji.

Nadalje, provedena je filogenetička analiza identificiranih proteina MATH-BTB pšenice, zajedno s proteinima MATH-BTB kukuruza (Juranić i sur., 2012), riže (Gingerich i sur., 2007.) i uročnjaka (Gingerich i sur., 2005; 2007). Metodom maksimalne vjerojatnosti utvrđeno je grupiranje proteina MATH-BTB u dvije skupine, osnovnu i proširenu, uz dodatno razdvajanje gena proširene skupine u pet podskupina, nazvanih E1 do E5, prateći nomenklaturu iz Juranić i Dresselhaus (2014). Dok je svih šest gena uročnjaka grupiralo u osnovnu skupinu, većina gena pšenice grupirala je u proširenu skupinu, što je u skladu s dosadašnjim saznanjima da je proširena skupina specifična za gene MATH-BTB trava (Juranić i Dresselhaus, 2014). Samo četiri proteina MATH-BTB pšenice grupirala su u osnovnu skupinu, i oni sadrže po četiri ili pet egzona, što je najčešći broj egzona gena BPM uročnjaka. Protein TaMAB2 grupirao je u podskupinu E3 proširene skupine.

S ciljem provjere evolucijske očuvanosti domena MATH i BTB u osnovnoj i proširenoj skupini, iz baza Pfam i CD preuzete su sekvence navedenih domena svih proteina pšenice proširene skupine, kao i svih proteina pšenice, kukuruza, riže i uročnjaka iz osnovne skupine. Višestruko sravnjenje sljedova pokazalo je manju očuvanost domene MATH proširene skupine u odnosu na domenu BTB, dok je u osnovnoj skupini domena MATH očuvanija od domene BTB. Ovaj rezultat u skladu je s postojećim indicijama o pojačanoj diverzifikaciji domene MATH proširene skupine, za koju se smatra da je posljedica diverzifikacije supstrata proteina MATH-BTB kao adaptera CUL3-E3 ligaze (Gingerich i sur., 2007) te je vezana uz okolišne čimbenike koji su specifično oblikovali obitelj MATH-BTB vrsta iz porodice trava (Juranić i Dresselhaus, 2014).

Drugi cilj ovog rada bio je istražiti funkcije dvaju predstavnika obitelji MATH-BTB, proteina pšenice iz proširene skupine, TaMAB2, i proteina uročnjaka iz osnovne skupine, AtBPM1 (nadalje BPM1). Budući da utišavanje gena *TaMAB2* u pšenici dovodi do letalnog fenotipa (Bauer i sur., 2019), za istraživanje fizioloških uloga proteina TaMAB2 nije bilo moguće koristiti homologni sustav. Stoga je za indirektno istraživanje funkcije proteina TaMAB2 korištena stabilna transgenična linija uročnjaka koja eksprimira protein TaMAB2 obilježen privjeskom GFP (TaMAB-GFP; Bauer i sur., 2019). Na sličan način, za istraživanje proteina BPM1, korištena je transgenična linija uročnjaka koja prekomjerno eksprimira BPM1-GFP. Oba gena stabilno su integrirana u genom i pod kontrolom su promotora virusa mozaika cvjetače 35S (eng. cauliflower mosaic virus, CaMV 35S), osiguravajući konstitutivnu ekspresiju fuzijskog proteina.

Prethodna istraživanja ukazala su na uloge proteina MEL-26 i ZmMAB1 kao adaptera ligaze CUL3-E3, u sklopu koje usmjeravaju ciljne proteine na razgradnju i tako sudjeluju u regulaciji citoskeleta. Kako bi se provjerila potencijalna povezanost proteina TaMAB2 i regulacije funkcije citoskeleta, provedena je analiza produžnog rasta korijena klijanaca uročnjaka s prekomjernom ekspresijom TaMAB2. Duljina primarnog korijena transgeničnih klijanaca bila je ista kao kod divljeg tipa, no duljina epidermalnih stanica korijena bila je statistički značajno veća kod transgenične linije u odnosu na divlji tip, ukazujući na potencijalnu ulogu proteina TaMAB2 u regulaciji funkcije citoskeleta. Nadalje, transgenični protoplasti s prekomjernom ekspresijom proteina TaMAB2 analizirani su metodom Duolink te je utvrđena kolokalizacija proteina TaMAB2 s ubikvitinom u citoplazmatskim nakupinama, ukazujući na moguću uključenost proteina TaMAB2 u sastav ligaze CUL3-E3 ovisne o ubikvitinu. Ovi rezultati u skladu su s ranije pokazanom lokalizacijom proteina TaMAB2 u citoplazmi i jezgri (Leljak-Levanić i sur., 2013) te zabilježenom

interakcijom između TaMAB2 i CUL3 (Bauer i sur., 2019). Sustavom dvaju kvašćevih hibrida (eng. *yeast two hybrid*, Y2H) provjerena je interakcija između proteina TaMAB2 i citoskeletnog regulatora Katanina iz pšenice, no zbog nespecifične interakcije u negativnoj kontroli, direktna interakcija s Kataninom nije potvrđena. Koristeći transgeničnu liniju uročnjaka koja prekomjerno eksprimira TaMAB2 prethodno je proveden ekspanzivni afinitetne kromatografije i spektrometrije masa (eng. *tandem affinity purification-mass spectrometry*, TAP-MS), te su otkriveni potencijalni interaktori proteina TaMAB2, između ostalih, podjedinica A faktora inicijacije translacije 4 i podjedinica G faktora inicijacije translacije 3 (Bauer i sur., 2019). Oba proteina analizirana su u sustavu Y2H, no interakcija s proteinom TaMAB2 nije potvrđena.

Dosadašnja istraživanja opetovano su ukazivala na funkciju proteina BPM uročnjaka u odgovoru na stres. S ciljem daljnje analize uloge proteina BPM1 u promijenjenim okolišnim uvjetima, biljke divljeg tipa uročnjaka i/ili transgenične linije koje prekomjerno ekspimiraju protein BPM1 izložene su uvjetima suše, solnog stresa, povišenoj temperaturi te različitim uvjetima osvjetljenja, te su potom analizirane različitim metodama. U divljem tipu je kvantitativnom metodom reverzne transkripcije i lančane reakcije polimeraze (eng. *quantitative reverse transcription polymerase chain reaction*, RT-qPCR) mjerena ekspresija svih šest gena *BPM*, dok je u transgeničnim linijama hibridizacijom po Westernu mjerena stabilnost fuzijskog proteina BPM1-GFP, dok je njegova unutarstanična lokalizacija analizirana fluorescencijskom mikroskopijom.

U svrhu induciranja solnog stresa, osmotskog stresa i signalne kaskade hormona ABA, biljke su tretirane natrijevim kloridom, manitolom odnosno hormonom ABA. U divljem tipu, ovi tretmani nisu uzrokovali značajnu promjenu u ekspresiji gena *BPM*, osim u slučaju gena *BPM5*, čija se ekspresija smanjila nakon tretmana manitolom, i gena *BPM6*, čija je ekspresija porasla nakon tretmana natrijevim kloridom. U transgeničnim linijama, razina proteina BPM1 nije se promijenila nakon izlaganja osmotskom stresu i hormonu ABA, dok je tretman solnim stresom smanjio količinu proteina BPM1, najvjerojatnije putem proteasomske degradacije. Nadalje, dok su osmotski stres i ABA inducirali snažnu akumulaciju proteina BPM1 u jezgri stanica korijena, solni stres je uzrokovao difuziju signala proteina BPM1 duž stele korijena. Osim toga, proveden je test klijavosti divljeg tipa i transgeničnih linija na hranjivim podlogama s dodatkom natrijevog klorida, manitola i hormona ABA. Test je pokazao da su transgenične linije otpornije od divljeg tipa na osmotski stres i stres uzrokovan hormonom ABA. S druge strane, transgenične linije bile su jednako podložne solnom stresu kao i divlji tip uročnjaka. Ovi rezultati ukazuju na potencijalnu

ulogu proteina BPM1 u odgovoru na sušu, no ne i na solni stres, pri čemu bi nakupljanje proteina u jezgri i stabilna količina raspoloživog proteina mogle imati značajnu ulogu.

Radi provjere učinka povišene temperature na ekspresiju gena *BPM* te stabilnost i lokalizaciju proteina BPM1, klijanci su inkubirani na 37 °C. U divljem tipu je nakon 3 sata tretmana zabilježen porast ekspresije gena *BPM1*, *BPM2* i *BPM3*, s najvećim povećanjem izmjerenim za gen *BPM2*. Ekspresija gena *BPM4* bila je blago smanjena, a gena *BPM5* i *BPM6* nepromijenjena. Nadalje, količina proteina BPM1 značajno je porasla nakon 1 sat i 3 sata tretmana povišenom temperaturom, a analiza korijena klijanaca ukazala je na njegovu snažnu akumulaciju u jezgrama epidermalnih stanica nakon 6 sati tretmana. Ovi rezultati ukazuju da su u uvjetima povišene temperature, proteini BPM, osim na razini genske ekspresije, regulirani i na post-translacijskoj razini, odnosno na razini stabilnosti proteina. Porast genske ekspresije u divljem tipu te stabilizacija proteina u transgeničnoj liniji ukazuju na nužnost povećane i stabilne razine raspoloživog proteina BPM1 u uvjetima povišene temperature, što je u skladu s opisanom ulogom proteina BPM kao regulatora količine transkripcijskog faktora DREB2A u sklopu odgovora na toplinski stres, radi sprječavanja mogućih negativnih posljedica nakupljanja DREB2A (Morimoto i sur., 2017).

S ciljem provjere učinka prekomjerne ekspresije proteina BPM1 na količinu transkripcijskog faktora DREB2A, napravljena je indirektna analiza ekspresije gena *HsfA3* i *AT4G36010*, čiju ekspresiju inducira DREB2A u uvjetima toplinskog stresa (Sakuma i sur., 2006b). Dok je u divljem tipu uročnjaka izlaganje povišenoj temperaturi uzrokovalo očekivan porast ekspresije gena *HsfA3* i *AT4G36010*, u transgeničnim linijama s prekomjernom ekspresijom proteina BPM1 taj je porast bio značajno manji, ukazujući na smanjenu količinu aktivnog transkripcijskog aktivatora DREB2A. Ovaj rezultat dodatno potvrđuje ulogu proteina BPM1 u degradaciji transkripcijskog faktora DREB2A.

Za gen *BPM2* zabilježen je najveći porast ekspresije u divljem tipu nakon izlaganja povišenoj temperaturi. Gen *BPM2* ujedno ima i najveći broj varijanti alternativnog prekrajanja RNA, koje mogu dati pet različitih proteinskih produkata (*BPM2.1* – *BPM2.5*). S ciljem provjere učinka povišene i snižene temperature na alternativno prekrajanje gena *BPM2*, klijanci divljeg tipa uročnjaka izloženi su 3 sata temperaturama 37 °C odnosno 4 °C te je metodom RT-qPCR mjerena količina triju transkripata gena *BPM2*, točnije *BPM2.3*, *BPM2.4* i *BPM2.5*. Dobiveni rezultati ukazali su da je količina transkripta *BPM2.5* značajno porasla nakon oba tretmana, ukazujući na dominantnu ulogu ove proteinske varijante u oba tipa temperaturnog stresa. Nadalje, povišena

temperatura povećala je količinu transkripta *BPM2.3*, a smanjila količinu transkripta *BPM2.4*, dok snižena temperatura nije imala značajnog utjecaja na količine ovih transkripata. Ovi rezultati ukazuju na dodatnu razinu regulacije aktivnosti proteina BPM uslijed temperaturnog stresa, uz regulaciju genske ekspresije i stabilnosti proteina, što potencijalno omogućava raznolikiji odgovor biljaka na stres. Osim toga, varijanta *BPM2.3*, čija se količina povećava na povišenoj temperaturi, ne sadrži potpunu domenu BTB, čime se otvara mogućnost dodatnih uloga proteina BPM u odgovoru na stres, koje ne zahtijevaju interakciju s proteinom CUL3 posredovanu domenom BTB. Količina svjetlosti je, kao i temperatura i količina dostupne vode, okolišni čimbenik koji oscilira s obzirom na doba dana ili godine. S ciljem provjere učinka fotoperioda na ekspresiju gena *BPM*, klijanci divljeg tipa uzgajani su u uvjetima dugog dana te su uzorkovani tijekom dana: u 12:00 i 17:00 te u 6:00 (kraj noćnog perioda). Ekspresija je analizirana metodom RT-qPCR. Za gene *BPM2* i *BPM6* pokazan je statistički značajan porast ekspresije na kraju noćnog perioda (6:00) u odnosu na 12:00 i 17:00, dok je kod ostalih gena zabilježen sličan trend, ali bez statističke značajnosti. Nadalje, klijanci transgenične linije uzorkovani su svaka 4 sata tijekom perioda od 24 sata i količina proteina BPM1 analizirana je imunodetekcijom. Rezultati ove analize pokazali su da se količina proteina BPM1 značajno smanjuje tijekom noći, ukazujući na smanjenu stabilnost i degradaciju proteina. Konačno, s ciljem provjere unutarstanične lokalizacije proteina BPM1 nakon dugotrajnog izlaganja svjetlosti odnosno mraku, klijanci transgenične linije analizirani su fluorescencijskom mikroskopijom. Dok je produljeno izlaganje svjetlosti uzrokovalo karakteristično nakupljanje proteina BPM1 u jezgrama epidermalnih stanica korijena, inkubacija u mraku dovela je do disperzije signala proteina BPM1 te naposljetku do translokacije u stelu korijena. Ovi rezultati ukazuju na regulaciju stabilnosti i unutarstanične lokalizacije proteina BPM1 ovisnu o fotoperiodu, što je u skladu s ranijim indikacijama o ulozi proteina BPM u regulaciji cvjetanja, gdje fotoperiod ima važnu ulogu (Chen i sur., 2015; Škiljaica i sur., 2020.)

S obzirom na utjecaj povišene temperature na ekspresiju gena iz obitelji *BPM*, posljednji cilj ovog rada bio je odabir i validacija referentnih gena za normalizaciju vrijednosti ekspresije u metodi RT-qPCR, u tkivima uročnjaka izloženima povišenoj temperaturi. Pregledom literature i javno dostupnih pokusa DNA mikročipova (eng. *microarray*) na tkivima uročnjaka izloženima raznim toplinskim tretmanima, odabrano je deset referentnih gena kandidata. Klijanci divljeg tipa uročnjaka i odrasle biljke u fazi cvatnje tretirane su s pet različitih povišenih temperatura nakon čega su uzorkovani čitavi klijanci, komadići listova i cvjetni pupovi. Ekspresija referentnih gena

kandidata mjerena je metodom RT-qPCR, nakon čega je stabilnost ekspresije analizirana pomoću četiri različita programa za validaciju referentnih gena. U konačnici je provedena empirijska validacija najstabilnijih gena u eksperimentu gdje je kao testni gen korišten *DREB2A*, a različite kombinacije referentnih gena korištene su za normalizaciju podataka. Za svaku vrstu tkiva predloženi su optimalni referentni geni za uporabu u analizama diferencijalne ekspresije gena uročnjaka izloženog povišenim temperaturama.

Ključne riječi: ABA, abiotski stres, *Arabidopsis*, MATH-BTB, povišena temperatura, prekrajanje RNA, pšenica, referentni geni, stabilnost proteina, ubikvitin

CONTENTS

1. INTRODUCTION	1
2. LITERATURE OVERVIEW	5
2.1. The ubiquitin pathway	5
2.2. MATH-BTB proteins as adaptors of CUL3-based E3 ligases	8
2.3. Phylogeny of the plant <i>MATH-BTB</i> family	10
2.4.1. Maize, wheat, tomato and rice MATH-BTB proteins	14
2.4.2. <i>Arabidopsis</i> BPM proteins	16
3. MATERIAL AND METHODS	21
3.1. Material	21
3.1.1. Bacterial strains	21
3.1.2. Yeast strains	21
3.1.3. <i>Arabidopsis</i> plant lines	21
3.2. Methods	22
3.2.1. Bioinformatics	22
3.2.1.1. Phylogenetic analysis	22
3.2.1.2. Multiple sequence alignments	22
3.2.1.3. Selection of temperature-stable candidate reference genes	23
3.2.1.4. RT-qPCR primer design	23
3.2.1.5. Candidate reference gene expression stability analysis	24
3.2.2. Plant growth conditions	24
3.2.3. Generation of plasmid constructs	25
3.2.4. Standard PCR reactions	26
3.2.5. Yeast-two-hybrid (Y2H) assay	26
3.2.6. Germination assay	27
3.2.7. Abiotic stress treatments	28
3.2.8. Root and epidermal cell length measurements	29
3.2.9. Protoplast isolation	29
3.2.10. Duolink <i>in situ</i> proximity ligation assay (PLA)	30
3.2.11. Plant tissue harvesting and homogenization	31
3.2.12. Whole protein extraction and Western blot analysis	31
3.2.13. Total RNA extraction	33
3.2.14. Quantitative reverse transcription PCR (RT-qPCR)	33
3.2.15. qPCR data analysis	34

3.2.16. Fluorescence microscopy	35
3.2.17. Statistical analysis	35
4. RESULTS.....	36
4.1. Phylogeny of Arabidopsis and wheat MATH-BTB proteins	36
4.1.1. Identification of TaMAB2 paralogs	36
4.1.2. Phylogenetic tree of plant MATH-BTB proteins	38
4.1.3. <i>Arabidopsis</i> BPM protein isoforms	42
4.2. Functional analysis of wheat TaMAB2.....	53
4.2.1. Overexpression of TaMAB2 affects epidermal cell length	53
4.2.2. TaMAB2 colocalization and protein interaction analysis	53
4.3. Functional analysis of <i>Arabidopsis</i> BPM1	56
4.3.1 ABA and osmotic stress affect BPM1 protein turnover	56
4.3.2. Temperature affects expression of <i>BPM</i> genes and BPM1 protein turnover	57
4.3.3. Photoperiod affects transgenic BPM1 protein stability	63
4.4. Evaluation of reference genes for RT-qPCR gene expression analysis in <i>Arabidopsis</i>	66
4.4.1. Expression variation of candidate reference genes.....	66
4.4.2. Evaluation of expression stability of candidate reference genes	68
4.4.3. Validation of top-ranked reference genes.....	70
5. DISCUSSION.....	76
5.1. Expansion of the MATH-BTB family in wheat	76
5.2. Putative roles of TaMAB2 during wheat embryogenesis.....	78
5.3. Environmental cues affect BPM1 turnover	81
5.3.1. BPM1 is involved in drought and heat stress response	81
5.3.2. Photoperiod and light signaling affect BPM1 stability	84
5.3.3 Transcriptional and post-translational regulation of BPM proteins	86
5.4. Evaluation of RT-qPCR candidate reference genes.....	90
6. CONCLUSIONS.....	94
7. REFERENCES	96
APPENDIX	106
APPENDIX A	106
APPENDIX B.....	109
LIST OF ABBREVIATIONS.....	116
CURRICULUM VITAE	cxviii

1. INTRODUCTION

The MATH-BTB family is comprised of proteins containing two domains, Meprin and TRAF Homology (MATH) and Broad-complex, Tramtrack, and Bric-à-brac (BTB). Several members of the MATH-BTB subfamily, containing both the MATH and BTB domain, have been described in animals and plants. These proteins act as substrate-specific adaptors of E3 ubiquitin ligases mediating proteasomal degradation of target proteins. While the BTB domain binds the Cullin 3 (CUL3) scaffold protein of the E3 ligase, the MATH domain binds the target protein. The target protein is thus brought in close proximity to an E2 ligase which ubiquitinates and thereby designates the protein for degradation on the 26S proteasome (Chen et al., 2013; Gingerich et al., 2005; Juranić et al., 2012; Stogios et al., 2005, among others). The first animal MATH-BTB proteins described as substrate-specific adaptor of an E3 ligase is MATERNAL EFFECT LETHAL-26 (MEL-26) of *Caenorhabditis elegans*. MEL-26 mediates ubiquitin-dependent degradation of MEI-1, the microtubule-severing Katanin protein. This occurs after meiosis and the process is essential for assembly of the mitotic spindle (reviewed in Pintard et al., 2004).

MATH-BTB proteins are also broadly represented in plants. While the *Arabidopsis* (*Arabidopsis thaliana* (L.) Heynh) genome encodes only six *MATH-BTB* genes (*Arabidopsis thaliana* *BTB/POZ-MATH1-6*; *AtBPM1-6*), a large expansion of *MATH-BTB* genes occurred in grasses (Gingerich et al., 2005; 2007; Juranić & Dresselhaus, 2014). For instance, there are 69 rice (*Oryza sativa* L.) *MATH-BTB* (*OsMBTB*) genes, and at least 41 estimated *MATH-BTB* pseudogenes (Gingerich et al., 2007). Plant *MATH-BTB* genes cluster into two clades: the smaller, more conserved core clade and the larger and more diversified expanded clade. While *Arabidopsis* *BPM* genes cluster exclusively into core clade, the expanded clade predominantly contains *MATH-BTB* genes of grasses, such as rice, maize, *Sorghum bicolor* and *Brachypodium distachyon* (Gingerich et al., 2005; 2007; Juranić & Dresselhaus, 2014).

A similar expansion of the *MATH-BTB* family was expected in wheat, another monocot grass species. Furthermore, different dynamics in sequence conservation were expected between core clade (*Arabidopsis*) and expanded clade (wheat) proteins. Therefore, the first research objective of this work was a phylogenetic analysis of wheat and *Arabidopsis* *MATH-BTB* proteins. Firstly, the Ensembl Plants database was searched against the wheat genome using TaMAB2 amino acid sequence as query, to retrieve putative *MATH-BTB* genes of wheat. Putative *MATH-BTB* proteins of wheat were subsequently used to build a phylogenetic tree, which also included maize, rice and

Arabidopsis MATH-BTB proteins. Additionally, amino acid sequences of putative MATH and BTB domains of selected core and expanded clade proteins were further analyzed to assess their conservation statuses.

At the beginning of this PhD study, the only functionally analyzed expanded clade protein was the maize (*Zea mays* L.) MATH-BTB1 (ZmMAB1) protein, expressed in the male and female germ lineages. Research on RNA interference (RNAi) mutants with downregulated *ZmMAB1* showed its involvement in nuclei positioning during mitosis-to-meiosis transition in the male and female gametophyte, as well as in spindle apparatus formation and function during meiosis (Juranić et al., 2012). Two wheat (*Triticum aestivum* L.) MATH-BTB genes (*TaMAB*) have also been studied. While *TaMAB1* is expressed exclusively in wheat egg cells, *TaMAB2* is expressed in both the zygote and two-celled proembryos. In tobacco Bright Yellow-2 (BY-2) cells transiently expressing TaMAB2 tagged with green fluorescent protein (GFP), the protein localizes in and around the nucleus, but its function in early embryogenesis has not been elucidated (Leljak-Levanić et al., 2013).

The small family of core clade *BPM* genes in *Arabidopsis* has been more extensively studied. By acting as substrate specific adaptors of CUL3-based E3 ligases, BPM proteins interact with members of several families of transcription factors and were therefore proposed as important regulators of various developmental processes and stress response. For instance, by mediating degradation of transcription factor ARABIDOPSIS THALIANA HOMEBOX 6 (ATHB6) and protein phosphatases type 2C (PP2Cs), BPM proteins regulate the abscisic acid (ABA) response, a fundamental mechanism of biotic and abiotic stress response in plants (Julian et al., 2019; Lechner et al., 2011). BPM proteins have also been linked to ethylene response. For instance, BPM proteins negatively regulate ethylene-responsive transcription factor WRINKLED1 (WRI1), thus affecting fatty acid metabolism and seed development in *Arabidopsis* (Chen et al., 2013). BPM proteins are involved in drought response through interaction with DEHYDRATION-RESPONSIVE ELEMENT BINDING 2A (DREB2A), a key transcription factor acting in drought and heat stress tolerance in *Arabidopsis* (Morimoto et al., 2017). Additionally, BPM proteins were shown to induce degradation of transcription factor MYB56, thus promoting flowering (Chen et al., 2015). The second research objective of this work was a functional analysis of TaMAB2 and AtBPM1 (further referred to as BPM1). Based on *TaMAB2* gene expression pattern, TaMAB2 is active during early embryogenesis and not surprisingly, its knockout caused lethality in wheat embryos

(Bauer et al., 2019). Therefore, transgenic *Arabidopsis* plants overexpressing TaMAB2 (Bauer et al., 2019) were used for further functional analyses of TaMAB2. Knockout of individual *BPM* genes does not cause phenotypic changes (Lechner et al., 2011). Therefore, *Arabidopsis* plants overexpressing BPM1 which exhibit multiple phenotypic differences compared to wild type (Škiljaica et al., 2020) were used for functional analyses of BPM1. Both TaMAB2- and BPM1-overexpressing transgenic lines were created by stable transformation using *Agrobacterium tumefaciens* carrying a plasmid-borne gene cassette encoding green fluorescent protein (GFP)-tagged TaMAB2 and GFP-tagged BPM1, respectively. Both genes are integrated into the genome and are under control of the cauliflower mosaic virus (CaMV) 35S promoter, ensuring constitutive transgene expression.

Previous findings on MEL-26 and ZmMAB1 indicated their involvement in cytoskeletal regulation via ubiquitin-dependent degradation of target proteins. To test possible involvement of TaMAB2 with cytoskeletal network in *Arabidopsis*, plants overexpressing TaMAB2 were analyzed for differences in primary root length and root epidermal cell length. Additionally, to test the hypothesis that TaMAB2 acts as an adapter in the ubiquitin-dependent Cul3-E3 ligase, the co-localization of TaMAB2 and ubiquitin was analyzed *in situ* using Duolink proximity ligation assay (PLA). Finally, based on results of a previous tandem affinity purification experiment using *Arabidopsis* plants overexpressing TAP-tagged TaMAB2, a yeast two hybrid (Y2H) assay was performed to analyze direct protein-protein interactions of TaMAB2 with two putative interactors, namely subunit A of the translation initiation factor 4 and subunit G of the translation initiation factor 3. Additionally, cytoskeletal regulator Katanin from wheat was tested for direct protein-protein interaction with TaMAB2 in Y2H.

Previous research showed that BPM proteins are involved in various stress response pathways. Therefore, the initial hypothesis was that various stress conditions and/or changes in environmental stimuli, such as the amount of light exposure, would affect BPM protein levels, either transcriptionally at the level of gene expression, or by differential splicing, or post-translationally at the level of protein degradation. To study the effect of salt stress, osmotic stress, ABA-induced stress and/or elevated temperature on endogenous *BPM* genes, wild type *Arabidopsis* seedlings were treated with NaCl, mannitol, ABA or elevated temperature, respectively, and differential gene expression was measured by quantitative reverse transcription PCR (RT-qPCR). To analyze the stability of transgenic BPM1 protein after exposure to the same stressors, transgenic BPM1-

overexpressing seedlings were treated and subsequently used for whole protein extraction and Western blotting using anti-GFP antibody. Additionally, subcellular localization of transgenic BPM1 protein was analyzed by fluorescence microscopy of seedling roots. To analyze tolerance of BPM1 overexpressors to salt, osmotic and ABA-induced stress, a germination assay was performed on wild type and transgenic seeds. BPM proteins presumably directly interact with DREB2A to mediate its proteasomal degradation in conditions of elevated temperature (Morimoto et al., 2017). To analyze the effect of BPM1 overexpression on the amount of transcription factor DREB2A, an indirect study was performed, measuring differential expression of DREB2A downstream targets, *HsfA3* and *AT4G36010*, in seedlings of wild type and BPM1 overexpressors after exposure to elevated temperature.

Compared to other *BPM* genes, *BPM2* showed highest upregulation after exposure to elevated temperature. To assess whether temperature affects differential splicing of *BPM2* gene, wild type seedlings were exposed to elevated temperature or cold stress and changes in transcript abundance of three *BPM2* splicing variants were analyzed by RT-qPCR.

Furthermore, the effect of light on *BPM* gene expression, and BPM1 protein stability and localization was analyzed. To test whether photoperiod affects expression of endogenous *BPM* genes, wild type *Arabidopsis* seedlings were harvested at different time points during the day and differential gene expression was analyzed. Additionally, transgenic BPM1 protein stability was analyzed by Western blotting, using seedlings harvested at different time points of the day. Finally, to assess whether continuous exposure to light or dark affects subcellular localization of transgenic BPM1 protein, seedlings were incubated in either light or dark and analyzed by fluorescence microscopy of seedling roots.

The third objective of this doctoral work was validation of reliable reference genes for use in RT-qPCR experiments employing elevated temperatures in different *Arabidopsis* tissues. Ten candidate reference genes were selected based on literature review and publicly available microarray data from experiments on *Arabidopsis* tissues exposed to various heat treatments. Wild type *Arabidopsis* seedlings and adult plants were exposed to a series of elevated temperatures, followed by harvesting of whole seedlings, leaves and flower buds. Expression levels of selected genes were measured by RT-qPCR. Expression stability of each gene was assessed with four different types of reference gene validation programs. For each tissue type, an optimal combination

of two reference genes was suggested for use in temperature-dependent relative gene expression analyses.

2. LITERATURE OVERVIEW

2.1. The ubiquitin pathway

Degradation of cellular proteins is an evolutionarily conserved, highly complex and tightly regulated process involved in various molecular pathways during a cell's lifespan. The importance of protein degradation is highlighted by genomic analyses of plant genomes. For instance, a remarkable 6% of the *Arabidopsis thaliana* genome encodes proteins involved in the ubiquitin/26S proteasome degradation system and related functions. This large assortment of more than 1400 gene loci produces a complex network of proteins which maintain and regulate molecular mechanisms involved in plant growth, hormonal signaling, abiotic stress, immunity, embryogenesis, and senescence (Sharma et al., 2016; Vierstra, 2009). The ubiquitin-dependent 26S proteasome pathway, or the ubiquitin (Ub) pathway is largely responsible for timely degradation of target proteins. The pathway is driven by the activity of three enzymes, named E1-3. First, the ubiquitin-activating enzyme E1 activates Ub in an ATP-dependent manner. Next, the activated ubiquitin is transferred to a cysteine residue of an E2 conjugating enzyme before the ubiquitin is covalently attached to the substrate protein. Finally, the E3 ubiquitin ligase enzyme plays the role of a mediator in this process: it “selects” and binds the substrate protein and positions it in close vicinity of the E2 conjugating enzyme, which allows its ubiquitination (Hershko & Ciechanover, 1998; Smalle & Vierstra, 2004). In general, during target ubiquitination, an isopeptide bond is formed between the C-terminus of ubiquitin and the ϵ -NH₂ group on a substrate lysine, and the protein ends up either monoubiquitinated, multi-monoubiquitinated or polyubiquitinated, the last modification usually leading to protein degradation in the 26S proteasome. The fate of a ubiquitinated protein additionally depends on the site of linkage formation within the ubiquitin molecule. For instance, Lys11-, Lys29-, Lys48-, and Lys63-linked chains often lead to proteasomal degradation, with Lys11- and Lys48-linked chains triggering degradation more frequently than other modifications (Komander & Rape, 2012). Additionally, Lys63 polyubiquitination was shown to have important proteasome-independent roles in cellular processes such as endocytosis,

autophagy and translation, and physiological processes such as hormonal responses, development, biotic interactions, nutrition and others (Romero-Barrios & Vert, 2018).

In general, plant genomes encode only a few E1 and E2 enzymes, and numerous E3 ligases. For example, the *Arabidopsis* genome encodes two E1 enzymes (Hattfield et al., 1997), 37 E2 enzymes (Kraft et al., 2005), but 1415 predicted E3 ligases (Mazzucotelli et al., 2006). The specificity of the Ub pathway is largely conferred by the differential activity of E3 ligases and their adaptor components which recognize and bind different target proteins (Genschik et al., 2013). Plant E3 ligases are classified into three major groups based on their subunit composition: (1) U-box E3 ligases, (2) HOMOLOGOUS TO THE E6-AP CARBOXYL TERMINUS (HECT) E3 ligases, and (3) REALLY INTERESTING NEW GENE (RING)-finger E3 ligases (Chen & Hellman, 2013). By regulating protein levels of their target proteins, E3 ligases are involved in many biological and developmental processes in plants, such as photomorphogenesis, hormone signaling, biotic stress, as well as abiotic stress responses, such as response to salt, drought, heat, and cold (Chen & Hellmann 2013; Al-Saharin et al., 2022).

RING-finger E3 ligases can be divided into single-subunit and multi-subunit complexes. The difference between the two groups of RING E3 ligases is indicated by their name: while the former type contains a single polypeptide bridge between the E2 enzyme and the substrate, the latter is constituted by several subunits, each with its own role in the complex. Multi-subunit RING E3s are the most diverse group of E3 ligases. The common architecture of all multi-subunit RING ligases is made up of three parts: (1) a central scaffolding subunit made up of a cullin (CUL) or a cullin-like protein, (2) a RING-finger protein which binds the E2 ligase and (3) an adaptor protein which binds substrates for ubiquitination. The cullin is bound to the RING-finger protein on one side and the adaptor protein on the other side (Chen & Hellmann, 2013). In plants, multi-subunit RING E3 ligases include CUL3-based E3 ligases, CUL1-based SKP1-CULLIN-F-BOX (SCF) complexes, CUL4-based E3 ligases and the ANAPHASE PROMOTING COMPLEX (APC) based on a cullin-like protein APC2 (reviewed in Chen & Hellmann, 2013; Genschik et al., 2013; Risseuw et al., 2003). The activity of cullin-RING E3s is regulated in different ways. For instance, the cullin protein can be covalently linked to a small, 76 amino-acid protein called RELATED TO UBIQUITIN (RUB; known in animals as NEDD8; neural precursor cell expressed, developmentally downregulated 8) in a process termed rubylation (neddylation). Cullin rubylation is promoted by a RING-finger protein RING-BOX 1 (RBX1), which is common for all cullin-

RING E3s. It was proposed that rubylation of cullin causes a conformational change in subdomains of the cullin and RBX1 subunits, which favors substrate ubiquitination (Schwechheimer & Mergner, 2014). It was also shown that association of human NEDD8 to CUL3 promotes dimerization of CUL3 and thus activates the E3 ligase (Wimuttisuk & Singer, 2007). The conjugate is removed in a process termed derubylation (deneddylation), and research indicates that a derubylated cullin state is necessary for binding of the exchange factor CULLIN ASSOCIATED NEDD8 DISSOCIATED 1 (CAND1), which promotes exchange of substrate receptor subunits and as such modulates the cell's repertoire of RING-E3s' substrates (Schwechheimer & Mergner, 2014). Regulation of cullin-RING E3 ligase activity by rubylation and derubylation is essential for plant growth and development, which is evidenced in *Arabidopsis* by an embryo lethal phenotype of a double knockout mutant of two redundant RUB proteins, RUB1 and RUB2 (Bostick et al., 2004).

Arabidopsis CUL3 proteins come in two functionally redundant forms, CUL3A and CUL3B (Figuroa et al., 2005; Risseuw et al., 2003). Due to their functional redundancy, there have been multiple attempts at obtaining a viable double *cul3* mutant in which both proteins are non-functional. Transgenic plants in which only the *CUL3B* gene is disrupted by a T-DNA insertion at the beginning of the coding sequence (*cul3b-1* line) develop normally and exhibit full fertility (Thomann et al., 2005). However, as multiple studies have shown, loss-of-function mutants of both *CUL3A* and *CUL3B* exhibit embryo lethality and plants are unable to develop past the embryonic stage (Figuroa et al., 2005; Gingerich et al., 2005; Thomann et al., 2005). The next attempt at creating a viable double mutant consisted in combining two T-DNA insertion lines, the aforementioned *cul3b-1* mutant and a *CUL3A* mutant called *cul3a-3* (Thomann et al., 2009). Like *cul3b-1*, the homozygous *cul3a-3* mutant plants are fully viable and fertile (Thomann et al., 2005, 2009). The *cul3a-3* mutant has an insertion at the very end of the *CUL3A* coding sequence, which creates a mutation by which the last two amino acids of the protein are replaced by an eight-residue peptide. The mRNA transcript is truncated and of lower abundance, and the resulting protein product is hyper-rubylated (Thomann et al., 2009). As mentioned previously, rubylation is a covalent modification of a cullin protein, which promotes an active conformational state favoring substrate ubiquitination by the E3 ligase, while derubylation promotes normal activity of cullin-RING E3 ligases by means of substrate exchange (Schwechheimer & Mergner, 2014). Derubylation of modified CUL3A appears to be hindered in the *cul3a-3* mutant (Thomann et al.,

2009). The double homozygous *cul3a-3 cul3b-1* mutant (termed the *cul3* hypomorph; *cul3^{hyp}*) is viable but a portion of its progeny exhibits several developmental defects, most apparent as seedlings with a single, three or fused cotyledons and abnormal cotyledon vasculature. At a later stage of development, *cul3^{hyp}* plants exhibit reduced rosette size and a delay in flowering (Thomann et al., 2009). These strong and weak double mutant phenotypes suggest an essential role of CUL3A and CUL3B during embryo development (Figueroa et al., 2005; Gingerich et al., 2005; Thomann et al., 2005) and post-embryonic stages of development (Thomann et al., 2009), respectively.

2.2. MATH-BTB proteins as adaptors of CUL3-based E3 ligases

Nearly two decades ago, several studies first showed the basic structure of plant CUL3-based E3 ligases. The central scaffold of the complex is the CUL3 protein which binds RBX1 as the RING-finger protein and a substrate adaptor from a family known as BTB/POZ proteins, or simply BTB proteins (Dieterle et al., 2005; Figueroa et al., 2005; Gingerich et al., 2005; Weber et al., 2005). The nucleotide sequence of the BTB domain was originally identified as a motif in a DNA virus and was later found in all known eukaryotes, in numbers which greatly vary between species. The BTB domain is a highly versatile protein-protein interaction domain which can enable dimerization and oligomerization in interactions involving either another BTB protein or a non-BTB protein (Perez-Torrado et al., 2006). The core BTB sequence consists of 95 amino acids organized in five α -helices and three β -strands, making up a highly conserved tertiary structure (Stogios et al., 2005). The variability of BTB domain-containing proteins is maintained through the secondary motif which usually follows the N-terminal core BTB region. For instance, in plants, the BTB domain is followed by motifs such as MATH, ankyrin, armadillo, pentapeptide and tetratricopeptide (TPR) repeats, and transcriptional adapter zinc finger (TAZ), and non-phototropic hypocotyl (NPH3) domains (Gingerich et al., 2005, 2007; Stogios et al., 2005). Not all secondary motifs are present in all species. For instance, the Kelch and Zinc finger motifs in combination with the BTB domain are highly represented in vertebrates but do not appear in higher plants (Gingerich et al., 2005; Perez-Torrado et al., 2006). Specificities also exist among species of the same kingdom. For example, BTB-NPH3 proteins are found in *Arabidopsis* but not in rice (Gingerich et al., 2007). With their high variability and versatility of association, proteins containing a BTB domain take part in multiple cellular processes, from actin dynamics (Hara et al., 2004), cell cycle regulation

(Masuda et al., 2008) to hematopoiesis and immunity (Siggs & Beutler, 2012), and their functions are often executed via transcriptional regulation (Perez-Torrado et al., 2006; Siggs & Beutler, 2012). Although BTB proteins serve a wide variety of purposes, they have been extensively described as substrate-specific adaptors of CUL3-based E3 ligases. In this complex, the BTB domain interacts with CUL3 and the specificity of substrate binding is ensured by the secondary motif, which binds specific substrates and targets them for proteolytic degradation (Canning et al., 2013; Lechner et al., 2011; Narahara et al., 2019; Weber et al., 2005; Weber & Hellmann, 2009, among others).

As mentioned previously, one of the secondary motifs present in plants is the MATH domain, which is also one of the five most prevalent secondary motifs in BTB domain-containing proteins (Perez-Torrado et al., 2006). The MATH domain is broadly represented in eukaryotes and is comprised of seven anti-parallel β -helices which allow it to participate in protein-protein interactions. Proteins containing a MATH domain commonly contain additional domains, such as peptidases, RING and zinc finger, filamin and RluA domains, the BTB domain, tripartite motif and astacin domains. Unlike BTB proteins, MATH-containing proteins seem to be exclusively involved in regulation of protein processing and ubiquitination (Zapata et al., 2007). Interestingly, in proteins containing both a MATH and a BTB domain (MATH-BTB proteins), the BTB domain is found C-terminal to its partner MATH domain, whereas a reversed scenario occurs in other BTB proteins. Additionally, unlike some other BTB subfamilies, MATH-BTB proteins are highly conserved across their full length (Stogios et al., 2005). The evolutionary stability of the MATH-BTB family is also highlighted by a study which calculated the frequency of two-domain combinations in proteins of organisms with completely sequenced genomes. Here, the MATH-BTB combination was the 10th most frequent one (Vogel et al., 2004).

In *Arabidopsis* BPM proteins, the BTB domain is followed C-terminally by the BTB AND C-TERMINAL KELCH (BACK)-AtBPM-like domain, further referred to as BACK domain (Pfam database, NCBI). The BACK domain has not been characterized in detail as part of MATH-BTB proteins in *Arabidopsis*. However, it was found to be highly conserved in metazoan genomes and often present in plant BTB-Kelch proteins (Stogios and Privé, 2004).

The first MATH-BTB protein described as a substrate-specific adaptor of a CUL3-based E3 ligase was MEL-26 of *C. elegans*. MEL-26 mediates proteolytic degradation of a microtubule-severing protein MEI-1, which is necessary for normal progression of the meiosis-to-mitosis transition.

Specifically, degradation of MEI-1 is a prerequisite for normal assembly of the mitotic spindle during early embryogenesis (Pintard et al., 2003). In *Drosophila melanogaster*, a MATH-BTB protein called Hh-INDUCED BTB (HIB) regulates the turnover of the transcription factor CUBITUS INTERRUPTUS (Ci), involved in the Hedgehog signaling pathway, and as such regulates eye development. By designating Ci for degradation, HIB inhibits its transcriptional activity in the *Drosophila* eye disc posterior to the morphogenic furrow, which in turn blocks the Hedgehog pathway and enables normal development of the eye (Zhang et al., 2006). This regulatory process is highly conserved between *Drosophila* and vertebrates. In the mouse genome, two HIB homologs exist, named SPECKLE-TYPE POZ PROTEIN (SPOP). It was shown that expression of SPOP in eye discs of *Drosophila hib* mutants also results in Ci degradation (Zhang et al., 2006). Additionally, experiments in mammalian cell lines showed that SPOP binds transcription factors Gli2 and Gli3 (homologs of Ci) and targets them for degradation, playing an important role during mouse development (Chen et al., 2009). The human genome also contains two genes encoding SPOP proteins, termed SPOP and SPOPL, which are highly similar in both sequence and function. Similar to other MATH-BTB substrate adaptors, the SPOP protein has an N-terminal MATH domain which binds targets for degradation, the internal BTB domain followed by the BACK domain, and a C-terminal nuclear localization sequence (Errington et al., 2012; Zhuang et al., 2009). DNA sequence mutations and aberrant expression levels of SPOP have been observed in human disease, specifically prostate tumors as well as in kidney, breast, colorectal, thyroid and other cancers (reviewed in Clark & Burleson, 2020).

To date, members of the plant MATH-BTB protein family have been researched in a handful of species, with *A. thaliana* being the primary model plant in these studies. The phylogeny and functions of known plant MATH-BTB proteins will be addressed in the following sections.

2.3. Phylogeny of the plant *MATH-BTB* family

The MATH-BTB family was shaped by species-specific evolutionary processes, resulting in different family profiles in species which diverged a long time ago, such as *Homo sapiens*, *C. elegans* and *A. thaliana* but also between more closely related groups of species. For instance, grass plant species had their own specific and rather robust evolutionary pathway compared to other land plant species. In *C. elegans*, there have been reports of 95 MATH proteins and 178 BTB proteins

(Stogios et al., 2005 and references cited therein). Of these two largely expanded groups, a subset of 46 proteins belongs to the MATH-BTB family, which makes this family broadly represented in *C. elegans* (Stogios et al., 2005). Like in *C. elegans*, the *H. sapiens* BTB family is also expanded, but the MATH-BTB expansion did not occur. In their review of CUL3-BTB complexes, Pintard et al. (2004) report 208 BTB proteins in *H. sapiens*, and a later phylogenetic analysis reports 183 BTB members, of which only two belong to the MATH-BTB family (Stogios et al., 2005).

Plants are equally diverse in this aspect. In *A. thaliana*, early studies report 59 *MATH* genes (Oelmüller et al., 2005) and 77 *BTB* genes (Stogios et al., 2005). Additional phylogenetic analyses of the *MATH-BTB* gene family reveal 80 *BTB* genes, of which six belong to the *MATH-BTB* family (Gingerich et al., 2005, 2007). Together, these early analyses indicate no significant expansion of the *MATH-BTB* family in a eudicot species *A. thaliana*.

However, a significant *MATH-BTB* expansion occurred in rice, a monocot species. The first preliminary study of *BTB* genes in the rice genome reports 112 potential genes (Gingerich et al., 2005). A more exhaustive study reports 149 BTB domain-encoding genes and 43 putative pseudogenes, of which at least 69 are *MATH-BTB* genes, with five additional *BTB* genes with *MATH*-related domains, and another 41 genomic loci predicted to be *MATH-BTB* pseudogenes (Gingerich et al., 2007). A phylogenetic inference of BTB domain-containing proteins in the most recent common ancestor (MRCA) of rice and *Arabidopsis* revealed an estimate of 56 *BTB* genes in the MRCA. While the *Arabidopsis* *BTB* family underwent a relatively slight (42%) increase since the monocot-eudicot split, the rice *BTB* family nearly tripled in size and this was largely due to the great expansion of the *MATH-BTB* family, which went from three members in MRCA to 74 members in rice (Gingerich et al., 2007). Another phylogenetic analysis confirmed the presence of 69 *MATH-BTB* rice genes (Juranić & Dresselhaus, 2014). However, a more recent study of MATH domain-encoding sequences in the rice genome reports 69 *MATH* genes, of which only 55 encode both a MATH and a BTB domain (Kushwaha et al., 2016).

A significant expansion was also reported in *Sorghum bicolor*, another grass monocot species, with 41 *MATH-BTB* genes and at least 27 *MATH-BTB* pseudogenes (Gingerich et al., 2007). A later analysis found additional 51 members, making up a total of 92 *MATH-BTB* genes in *Sorghum* (Juranić & Dresselhaus, 2014). These results indicated similar evolutionary dynamics as those that shaped the rice *MATH-BTB* family. Two other grass species are characterized by expansion of the *MATH-BTB* gene family. Maize, a grass monocot related to *Sorghum*, contains 31 *MATH-BTB*

genes (Juranić et al., 2012) and *Brachypodium dystachion*, a grass monocot species closely related to wheat and barley, contains 49 *MATH-BTB* genes (Juranić & Dresselhaus, 2014).

Not all plant species underwent an expansion of the *MATH-BTB* family. An analysis of *MATH* genes in the *Brassica rapa* genome revealed 90 *MATH* domain proteins, of which 11 are *MATH-BTB* proteins (Zhao et al., 2013). An analysis of *BTB* genes in the *Solanum lycopersicum* genome revealed 38 *BTB* genes, of which two are confirmed as *MATH-BTB* genes and additional three cluster alongside them into a *MATH*-related subclade of tomato *BTB* genes (Li et al., 2018). Multiple other land plant species, including monocots (ancestral wheat *Triticum monococcum*, and banana *Musa acuminata*), eudicots (*Medicago truncatula*, poplar *Populus trichocarpa* and grapevine *Vitis vinifera*), gymnosperms (pine *Pinus taeda*), mosses (*Physcomitrella patens*) and bryophytes (*Selaginella moellendorffi*) were all reported to contain less than eight *MATH-BTB* genes, indicating no significant expansion of this gene family (Gingerich et al., 2007; Juranić & Dresselhaus, 2014).

The two most comprehensive phylogenetic analyses of all known plant *MATH-BTB* genes have led to similar yet, in one aspect, markedly different conclusions. The first analysis by Gingerich *et al.* (2007) shows clustering of *MATH-BTB* genes into two distinct clades. One is the smaller core clade, and the other is the large, expanded clade. The core clade contains *MATH-BTB* genes of eudicots *A. thaliana*, *M. truncatula* and poplar, and all other non-monocot species in which no expansion occurred. The core clade also contains two rice and four *Sorghum* genes, as the only examples of a monocot species genes. The expanded clade contains the remaining 64 rice and 39 *Sorghum* *MATH-BTB* genes as well as the single *MATH-BTB* gene which was, at the time, identified in the monocot *T. monococcum*. The clustering of genes seemed to be based on whether they belonged to a monocot or a non-monocot species, which led to the hypothesis that the expanded clade is monocot-specific. The authors suggest that the large expansion of the *MATH-BTB* family characterized the evolution of monocot plants, as a means of adaptation to increasingly dynamic changes in environment following the monocot-dicot split (Gingerich et al., 2007). This original phylogenetic analysis was extended by Juranić & Dresselhaus (2014) in a study which includes the *MATH-BTB* sequences used in Gingerich et al. (2007), and additional sequences of genomes which have become available in the meantime, such as maize (a grass monocot) and banana (a non-grass monocot). Again, *MATH-BTB* genes clustered into core clade and expanded clade. However, unlike the original analysis in which all monocot species were also members of

the Poaceae family (grasses), here a non-grass monocot species (banana) was included and surprisingly, its genes clustered into the core-clade, along with other non-monocot genes, while the expanded clade consisted exclusively of grasses' *MATH-BTB* sequences. This analysis showed that the expanded clade is, in fact, grasses-specific and that the significant expansion of *MATH-BTB* genes is an adaptation to specific evolutionary pathways shaping the Poaceae family, and not the monocot lineage (Juranić & Dresselhaus, 2014).

The two clades of *MATH-BTB* genes significantly differ at the level of evolutionary conservation. The core clade is highly conserved among nine diverse land plant species analyzed in Gingerich et al. (2007), which was additionally confirmed by the calculation of 60 to 84% amino acid identity with almost no gaps between sequence alignments of core clade proteins (Juranić & Dresselhaus, 2014). Additionally, core clade genes are conserved at the level of gene structure, with most genes containing four exons, and the positions of the intron/exon junctions conserved to the nucleotide (Gingerich et al., 2007). By contrast, the grasses-specific expanded clade shows high levels of sequence divergence (Gingerich et al., 2007), with an average of 45% identical amino acids between sequence alignments (Juranić & Dresselhaus, 2014). Sequence divergence among expanded clade members is particularly prominent within the target-hunting MATH domain, which is more diverged than the scaffold-binding BTB domain (Gingerich et al., 2007). The highly divergent expanded clade further clusters into five smaller subclades, annotated E1 to E5 (Juranić & Dresselhaus, 2014). Unlike core clade members, the coding regions of expanded clade *MATH-BTB* loci contain only one predicted exon uninterrupted by obvious introns (Gingerich et al., 2007). Another interesting distinction between core and expanded clade genes is their chromosomal location. While core clade genes are exclusively single copies scattered on different chromosomal locations, the majority of *Sorghum*, *Brachypodium*, and rice *MATH-BTB* genes of the expanded clade are located in gene clusters or in close proximity on the same chromosome (Juranić & Dresselhaus, 2014).

Clustering of *MATH-BTB* genes into two groups with distinct evolutionary backgrounds prompted questions regarding the function of each group. Evolution of protein-coding genes is driven, among other mechanisms, by point mutations. Point mutations can lead to either a synonymous nucleotide substitution, encoding the same amino acid as before the mutation, and a non-synonymous nucleotide substitution, encoding a new amino acid. Evaluation of the ratio of nonsynonymous distance (K_A) to synonymous distance (K_S) in the core and expanded clades showed that in the core

clade, the *MATH* domain is under a strong purifying selection, meaning that synonymous nucleotide substitutions are favored in order to prevent a change in amino acids. On the other hand, the diversification of the expanded clade seems to be driven by positive selection of nonsynonymous substitutions (Gingerich et al., 2007). It was suggested that the overrepresentation of positively selected sites in the expanded group reflects a pressure for diversification aimed at coping with diversification of their fast-evolving targets (Gingerich et al., 2007). For instance, Thomas (2006) suggests that possible substrates of the highly expanded MATH-BTB family in *C. elegans* are pathogen proteins, which are under strong positive selection to avoid detection and inactivation by the host. Conversely, proteins of the highly conserved core group most likely recognize targets with more stable evolutionary histories, which are possibly involved in essential cellular functions (Gingerich et al., 2007; Juranić & Dresselhaus, 2014).

2.4. Functional roles of plant MATH-BTB proteins

2.4.1. Maize, wheat, tomato and rice MATH-BTB proteins

The first functionally studied MATH-BTB protein belonging to a grass species was ZmMAB1 protein of maize. The *ZmMAB1* gene is expressed in the male and female germline, especially post-meiosis and during early mitotic stages of embryo development (Juranić et al., 2012; Juranić & Dresselhaus, 2014), as well as in the maize zygote during asymmetric cell division (Juranić et al., 2012). The maize *ZmMAB1* mutant exhibits severe developmental defects in the male and female germlines. In 40% of *mab1* (RNAi) mutants of maize, polar nuclei separation and migration is arrested during the first mitotic division of female germline cells. Developmental arrests occur either at the one- or two-nucleate stage, containing both nuclei attached to each other or two nuclei that are not properly separated (Juranić et al., 2012). Additionally, in a subset of *mab1* (RNAi) mutants there is no asymmetric cell division during the first mitotic divisions of the male germline. Instead, several mutant phenotypes occur, such as the formation of two attached vegetative-like nuclei of identical size containing large nucleoli but lacking cellularization, or two separated vegetative-like nuclei lacking cellularization (Juranić et al., 2012). During male meiosis in *mab1* (RNAi) mutant microsporocytes, some chromosomes are not properly pulled toward spindle poles and are lost during the anaphase–telophase transition at meiosis I. During meiosis II,

the spindle apparatus is significantly shorter in mutant dyads than in wild type and the resulting tetrads consist each of two pairs of microspores containing nuclei not properly separated from each other. A large portion of these tetrads undergo apoptosis (Juranić et al., 2012).

ZmMAB1 interacts with CUL3, itself and Katanin subunit p60 of Arabidopsis, suggesting ZmMAB1-mediated regulation of Katanin degradation via CUL3-based E3 ligase activity (Juranić et al., 2012). Expression of two closely related maize *MATH-BTB* genes, *ZmMAB2* and *ZmMAB3* is also germline-specific. In the male gametophyte, *ZmMAB2* is most strongly expressed during meiosis and at the uninucleate stage, while *ZmMAB3* expression is barely detectable during all developmental stages. In the female gametophyte, *ZmMAB2* is constitutively expressed at all stages and *ZmMAB3* mostly during late cellularization events. Based on their expression profiles, the authors suggest temporally and spatially specific functions of the three ZmMAB proteins (Juranić & Dresselhaus, 2014).

To date, three *MATH-BTB* genes of wheat were studied at the level of gene expression, namely *TaMAB1-3*. Similar to *ZmMAB* genes of maize, *TaMAB1* and *TaMAB2* exhibit temporally and spatially different expression profiles during reproductive development of wheat. *TaMAB1* is expressed exclusively in wheat egg cells, while *TaMAB2* is expressed in the zygote and two-celled proembryos. Conversely, *TaMAB3* is expressed in a ubiquitous manner, throughout all tested generative and vegetative tissues (Leljak-Levanić et al., 2013). Finally, in tobacco BY-2 cells transiently transformed with GFP-tagged TaMAB2, the fusion protein localizes in and around the nucleus, but its function in wheat reproduction has not been determined (Leljak-Levanić et al., 2013).

Compared to known *MATH-BTB* genes of maize and wheat, a somewhat different expression profile has been reported for *MATH-BTB* genes of tomato, a non-grass species. Here, microarray data analysis showed that all five *BTB* genes in a MATH-related cluster are constitutively expressed in various vegetative tissues at various developmental stages (Li et al., 2018).

Using microarray data, Kushwaha et al. (2016) analyzed the expression of 54 rice genes encoding a single MATH and a single BTB domain (annotated as OsMB) in order to elucidate genes with higher expression throughout all developmental stages and tissues, as well as during biotic stresses. Several highly expressed genes were additionally validated by RT-qPCR after exposure to drought and salt stress. Out of all highly expressed genes, *OsMB11* seems to be ubiquitously expressed in all the tissues, developmental stages, as well as during biotic and abiotic stresses, however,

functional analyses are yet to be published (Kushwaha et al., 2016). To the best of my knowledge, no rice MATH-BTB proteins with more specific expression profiles have been studied in detail at the time of writing this dissertation.

2.4.2. *Arabidopsis* BPM proteins

A small family of *Arabidopsis* MATH-BTB genes (*BPMs*) was more extensively studied. Lechner et al. (2011) report similar levels of expression of all six *BPM* genes in various organs, with highest expression in flower buds and open flowers. Although two earlier studies report more pronounced differences in tissue-specific expression levels between individual genes (Weber et al., 2005; Weber & Hellmann, 2009), all studies confirm constitutive expression of *BPM* genes and suggest functional redundancy. Furthermore, *Arabidopsis* T-DNA insertion lines of several individual *BPM* genes were found to exhibit wild type-like phenotype under control conditions (Lechner et al., 2011).

BPM proteins interact with several types of transcription factors and target them for proteasomal degradation via CUL3-based E3 ligase activity and thus play regulatory roles in various cellular and developmental processes (Lechner et al., 2011; Chen et al., 2013, 2015; Morimoto et al., 2017). For instance, *BPM* proteins were shown to regulate flowering, a developmental process which is also dependent on environmental conditions. In *Arabidopsis*, a transcription factor MYB56 of the R2R3-MYB family negatively regulates the expression of *FLOWERING LOCUS T* (*FT*, also referred to as the *florigen*), which is a key activator of flowering (Chen et al., 2015). *BPM* proteins are directly involved in regulation of flowering through binding of MYB56, which results in MYB56 instability and consequently, promotion of flowering (Chen et al., 2015). Similarly, *BPM* proteins were shown to directly interact with MYB106, another negative regulator of *FT* expression. The authors suggest that MYB106 protein levels are modulated via Cul3-based E3 ligase activity, which in turn regulates *FT* expression and flowering (Hong et al., 2021).

Involvement of *BPM* proteins in flowering was also demonstrated by phenotypic changes of 6xami*BPM* mutant *Arabidopsis* lines with significantly reduced expression of all six *BPM* genes. Besides a significant delay in primary root growth, reduced number of lateral roots and aberrations in shoot development, the 6xami*BPM* plants are heavily affected in flower development, exhibiting

a late flowering phenotype, fewer leaves at the beginning of flowering, reduced rosette size and smaller flowers in fewer numbers (Chen et al., 2013).

Several other MYB transcription factors were indicated as potential targets of BPM proteins, namely MYB1, MYB25 and MYB109. Although the authors do not directly show that the Cul3-BPM complex mediates degradation of these transcription factors, they show that BPMs directly interact with all three transcription factors, and provide evidence that their degradation is mediated by the 26S proteasome (Beathard et al., 2021). Contrary to the two previously mentioned MYB transcription factors which are involved in flowering regulation, MYB25 was shown to have a role in abiotic and biotic stress response (Beathard et al., 2021).

BPMs are additionally involved in regulation of phytohormone ABA response (Julian et al., 2019; Lechner et al., 2011), a central mechanism by which plants respond to adverse environmental circumstances. During abiotic and biotic stress, ABA levels generally rise and the newly abundant phytohormone introduces various physiological changes with the aim to protect the plant from negative consequences of stress exposure. For instance, ABA promotes stomatal closure to prevent intracellular water loss and inhibits seed germination to postpone seedling growth to a period of more favorable external conditions (reviewed in Tuteja, 2007). ABA triggers abiotic stress response through multiple transcriptomic pathways, i.e. by regulating expression of various stress-responsive genes (reviewed in Cutler et al., 2010; Sreenivasulu et al., 2012; Vishal & Kumar, 2018, among others). During drought, ABA triggers accumulation of osmolytes and synthesis of proteins which maintain cellular water status and protect other proteins and cellular organelles from collapsing under water stress (Sreenivasulu et al., 2012). Additionally, cellular ABA levels fluctuate depending on intrinsic developmental programs (Finkelstein et al., 2002; Vishal & Kumar, 2018). ABA signaling begins with, among others, a class of protein phosphatases type 2C (PP2Cs) which inhibit the activity of a class of SNF1-related protein kinases (SnRK2s). Upon stress exposure, PP2Cs are inactivated and SnRK2s are relieved of inhibition and can phosphorylate and thus enhance the activity and stability of many ABA-responsive transcription factors, among other types of mediators. These TFs act as master switches which regulate transcription of downstream gene targets (reviewed in Cutler et al., 2010). One example is *ATHB6*, a member of the class I homeodomain-leucine zipper (HD-Zip) family of transcription factors. *ATHB6* binds to its own promoter and induces *ATHB6* upregulation (Himmelbach et al., 2002; Söderman et al., 1999) and the accumulated TF acts as a negative regulator of ABA response (Himmelbach et al., 2002). This

is where BPM proteins come into play. First, it was shown that all six BPMs bind ATHB6 and target it for proteasomal degradation, thus acting as positive regulators of ABA response (Lechner et al., 2011). Secondly, a recent study reported that two members of the BPM family, namely BPM3 and BPM5 also target the major inhibitors of ABA-response, PP2Cs, for proteasomal degradation (Julian et al., 2019). This was an important finding in light of the fact that most PP2Cs are significantly upregulated (up to 75-fold) in response to ABA treatment, drought, salt and osmotic stress, a phenomenon explained in terms of higher plasticity of ABA response (Szostkiewicz et al., 2010). Julian et al. (2019) suggest that degradation of PP2Cs by BPMs serves to counteract ABA-induced accumulation of PP2Cs and to restore phosphatase levels that allow efficient ABA signaling (Julian et al., 2019). The role of BPM proteins in ABA response was also shown by phenotypic analyses of mutant plants. The *amiR-bpm* mutant line with reduced expression of *BPM1*, 4, 5, and 6 exhibits reduced leaf blade size, serrated leaves, a reduced, bushy stature and altered flower development. The flowers have shorter pedicels, exaggerated opening, shorter stamens, protruding gynoecium and short siliques (Lechner et al., 2011). *AmiR-bpm* seeds are ABA insensitive, with no inhibition of germination after ABA treatment. Grown *amiR-bpm* plants exhibit reduced stomatal closure after ABA treatment and under nonstress conditions (darkness). Reduced stomatal closure was also indirectly measured as lower leaf temperature after dehydration stress (Lechner et al., 2011). These findings were confirmed by Julian et al. (2019), who additionally generated a loss-of-function double mutant *bpm3 bpm5*. Similar to *amiR-bpm* plants, the *bpm3 bpm5* mutant exhibits reduced sensitivity to ABA-mediated inhibition of seedling establishment and root growth. The mutant also exhibits lower leaf temperature, an indicator of reduced stomatal closure, but the effect is not as pronounced as in *amiR-bpm* and the authors conclude that overall, the mutant shows no significant alteration in ABA-mediated stomatal closure (Julian et al., 2019). Conversely, overexpression of either BPM3 or BPM5 leads to enhanced ABA sensitivity, with inhibition of seed germination, seedling establishment, and root growth (Julian et al., 2019). Plants overexpressing BPM3 or BPM5 also show reduced water loss, which is an indirect reflection of increased stomatal closure. Additionally, OE BPM5 plants show enhanced drought resistance under greenhouse conditions (Julian et al., 2019).

Besides ABA, ethylene is another hormone whose production is induced by stress and which regulates the activity of many transcription factors of the APETALA2/ETHYLENE RESPONSE FACTOR (AP2/ERF) family. AP2/ERFs contain an AP2/ETHYLENE RESPONSIVE ELEMENT

BINDING FACTOR (EREB) domain and are divided into four subfamilies, depending on their DNA binding preferences, i.e. the response elements they recognize (reviewed in Xie et al., 2019). CUL3-based E3 ligase activity of BPMs has been linked to different AP2/ERFs and consequently to different physiological processes (Weber & Hellmann, 2009; Chen et al., 2013; Morimoto et al., 2017). WRI1 is a member of the ERF subfamily which recognizes an ETHYLENE RESPONSE ELEMENT (ERE) (Xie et al., 2019, and references cited therein) and it was shown that by targeting WRI1 for degradation, BPMs regulate fatty acid metabolism during seed development (Chen et al., 2013).

Another AP2/ERF transcription factor is RAP2.4, a member of DEHYDRATION-RESPONSIVE ELEMENT BINDING (DREB) proteins and additionally categorized within a smaller DREB subgroup of proteins which recognize both a DEHYDRATION-RESPONSIVE ELEMENT (DRE) and an ERE (Xie et al., 2019, and references cited therein). RAP2.4 has been described previously as a regulator of abiotic stress tolerance and red light response (Lin et al., 2008) and BPM proteins were suggested as mediators of its proteasomal degradation (Weber & Hellmann, 2009).

Another DREB protein has been implicated as a target of BPM proteins (Morimoto et al., 2017). DREB2A is a key transcription factor acting in drought and heat stress response in *Arabidopsis*. Exposure of plants to these stresses induces expression of the *DREB2A* gene via cis-acting elements in its promoter (Yoshida et al., 2011), which is followed by transcriptional activation of genes encoding downstream transcription factors involved in heat and drought stress response (Sakuma et al., 2006a; 2006b). Heat shock factors (HSF) play a key role in heat-stress response, acting as transcriptional activators both upstream and downstream of DREB2A; for instance, Hsf1A induces expression of DREB2A which then regulates expression of downstream target genes in the transcriptional cascade, such as heat shock proteins (HSPs) (Yoshida et al., 2011). *HsfA3* is a well-characterized DREB2A target, known to be up-regulated by DREB2A in conditions of heat and drought stress in wild type plants (Sakuma et al., 2006b). Furthermore, accumulation of DREB2A in the amiBPM line with downregulated *BPM* genes causes upregulation of *HsfA3* (Morimoto et al., 2017), making it a convenient candidate to indirectly measure levels of available DREB2A. In order to induce expression of target genes during stress exposure, DREB2A needs to be post-translationally stabilized via its negative regulatory domain, NRD (Morimoto et al., 2013; Sakuma et al., 2006b). It was shown that members of the BPM family interact with the NRD of DREB2A, promote its degradation via CUL3-based E3 ligase activity and negatively regulate heat stress

response (Morimoto et al., 2017). This is believed to serve as a protective mechanism against any adverse effects that stress-induced accumulation of DREB2A could have on numerous physiological processes this protein is involved in (Morimoto et al., 2017). The dynamic between BPM proteins and DREB2A resembles the proposed model of PP2C protein level regulation by BPMs during ABA response (Julian et al., 2019).

Via their CUL3-based E3 ligase activity, BPM proteins also regulate members of the basic helix-loop-helix (bHLH) family of TFs, namely the three MYC proteins, MYC2, MYC3, and MYC4. MYC proteins are one of the key players of a signaling pathway induced by jasmonates (JAs), oxygenated lipid derivatives which act as essential phytohormones. JA signaling affects expression of numerous genes and thus regulates biotic and abiotic stress responses and coordinates several developmental processes such as root growth and fertility (Wasternack & Hause, 2013). Several BPMs were shown to regulate MYC levels, most likely to reset JA signaling and to reduce possible harmful effects of MYC activity (Chico et al., 2020), similar to the hypothesized role of BPMs in regulation of DREB2A and PP2Cs (Julian et al., 2019; Morimoto et al., 2017). Furthermore, BPM proteins have been linked to JA signaling via interaction with an AP2/ERF transcription factor REDOX-RESPONSIVE TF 1 (RRTF1), which promotes resistance to pathogens (Li et al., 2021). The *Arabidopsis* plant line bpm235 is a triple mutant obtained by crossing the three T-DNA insertion lines for *bpm2*, *bpm3* and *bpm5* (Chico et al., 2020). According to the characterization of individual SALK lines, the authors show that the bpm235 line is a knockout mutant for *BPM2* and *BPM5*, and a knockdown for *BPM3*. The line exhibits a slightly shorter root than wild type, indicative of a mild constitutive JA response (Chico et al., 2020).

Taken together, these findings implicate BPMs as posttranslational regulators of proteins involved in various kinds of abiotic stress response and stress-induced hormone-signaling. Interestingly, while all six BPMs were shown to interact with proteins such as ATHB6, WRI1, MYB56 and DREB2A (Lechner et al., 2011; Chen et al., 2013, 2015, Morimoto et al., 2017), only specific members have been shown to interact with PP2ACs (Julian et al., 2019) and a similar bias exists between different BPMs for binding of the three MYC proteins (Chico et al., 2020). Additionally, only BPM1, BPM2 and BPM4 interact with MYB106 (Hong et al., 2021), only BPM1 and BPM3 interact with RRTF1 (Li et al., 2021). This implies both functional redundancy and the existence of individual roles within this highly conserved protein family, some of which possibly manifest under specific environmental circumstances.

3. MATERIAL AND METHODS

3.1. Material

3.1.1. Bacterial strains

Escherichia coli strain HST04 (StellarTM Competent Cells, Clontech, #636763) was used for cloning, as prepared by the manufacturer.

3.1.2. Yeast strains

Saccharomyces cerevisiae strain Hfc7 [MAT ura3-52 his3-200 ade2-101 lys2-801 trp1-901, leu2-3112 gal4-542 gal 80-538 LYS2::GAL1UAS-G-AL1TATA-HIS3URA3::GAL417mers (x3) - CyC1TATA-lacZ] was used for Y2H screens. The Hfc7 strain contains reporter genes (*HIS3* and *lacZ*) integrated into the genome (Feilotter et al., 1994).

3.1.3. *Arabidopsis* plant lines

Arabidopsis thaliana accession Columbia-0 (Col-0) line was used as wild type control in all experiments, unless stated otherwise. Two previously created *Arabidopsis* transgenic plant lines overexpressing TaMAB2-GFP (Bauer et al., 2019) and BPM1-GFP (Škiljaica et al., 2020) were used for functional analyses of TaMAB2 and BPM1, respectively. Both transgenic lines were made in the genetic background of *A. thaliana* accession Col-0, with the gene of interest functionally fused to the *GFP* sequence and integrated into the genome under control of the CaMV 35S promoter, ensuring constitutive expression of the fusion protein.

3.2. Methods

3.2.1. Bioinformatics

3.2.1.1. Phylogenetic analysis

The *Triticum aestivum* proteome available in Ensembl Plants database (<https://plants.ensembl.org>) was searched using the Protein BLAST tool with TaMAB2 amino acid sequence as query. A list of 46 putative wheat *MATH-BTB* genes was obtained and annotated *TaMAB1-46*. Non-redundant full-length amino acid TaMAB sequences were aligned with known MATH-BTB proteins from maize, *Z. mays* (ZmMAB; Juranić et al., 2012), rice, *O. sativa* (OsMBTB; Gingerich et al., 2007), and *A. thaliana* (AtBPM; Gingerich et al., 2005; 2007) using Clustal Omega v1.2.4 (Sievers et al., 2011). A phylogeny of MATH-BTB sequences was inferred in SeaView v4.6.1 (Gouy et al., 2010) using the maximum likelihood (ML) method with nearest-neighbor interchange (NNI) and supported with the Shimodaira–Hasegawa (SH) approximate likelihood ratio test (aLRT) at every bifurcation. The tree was visually adjusted using FigTree v1.4.2 (<http://tree.bio.ed.ac.uk/>). Images were processed in Inkscape 1.0 (<https://inkscape.org/>).

3.2.1.2. Multiple sequence alignments

For multiple sequence alignments of MATH and BTB domains of all BPM proteins' splicing variants, 16 known BPM sequences were pooled from the Ensembl Plants and UniProt database (www.uniprot.org). For multiple sequence alignments of MATH and BTB domains of all core clade proteins and expanded clade TaMAB proteins, amino acid sequences of relevant *Arabidopsis*, rice, maize and wheat MATH-BTB proteins were used. Each protein sequence was searched against the corresponding plant genome using NCBI Protein BLAST Tool. From here, putative MATH and BTB domain sequences were extracted from the Protein family (Pfam) or Conserved Domains (CD) database. Individual MATH or BTB sequences were aligned using ClustalX v.2.0 (Larkin et al., 2007) or Clustal Omega v1.2.4 (Sievers et al., 2011) and alignments with visible conservation statuses were displayed using Jalview v.2 (Waterhouse et al., 2009). Exon, 5' UTR and 3' UTR delineations of *BPM2* splicing variants were extracted from the *Arabidopsis thaliana*

Araport11 genome (genome ID:447) in the Phytozome database (<https://phytozome-next.jgi.doe.gov>). For calculation of similarity and identity between multiple sequence alignments, an online calculator was used to calculate pairwise sequence identities (Stothard, 2000), which were then averaged to obtain a general sequence identity value. Images were processed in Inkscape 1.0 (<https://inkscape.org/>).

3.2.1.3. Selection of temperature-stable candidate reference genes

Expression profiling data (ATH1 Genome Array datasets) obtained on several *Arabidopsis* tissues exposed to different temperature treatments (4 to 40 °C) were used to select candidate reference genes with minimum expression variation. Additionally, available literature was searched for RT-qPCR reference genes adhering to the following criteria: they belonged to traditional reference genes (“housekeeping genes”) and/or they had already been identified as potential reference genes for experiments employing specific temperatures in *Arabidopsis* (Hong et al., 2010). Microarray data processing and selection of candidate reference genes was performed by Lucija Markulin, according to the protocol described in Škiljaica et al. (2022).

3.2.1.4. RT-qPCR primer design

To design gene-specific primers suitable for RT-qPCR, genomic sequences and transcript sequences with designated exons, introns, 5' and 3' untranslated regions were retrieved from the Phytozome database. Gene-specific RT-qPCR primers were designed using PerlPrimer software (Marshall, 2004) with the criteria set to filter primer pairs with amplicon length of 100 to 250 bp, T_m of $59\text{ °C} \pm 1\text{ °C}$ and GC content of 40% to 60%. When possible, primers were designed to span an exon-exon junction. For genes with multiple transcripts, primers were designed to bind all transcripts which were known at the time of experimental design, yielding amplicons of identical sequence and size. Because it was not possible to design primers which would bind all three splicing variants of endogenous *BPM1*, two primer pairs were designed, one specific for both *BPM1.1* and *BPM1.3*, and the other specific for *BPM1.2*. Three primer pairs used for relative gene expression analysis of individual *BPM2* splicing variants (*BPM2.3*, *BPM2.4* and *BPM2.5*) were

designed to bind only the specified splicing variant. The specificity of each primer pair was verified using NCBI Primer BLAST Tool against the *A. thaliana* transcript database. Primers were ordered from Macrogen (Macrogen Europe, Amsterdam, Netherlands) and prepared according to the manufacturer's instructions. All primer sequences and corresponding gene annotations, their average primer efficiencies, amplicon sizes in base pairs (bp) and numbers of primer-bound transcript variants are listed in **Appendix A1**.

3.2.1.5. Candidate reference gene expression stability analysis

To assess the expression stability of candidate reference genes in *Arabidopsis* seedlings, leaves and buds after temperature treatments, the obtained C_q data was analyzed with four validation algorithms: BestKeeper, geNorm, NormFinder and comparative ΔC_q method. For each candidate reference gene, correlation coefficient (BestKeeper), M value (geNorm), stability value (NormFinder) and meanSD (comparative ΔC_q method) were calculated for individual tissue samples (seedlings, leaves, buds) and all three tissues combined. Expression stability analysis was performed by Lucija Markulin, according to the protocol described in Škiljaica et al. (2022). The entire code used for data analyses is deposited at <https://github.com/Edlenil/Reference-genes> (courtesy of Lucija Markulin).

3.2.2. Plant growth conditions

Arabidopsis thaliana seeds (approximately 100 per sample) were washed in 70% ethanol followed by surface-sterilization for 10 min in 1% Izosan G (100% sodium dichloroisocyanurate dihydrate, Pliva) and 0.01% Mucosal™ (Sigma-Aldrich). Seeds were rinsed five times in sterile distilled H₂O and plated on Murashige and Skoog (MS) medium (Murashige & Skoog, 1962) containing 20 g/L sucrose, 100 mg/L myo-Inositol, 0.5 mg/L niacin, 0.1 mg/L thiamin, 0.5 mg/L pyridoxine, 2 mg/L glycine (pH 5.8) and solidified with 0.8 % agar (Sigma-Aldrich). For selection of transgenic plants, MS medium was supplemented with 30 mg/L glufosinate ammonium (Sigma-Aldrich). Germination plates were stratified at 4 °C for 3 days, followed by incubation in short day conditions (8 h light/16 h dark cycles, 120 $\mu\text{mol m}^{-2} \text{s}^{-1}$, 24 °C) for two weeks. After formation of first leaves

(not counting cotyledons), plantlets were transferred to a soil mixture of white peat and perlite (Steckmedium KLASMANN, Klasmann-Deilmann GmbH) and kept for approximately two weeks in short day conditions. To reach maturity, plantlets were transferred to long day conditions (16 h light/8 h dark, $120 \mu\text{mol m}^{-2} \text{s}^{-1}$, $24 \text{ }^\circ\text{C}$) with 50% relative humidity. For selection and validation of RT-qPCR reference genes, seeds were plated as described above and kept for 12 days in long day conditions and a light intensity of approximately $70 \mu\text{mol m}^{-2} \text{s}^{-1}$. Twelve-day old seedlings were transferred to soil and kept for one week in short day conditions ($70 \mu\text{mol m}^{-2} \text{s}^{-1}$). Plants were then transferred to long day conditions ($70 \mu\text{mol m}^{-2} \text{s}^{-1}$) until they reached the age of 5 weeks.

3.2.3. Generation of plasmid constructs

Gene-specific primers were designed using In-Fusion Primer Design Tool for cloning into EcoRI and BamHI restriction sites (Clontech, Takara Bio Inc.; **Appendix A2**). Genes *eIF4A1* (AT4G11420) and *eIF3G1* (AT3G11400) were amplified using the $1\times$ In-Fusion CloneAmp™ HiFi PCR Premix (Clontech, Takara Bio Inc.) according to the manufacturer's instructions. Coding sequences for proteins of interest were cloned into the plasmid pGBT9, to yield the protein of interest N-terminally fused with the DNA-binding domain of the GAL4 transcription factor (pGBT9-eIF4A1 and pGBT9-eIF3G1). For all cloning procedures, In-Fusion technology (Clontech, Takara Bio Inc.) was used, following the manufacturer's instructions (In-Fusion® HD Cloning Kit User Manual). In-Fusion products were subsequently transformed into *E. coli* strain HST04 using heat-shock transformation, as follows. Up to 5 ng of DNA (2.5 μL of the In-Fusion reaction) was added to 45 μL of bacterial cells in a sterile round-bottom tube and the suspension was incubated on ice for 30 min. The tube was immersed in a water-bath at $42 \text{ }^\circ\text{C}$ for 45 sec (heat-shock) and transferred to ice for 2 min. For cell recovery, 500 μL of SOC medium (5 g/L yeast extract, 20 g/L tryptone, 10 mM NaCl, 2.5 mM KCl, 10 mM MgCl_2 , 10 mM MgSO_4 , 20 mM glucose) was added to each tube and suspensions were incubated for 1 h at $37 \text{ }^\circ\text{C}$ and 250 rpm. Bacterial suspension was plated on solid LB medium (5 g/L yeast extract, 10 g/L tryptone, 10 g/L NaCl pH 7.0, 15 g/L agar) supplemented with 0.1 mg/mL ampicillin and incubated overnight at $37 \text{ }^\circ\text{C}$. For isolation of plasmid DNA, a single colony was picked and cultured overnight at $37 \text{ }^\circ\text{C}$ and 250 rpm in 3 mL of liquid LB medium (without agar) supplemented with 0.1 mg/mL ampicillin.

Cells were harvested by one-step centrifugation (5 min, 14000 rpm) and plasmid DNA was isolated using the Wizard[®] Plus SV Minipreps DNA Purification System (Promega) according to the manufacturer's instructions. Concentrations of plasmid DNA were subsequently measured using the NanoVue[™] spectrophotometer (GE Healthcare, Life Sciences). The sequence of final plasmid constructs was verified by DNA sequencing (Macrogen Europe, Amsterdam, Netherlands). Plasmid DNA was stored at -20 °C until further use.

3.2.4. Standard PCR reactions

Standard PCR mixtures contained 1× EmeraldAmp[®] GT PCR Master Mix (Takara Bio Inc.), 300 nM forward and reverse primer and 100-200 ng of DNA as template in a total volume of 25 µL. PCR was performed in a gradient thermocycler (Eppendorf Mastercycler) with the initial denaturation step set to 95 °C for 2 min, followed by 40 cycles of denaturation at 95 °C for 30 s, annealing at 58 or 60 °C for 30 s, extension at 72 °C for 3 min and a final extension step at 72 °C for 5 min. PCR samples were loaded onto a 1% agarose gel in TAE buffer (40 mM Tris base, 20 mM glacial acetic acid, pH 8.0, 1 mM EDTA) and DNA fragments were separated by gel electrophoresis for 30 min at 100 V (RunOne[™] System, Embi Tec). The gel was stained using 10 ng/L ethidium bromide and illuminated by UV light using a Kodak EDAS 290 hood, with 2 s exposure time and 100% UV strength.

3.2.5. Yeast-two-hybrid (Y2H) assay

Plasmid constructs used for Y2H were described in section 3.2.3. Two previously generated plasmid constructs were also used, namely pGBT9-KAT, encoding the wheat Katanin protein fused to the binding domain of GAL4, and pGAD424-TaMAB2, encoding the wheat TaMAB2 protein fused to the activation domain of GAL4 (Škiljaica, 2016). Additionally, for positive control, plasmid constructs pGAD424-RDM1 and pGBT9-DMS3 were used (described in Sasaki et al., 2014; courtesy of Zdravko Lorković). The yeast strain Hfc7 was cultivated in liquid YPD medium (10 g/L yeast extract, 20 g/L peptone, 20 g/L glucose) and co-transformed with bait and prey constructs using a standard lithium-acetate (LiAc) technique (Agatep et al., 1988), following the

protocol described in the Yeast Protocols Handbook (Clontech, Takara Bio Inc.). Co-transformants were selected on solid YC medium lacking leucine and tryptophan (6.7 g/L yeast nitrogen base, 20 g/L glucose, 0.62 g/L DO Supplement –Leu/–Trp [Takara Bio Inc.]; YC/–Leu/–Trp). For the histidine prototrophy assay, individual colonies of all co-transformants were scraped from the YC/–Leu/–Trp plate, diluted in 100 μ L sterile distilled water and 10 μ L of each suspension was plated in a grid pattern on selective medium lacking histidine, leucine and tryptophan (prepared as described before, but using 0.62 g/L DO Supplement–His/–Leu/–Trp [Takara Bio Inc.]). The YC/–His/–Leu/–Trp medium was supplemented with 13 mM 3-AT (3-amino-1,2,4-triazole) for elimination of non-specific protein-protein interactions. The β -galactosidase assay was performed using X-gal (5-bromo-4-chloro-3-indolyl- β -D-galactopyranoside) in the Colony-lift Filter Assay following the protocol described in the Yeast Protocols Handbook (Clontech, Takara Bio Inc.), with some adjustments. First, individual colonies of all co-transformants were diluted in water and plated in a grid pattern on a YC/–Leu/–Trp plate, following the same procedure as described for the His prototrophy assay. For the assay, an 80-mm filter (Whatman) was pressed against the colonies and immediately immersed in liquid nitrogen several times. The filter was placed in an open Petri dish and overlaid with a 10 mL solution containing 0.7% agarose in Z buffer (60 mM $\text{Na}_2\text{HPO}_4 \cdot 7\text{H}_2\text{O}$, 40 mM $\text{NaH}_2\text{PO}_4 \cdot \text{H}_2\text{O}$, 10 mM KCl, 1 mM $\text{MgSO}_4 \cdot 7\text{H}_2\text{O}$), 165 μ L of X-gal stock solution (20 mg/mL in dimethylformamide) and 27 μ L β -mercaptoethanol (Sigma-Aldrich). Colonies which resulted with a detectable blue color in less than 30 min were considered to represent strong interactions. For detection of weaker interactions, incubations of up to five hours were allowed. For negative controls, all constructs were co-transformed together with the bait or prey construct without insertion. All components of DO Supplements are described in the Yeast Protocols Handbook (Clontech, Takara Bio Inc.). All plates were incubated for 2-3 days at 30 $^\circ\text{C}$ for colonies to appear. Three individual co-transformants of each co-transformation were used for the His prototrophy and β -galactosidase assay.

3.2.6. Germination assay

Arabidopsis thaliana seeds were sterilized as described in section 3.2.2. and plated on MS medium supplemented with 0.5 g/L 2-(N-morpholino)ethanesulfonic acid (MES). The MS-MES medium

was supplemented with different concentrations of NaCl (25, 50 and 100 mM), mannitol (100, 200 and 300 mM) or ABA (0.5 and 1 μ M). For ABA treatments, sucrose was omitted from the medium. For control, seeds were germinated on MS-MES medium. Control medium for ABA treatment did not contain sucrose. To ensure equal distribution of nutrients among seedlings and uninterrupted root growth, seeds were plated individually across the surface of the medium. Seeds were stratified for three days at 4 °C and transferred to a plant chamber with constant light (120 μ mol m⁻² s⁻¹, 24 °C) at 24 °C. Germination rate was measured as percentage of seeds with radicle emergence. Radicle emergence was evaluated 48 h after imbibition by placing sealed Petri dishes under a binocular magnifier and counting the seeds with visible embryonic root emerging through the micropyle. Three independent experiments were performed for all assays, with n > 100 in each experiment.

3.2.7. Abiotic stress treatments

Seeds were sterilized and germinated as described in section 3.2.2. For ABA, NaCl and mannitol treatments, 12-day-old seedlings were incubated for 6 h in liquid MS-MES medium without sucrose and supplemented with 50 μ M ABA, 150 mM NaCl or 300 mM mannitol. These concentrations were shown to be effective in preliminary experiments performed by Nataša Bauer. Liquid MS-MES was prepared as described in section 3.2.6, but without the agar and sucrose. For control, seedlings were incubated in a mock solution (liquid MS-MES medium without sucrose). Treatments were performed in 24-well plates, with 3-5 seedlings per well.

Elevated temperature treatments were carried out in Incubator Hood TH 30 (Edmund Bühler GmbH). Low temperature treatments were carried out in a cold room permanently maintained at 4 °C. Twelve-day-old seedlings on solid MS medium in sealed Petri dishes were incubated for 1, 3 or 6 h at 37 °C or 4 °C. Control plates were kept at 24 °C. There were approximately 50 seedlings per plate.

For selection and validation of RT-qPCR candidate reference genes, temperature treatments were carried out in Plant growth chamber RK-500 CH (Kambič) at 70 μ mol m⁻² s⁻¹ light intensity. Three hours after the beginning of light period, 12-day-old seedlings germinated and cultured on MS medium in sealed Petri dishes and 5-week-old plants in soil were incubated for 3 h at five different temperatures (22 °C, 27 °C, 32 °C, 37 °C and 42 °C).

3.2.8. Root and epidermal cell length measurements

Seeds were sterilized and germinated as described in section 3.2.2. To ensure equal distribution of nutrients among seedlings and uninterrupted root growth, approximately 15 seeds were plated individually in a straight line at the top of the plate. After 5 days, plates were scanned using the Epson Perfection V700 Photo scanner (Epson) and primary root length was measured using the Segmented Line Tool in ImageJ v.1.49 (Schneider et al., 2012). Two independent experiments were performed ($n = 40$). For root epidermal cell measurements, 5-day old seedlings were transferred to microscopic slides in a drop of water and covered with a coverslip. Images of the root hair initiation zone were acquired using Zeiss Axiovert 200 M microscopy system (20 \times objective) equipped with AxioCam MRc microscope camera and Zeiss binocular magnifier (STEMI 2000-C). Epidermal cell length was measured in AxioVision v4.5 (Zeiss). Two independent experiments were performed ($n_1 = 120$, $n_2 = 75$).

3.2.9. Protoplast isolation

Protoplasts were isolated from 14-day-old seedlings using the method described in Zhai et al. (2009). Seeds were sterilized and germinated as described in section 3.2.2. The following steps were performed at room temperature. Two grams of seedlings were sliced in 15 mL of TVL solution (0.3 M sorbitol, 50 mM CaCl_2) and the tissue was transferred to a 200 mL beaker along with 15 mL Enzyme Solution (0.5 M sucrose, 10 mM MES-KOH pH 5.7, 20 mM CaCl_2 , 40 mM KCl, 1% Cellulase Onozuka R10, 1% Maceroenzyme Onozuka R10). The tissue was mixed at 35 rpm in the dark for 16-18 h. The released protoplasts were collected into a 15 mL Falcon tube by sieving through sterile filters (Sysmex CellTrics, 100 μm pore size), pre-wet in W5 Solution (0.1% glucose, 2 mM MES-KOH pH 5.7, 1.84% CaCl_2 , 0.08% KCl, 0.9% NaCl). The filter was washed with 10 mL of W5 Solution and the protoplasts were carefully overlaid with another 10 mL of W5 Solution. The solution was centrifuged for 7 min at 100 \times g. Using a 10 mL pipette and a sterile tip, 10 mL of solution at the interface of Enzyme Solution and W5 Solution was collected and transferred to a new 50 mL Falcon tube. Protoplasts were washed twice in 15 mL W5 Solution, with two centrifugation steps for 5 min at 60 \times g. The supernatant was removed after the last centrifugation and protoplasts were left in approximately 500 μL of solution. Protoplasts were

pipetted onto positively charged silane-coated slides (BioGnost) and left to adhere for 1-2 h. Adhered protoplasts were fixed with 4% paraformaldehyde (Santa Cruz Biotechnology) for 10 min, washed with phosphate-buffered saline (137 mM NaCl, 2.7 mM KCl, 10 mM Na₂HPO₄, 1.8 mM KH₂PO₄) with 0.5% Triton (PBS-T) for 5 min to ensure membrane permeabilization. Protoplasts were washed again with PBS for 5 min and left to dry for 20 min. Slides with adhered protoplasts were stored at 4 °C until use.

3.2.10. Duolink *in situ* proximity ligation assay (PLA)

Duolink In Situ PLA detects both direct and indirect interactions *in situ* (Söderberg et al., 2006). In this test, two secondary antibodies labelled with complementary oligonucleotide probes (PLA probes) attach to corresponding primary antibodies which are bound to the assumed interactors. When PLA probes are in close proximity, they can hybridize and form a fluorescent signal through DNA amplification. Duolink *in situ* PLA was performed using components of the Duolink *in situ* Detection Reagents Red (Sigma-Aldrich, Merck). All volumes and incubation times were applied according to the Duolink *in situ* – Fluorescence User Guide (Sigma-Aldrich, Merck). First, protoplasts were blocked using Duolink PLA Blocking Solution and incubated in Duolink PLA Antibody Diluent containing custom-choice primary antibodies. The primary antibodies were mouse monoclonal anti-GFP (1:400, 11814460001, Roche) and rabbit polyclonal anti-ubiquitin antibody (1:2000, AB1690, Chemicon International). Protoplasts were incubated in primary antibody solution for 2 h at room temperature followed by overnight incubation at 4 °C, and washed in Washing Buffer A. This was followed by incubation with PLA probe PLUS (anti-rabbit) and PLA probe MINUS (anti-mouse) diluted 1:5 in Duolink PLA Antibody Diluent for 1 h, after which the protoplasts were incubated first in the Ligase solution and then in the Polymerase solution. After each step, protoplasts were washed twice in Washing buffer A. Finally, protoplasts were washed twice in Washing Buffer B and once in Washing Buffer B diluted 1:100 in deionized water. The slides were covered with a coverslip and mounted with a minimal volume of Duolink In Situ Mounting Medium with DAPI, and left in the dark for 20 min. PLA signals were detected by fluorescence microscopy (described in section 3.2.16). Three independent experiments were performed, with detection of at least 30 protoplasts emitting a PLA signal.

3.2.11. Plant tissue harvesting and homogenization

Plant tissues were harvested in 1.5 mL tubes containing 5-10 glass homogenization beads (SiLibeads Type S, Sigmund Linder). Approximately ten 12-day-old seedlings per sample were harvested for whole protein extraction and RNA isolation. For selection and validation of RT-qPCR reference genes, ten 12-day-old seedlings, three rosette leaves (approximately 2 cm long from base to apex) from three individual 5-week-old plants and flower buds from 6-12 individual 5-week-old plants were pooled to comprise the 'seedlings', 'leaves' and 'buds' samples, respectively. Each sample of 'seedlings', 'leaves' and 'buds' contained approximately 20, 80 and 20 mg of tissue, respectively. Plant samples were frozen along with glass beads in liquid nitrogen and stored at -80 °C. The tissues were homogenized by bead-induced rupture in a GC Silvermix 90 mixer (GC 900548) at 50 Hz for 8 sec, followed by immersion of the tube in liquid nitrogen and a second homogenization step in the mixer.

3.2.12. Whole protein extraction and Western blot analysis

Tissue harvesting and homogenization were performed as described in section 3.2.11. Each tissue sample was mixed with Extraction Buffer (50 mM Tris-HCl pH 6.8, 3% SDS, 10% glycerol, 0.1% bromophenol blue and 2.5 mM 1,4-dithioerythritol) and the tube was gently shaken until the material thawed. Samples were incubated at 95 °C for 5 min and centrifuged at 14000 × g for 15 min at 25 °C. During centrifugation, glass beads and tissue fragments were pelleted, and extracted proteins remained in the supernatant. Protein samples were mixed with the Sample Loading Buffer (125 mM Tris-HCl pH 6.8, 4% SDS, 32% glycerol, 10% β-mercaptoethanol, 0.01% bromphenol-blue) and loaded onto polyacrylamide mini gels comprised of a 12% resolving gel and a 4% stacking gel (components listed in **Table 1**). Proteins were separated by SDS-PAGE (sodium dodecyl sulfate-polyacrylamide gel electrophoresis) in a Laemmli Buffer (3 g/L Tris, 14.4 g/L glycine, 1 g/L SDS pH 8.3). Electrophoresis was performed in a MINI Vertical Dual Plate Electrophoresis Unit (Carl Roth) for 30 min at 90 V, followed by 1.5 h at 190 V (Consort EV243 Power Supply). To standardize protein concentrations, two SDS-PAGE runs were performed. An

equal volume of each sample was loaded onto the first gel, followed by SDS-PAGE, protein staining with 0.1% Coomassie Brilliant Blue R-250 in 10% methanol and 10% acetic acid, and destaining in 10% methanol and 10% acetic acid. The stained gel was scanned and color intensity of each lane was measured using ImageJ v.1.49 (Schneider et al., 2012). Based on the calculated difference in concentration, the volumes for the second gel were adjusted so that an equal amount of protein (approximately 20 µg) was loaded for every sample. This was followed by SDS-PAGE and transfer to membrane. Proteins were transferred onto a PVDF (polyvinylidene difluoride) membrane (Immobilon-P, Sigma-Aldrich) for 120 min at 200 mA in a Mini-PROTEAN 3 and Trans-Blot Cell (BioRad). The electroblotting unit was immersed in pre-chilled Transfer Buffer (20 mM Tris–HCl, 150 mM glycine, 10% methanol). Precision Plus Protein™ Dual Color Standard (BioRad) was used as a molecular ladder. The membrane was blocked with Western Blocker™ Solution for HRP detection systems (Sigma-Aldrich) for 1 h. The same solution was used for dilution of the primary (1:1000, anti-GFP, Roche) and secondary antibody (1:5000, anti-mouse HRP, Sigma-Aldrich). The membrane was incubated with primary antibody at 4 °C overnight without shaking, and with secondary antibody at room temperature for 2 h, with gentle agitation on orbital shaker at 50 rpm. After incubation with antibodies, the membrane was washed three times in PBS and signals were detected by chemiluminescence using Luminata Forte Western HRP substrate (Merck) followed by exposure to autoradiographic film (Hyperfilm, Amersham Pharmacia Biotech). The membrane was stained with 0.1% Coomassie R-250 in 40% methanol and 10% acetic acid, and destained in 40% methanol and 10% acetic acid.

Table 1. Components for a polyacrylamide mini gel comprised of a 12% resolving gel and a 4% stacking gel.

COMPONENT	RESOLVING GEL (12%)	STACKING GEL (4%)
reH ₂ O	1.675 mL	1.201 mL
0.5 M Tris-HCl pH 8.8	1.25 mL	-
0.5 M Tris-HCl pH 6.8	-	0.5 mL
30% acrilamide/bisacrilamide	2 mL	0.267 mL
10% SDS	50 µL	20 µL
10% ammonium persulfate	25 µL	10 µL
TEMED (N,N,N',N'- Tetramethylethylenediamine)	5 µL	5 µL

3.2.13. Total RNA extraction

Tissue harvesting and homogenization were performed as described in section 3.2.11. Total RNA was extracted using the MagMAX Plant RNA Isolation Kit (Applied Biosystems, Thermo Fisher Scientific) following the manufacturer's instructions. RNA purity and concentrations were determined using NanoDrop™ 1000 Spectrophotometer (Thermo Fisher Scientific). Two independent extractions (biological replicates) were prepared for every sample.

3.2.14. Quantitative reverse transcription PCR (RT-qPCR)

Reverse transcription (RT) was performed in a total volume of 20 µL using 200 units of RevertAid H Minus Reverse Transcriptase, 1× Reaction Buffer (Thermo Fisher Scientific), 20 units of RiboLock RNase inhibitor (Thermo Fisher Scientific), 0.5 mM dNTPs (Sigma-Aldrich), 5 µM Oligo(dT)₁₈ primer (Thermo Fisher Scientific) and 1 µg of total RNA. RT reaction mixture was incubated for 5 min at 65 °C, 45 min at 42 °C and 15 min at 70 °C. Prior to qPCR, cDNA samples were diluted five times. For all experiments, the PCR reaction mixture contained 1× GoTaq qPCR Master Mix reagent, 130 nM of forward and reverse primers and 2 µL cDNA sample in a total volume of 15 µL. All qPCR reactions were performed in two technical replicates. For the majority of experiments, qPCR reactions were performed in an optical 96-well plate using an Applied Biosystems™ 7500 Fast Real Time PCR system. SYBR Green was used to monitor dsDNA synthesis. The thermal profile was as follows: 50 °C for 20 s, 95 °C for 10 min followed by 40 cycles of 95 °C for 10 s and 58 °C for 40 s, except for *OGIO*, *PP2AA3* and *DWAI* genes where the annealing/extension step was carried out at 60 °C. The presence of a single amplicon was confirmed by agarose gel electrophoresis of PCR products (as described in section 3.2.4, but using a 2% agarose gel) and by the presence of a single peak in the melting curve obtained after amplification using the following parameters: 30 °C to 95 °C with ramp speed of 1 °C per minute. For each primer set, C_q values and primer efficiencies were calculated from raw amplification data in the exponential phase of each individual amplification plot using LinRegPCR software (Ramakers et al., 2003). For the *DREB2A* relative gene expression analysis used for validation of selected candidate reference genes, PCR reactions were performed in strip tubes using a MIC qPCR Cycler

(Bio Molecular Systems). The thermal profile was as follows: 95 °C for 5 min, 40 cycles of 95 °C for 10 s, and 60 °C for 10 s and the presence of a single amplicon was confirmed as described previously. For analysis of relative gene expression of *BPM2* splicing variants, PCR reactions were performed using a MIC qPCR Cycler (Bio Molecular Systems). The thermal profile was as follows: 50 °C for 20 s, 95 °C for 5 min, followed by 40 cycles of 95 °C for 5 s and 59 °C for 10 s. The presence of a single amplicon was confirmed by a single peak in the melting curve obtained after amplification using the following parameters: 40 °C to 95 °C with ramp speed of 0.5 °C per minute. In experiments where the MIC qPCR Cycler was used, C_q values and primer efficiencies were automatically calculated by the MIC qPCR Cycler software (Bio Molecular Systems). For all qPCR experiments, one independent experiment was performed.

3.2.15. qPCR data analysis

C_q values obtained for technical replicates were averaged prior to normalization and calibration. Gene expression was normalized to expression of a reference genes and relative expression profiles were generated using the $\Delta\Delta C_t$ method described by Vandesompele et al. (2002). Expression of *BPMs* in treated wild type samples was calibrated to expression of *BPMs* in untreated wild type control. Expression of *HsfA3* and *At4G36010* in temperature-treated wild type as well as untreated and temperature-treated transgenic line(s) was calibrated to expression of *HsfA3* and *At4G36010*, respectively, in untreated wild type control. Expression of *BPM2.3*, *BPM2.4* and *BPM2.5* in temperature-treated wild type samples was calibrated to expression of *BPM2.3*, *BPM2.4* and *BPM2.5*, respectively, in untreated wild type control. Expression of *BPM1-6* during daily rhythm was calibrated to expression of *BPM1-6*, respectively, at 12 p.m. (noon). For the *DREB2A* relative gene expression analysis used for validation of selected candidate reference genes, single and multiple candidate reference genes were used for data normalization. When multiple genes were used for normalization, geometric mean values were applied. Expression of *DREB2A* in samples corresponding to elevated temperature treatments was calibrated to expression of *DREB2A* in samples corresponding to 24 °C treatment. When multiple tissues were analyzed simultaneously, the calibrator sample was “seedlings at 24 °C”.

3.2.16. Fluorescence microscopy

For Duolink PLA analysis, Zeiss Axiovert 200 M fluorescence microscopy system was used, equipped with AxioCam MRc microscope camera and Zeiss binocular magnifier (STEMI 2000-C), using the 63× objective. Image acquisition was controlled by AxioVision imaging software v4.5 (Zeiss). Red PLA signals (TX Red) were detected using Zeiss filter set 31 (BP 565/30 nm excitation, BP 620/60 emission) and blue DAPI signals were detected using Zeiss filter set 49 (G365 nm excitation, BP 445/50 nm emission).

Confocal fluorescence microscopy images were acquired using a Leica TCS SP8X FLIM confocal microscopy system (Microsystems Wetzlar, Germany) with an Argon laser. Detection parameters for GFP were set to 488 nm excitation and 500-550 nm emission. Images were acquired via service of Ruđer Bošković Institute (Zagreb, Croatia), by Lucija Horvat. All images were processed in Inkscape 1.0 (<https://inkscape.org/>).

3.2.17. Statistical analysis

All statistical analyses were performed using a two-tailed Student's T-test. Root length and root epidermal cell length were analyzed between means of wild type and transgenic line. Germination rates and expression levels of endogenous *BPM* genes, *HsfA3*, *At4G36010* and *BPM2* splicing variants were analyzed between means of untreated and treated samples. *BPM* gene expression during daily rhythm was analyzed between means of 12 p.m. (control), and 5 p.m. or 6 a.m. Differences with a P value of < 0.05 were regarded as significant.

4. RESULTS

4.1. Phylogeny of Arabidopsis and wheat MATH-BTB proteins

4.1.1. Identification of TaMAB2 paralogs

An Ensembl Plants database search against the wheat proteome using the TaMAB2 sequence as query revealed 46 putative *MATH-BTB* genes in wheat (**Table 2**). Gene sequences retrieved in this search were analyzed for presence of splicing variants and the number of exons within the coding region, according to estimates available in the Ensembl Plants database at the time of analysis (July 11th 2017). The 44 novel sequences were annotated following the nomenclature previously proposed for *TaMAB1-2* (*Triticum aestivum* *MATH-BTB*; Leljak-Levanić et al., 2013). The *TaMAB3* clone found in the cDNA transcript library prepared by Leljak-Levanić et al. (2013) did not contain a complete open reading frame (ORF) and does not correspond to *TaMAB3* gene listed in **Table 2**. Genes were annotated by the order of their appearance on the retrieved TaMAB2 paralog list in the Ensembl Plants database. All putative TaMAB protein sequences were searched in the NCBI database using the Protein BLAST Tool to retrieve putative MATH and BTB domains. All TaMAB proteins were predicted to contain an N-terminal MATH domain and a C-terminal BTB domain. The only exception was TaMAB46, which was predicted to contain two MATH and two BTB domains. The majority of putative *TaMAB* genes encode a single splicing variant. Only four members, *TaMAB25*, *TaMAB36*, *TaMAB40* and *TaMAB41* contain two splicing variants. Plant MATH-BTB proteins cluster into two clades: core and expanded clade (Gingerich et al., 2007; Juranić & Dresselhaus, 2014). Four TaMAB proteins (TaMAB28, -33, -39 and -41) cluster into the core clade and contain four or five exons (**Table 2**). Forty-two TaMAB proteins, including TaMAB2, cluster into the expanded clade. One half of genes encoding expanded clade TaMAB proteins (21), including TaMAB2, contain a single exon, and the next largest subset is made of 12 genes containing two exons. The remaining expanded clade members contain three, four or, in one case, eight exons within the coding region (**Table 2**).

Table 2. Putative *MATH-BTB* genes of wheat. Forty-six genes were annotated following the nomenclature proposed for *TaMAB1-3* (*Triticum aestivum* *MATH-BTB*; Leljak-Levanić et al., 2013). Listed in the table are each gene's Locus ID or sequence identifier from the Ensembl Plants or NCBI database, the number of splicing variants, length of protein product (aa) and number of exons within the coding sequence as predicted in the Ensembl Plants database. For genes with two splicing variants, number of aa and exons of the variant which was not used for phylogenetic analysis is listed in parentheses. Highlighted in blue are *TaMAB* genes of the core clade. The databases were accessed and the sequences retrieved on July 11th, 2017.

GENE SYMBOL	SEQUENCE IDENTIFIER (LOCUS ID)	NUMBER OF SPLICING VARIANTS	LENGTH (aa)	NUMBER OF EXONS
<i>TaMAB1</i>	ACO56076.1	1	362	1
<i>TaMAB2</i>	TRIAE_CS42_2AL_TGACv1_092982_AA0268610	1	357	1
<i>TaMAB3</i>	TRIAE_CS42_2AL_TGACv1_096559_AA0319850	1	364	1
<i>TaMAB4</i>	TRIAE_CS42_5AL_TGACv1_377128_AA1244320	1	317	2
<i>TaMAB5</i>	TRIAE_CS42_5AL_TGACv1_377128_AA1244310	1	392	1
<i>TaMAB6</i>	TRIAE_CS42_2AL_TGACv1_093589_AA0283260	1	340	1
<i>TaMAB7</i>	TRIAE_CS42_2AL_TGACv1_097139_AA0323130	1	360	1
<i>TaMAB8</i>	TRIAE_CS42_2AL_TGACv1_094207_AA0294330	1	263	1
<i>TaMAB9</i>	TRIAE_CS42_2AL_TGACv1_095687_AA0313810	1	292	3
<i>TaMAB10</i>	TRIAE_CS42_2AL_TGACv1_095098_AA0306890	1	350	1
<i>TaMAB11</i>	TRIAE_CS42_5AS_TGACv1_393725_AA1275520	1	314	2
<i>TaMAB12</i>	TRIAE_CS42_2AL_TGACv1_094093_AA0292460	1	362	1
<i>TaMAB13</i>	TRIAE_CS42_4AL_TGACv1_289938_AA0979150	1	362	2
<i>TaMAB14</i>	TRIAE_CS42_5AL_TGACv1_374946_AA1212500	1	363	2
<i>TaMAB15</i>	TRIAE_CS42_4AL_TGACv1_288972_AA0962340	1	356	1
<i>TaMAB16</i>	TRIAE_CS42_1AS_TGACv1_019715_AA0070420	1	348	2
<i>TaMAB17</i>	TRIAE_CS42_2AL_TGACv1_094494_AA0298800	1	492	3
<i>TaMAB18</i>	TRIAE_CS42_5AS_TGACv1_393757_AA1275790	1	352	1
<i>TaMAB19</i>	TRIAE_CS42_7AS_TGACv1_570151_AA1831260	1	289	1
<i>TaMAB20</i>	TRIAE_CS42_2AL_TGACv1_093837_AA0287870	1	335	1
<i>TaMAB21</i>	TRIAE_CS42_2AL_TGACv1_096120_AA0317270	1	423	2
<i>TaMAB22</i>	TRIAE_CS42_2AL_TGACv1_095938_AA0315890	1	358	1
<i>TaMAB23</i>	TRIAE_CS42_7AL_TGACv1_559365_AA1799340	1	316	4

Table 2. – continued.

TaMAB24	TRIAE_CS42_2AL_TGACv1_094138_AA0293200	1	348	3
TaMAB25	TRIAE_CS42_6AL_TGACv1_471674_AA1512560. 2	2	(367) 372	(2) 2
TaMAB26	TRIAE_CS42_5AL_TGACv1_374651_AA1205580	1	359	2
TaMAB27	TRIAE_CS42_5AS_TGACv1_394663_AA1281400	1	390	1
TaMAB28	TRIAE_CS42_2AS_TGACv1_113137_AA0351730	1	268	4
TaMAB29	TRIAE_CS42_2AL_TGACv1_097570_AA0324530	1	368	1
TaMAB30	TRIAE_CS42_2AL_TGACv1_093970_AA0290420	1	358	1
TaMAB31	TRIAE_CS42_5AL_TGACv1_378253_AA1252240	1	351	2
TaMAB32	TRIAE_CS42_3AS_TGACv1_210508_AA0674190	1	362	2
TaMAB33	TRIAE_CS42_2AL_TGACv1_094379_AA0296760	1	396	5
TaMAB34	TRIAE_CS42_7AL_TGACv1_559746_AA1800670	1	363	1
TaMAB35	TRIAE_CS42_5AS_TGACv1_393725_AA1275530	1	404	1
TaMAB36	TRIAE_CS42_7AL_TGACv1_557344_AA1780000. 1	2	350 (350)	3 (2)
TaMAB37	TRIAE_CS42_2AL_TGACv1_093694_AA0285330	1	353	1
TaMAB38	TRIAE_CS42_3AL_TGACv1_193930_AA0622810	1	344	2
TaMAB39	TRIAE_CS42_2AS_TGACv1_112642_AA0342790	1	426	4
TaMAB40	TRIAE_CS42_7AS_TGACv1_571267_AA1846430. 1	2	355 (355)	3 (3)
TaMAB41	TRIAE_CS42_5AL_TGACv1_374210_AA1193750. 1	2	467 (437)	4 (5)
TaMAB42	TRIAE_CS42_7AL_TGACv1_559365_AA1799350	1	331	3
TaMAB43	TRIAE_CS42_2AL_TGACv1_094115_AA0292750	1	323	8
TaMAB44	TRIAE_CS42_2AL_TGACv1_094115_AA0292730	1	268	1
TaMAB45	TRIAE_CS42_7AL_TGACv1_560700_AA1802530	1	310	2
TaMAB46	TRIAE_CS42_2AL_TGACv1_095938_AA0315880	1	504	4

4.1.2. Phylogenetic tree of plant MATH-BTB proteins

To better understand the phylogeny of wheat MATH-BTB proteins, 46 TaMAB amino-acid sequences were aligned with six MATH-BTB sequences of *Arabidopsis* (AtBPM; Gingerich et al., 2005, 2007), 31 MATH-BTB sequences of maize (ZmMAB; Juranić et al., 2012) and 69 MATH-

BTB sequences of rice (*OsMBTB*; Gingerich et al., 2007), and their phylogeny was inferred using the maximum likelihood method (**Figure 1** and **Figure 2**).

Five *Arabidopsis*, nine maize and five rice genes encode more than one splicing variant. For those sequences, one splicing variant was used, as originally selected by Juranić & Dresselhaus (2014). Two types of phylogenetic trees were built, an unrooted tree portraying relationships between proteins of different species without assuming ancestry (**Figure 1**), and an arbitrarily rooted tree with a single lineage at the base (**Figure 2**). Protein annotations from different species were labelled with different colors for convenience. In the rooted tree, every branch node was labelled with an SH bootstrapping index representing a measure of support for the node, i.e. the probability that the sequences in the node cluster together and not with any others sequences. The value of 1.0 represents the highest level of support for a node (**Figure 2**).

The majority of MATH-BTB sequences, however, clustered into the grasses-specific expanded clade, predominantly in subclades E1, E3 and E4. Interestingly, subclade E2 does not contain any TaMAB proteins, and subclade E5 contains a single wheat protein, TaMAB1. TaMAB2 clustered into subclade E3 along with 13 other wheat (*TaMAB3-10*, 12, 17, 21, 22, and 46) and three rice proteins (*OsMBTB6-8*) but no maize proteins. Of the three rice proteins, *OsMBTB7* clustered together with TaMAB3 with the SH index of 1.0, indicating that the two proteins might be orthologs. Neither gene contains introns or is predicted to have splicing variants, and the two genes encode proteins of similar length, 366 and 364 aa, respectively. RNA-Seq expression values available in the TIGR Rice Genome Annotation Project show that *OsMBTB7* is ubiquitously expressed, with highest expression value in embryos (12.76), immature seeds (14.40), pistils (15.74) and post-emergence inflorescence (13.47). Expression in all other tissues is 2-3 times lower. RNA-Seq expression values of *OsMBTB6* and *OsMBTB8* are 0 in all tissues, indicating no or very low expression. Gametophyte-specific *ZmMAB1* of maize clustered into subclade E2, as shown previously (Juranić & Dresselhaus, 2014), along with four other maize (*ZmMAB2-6*) and four rice proteins (*OsMBTB 29, 30, 31, 32*).

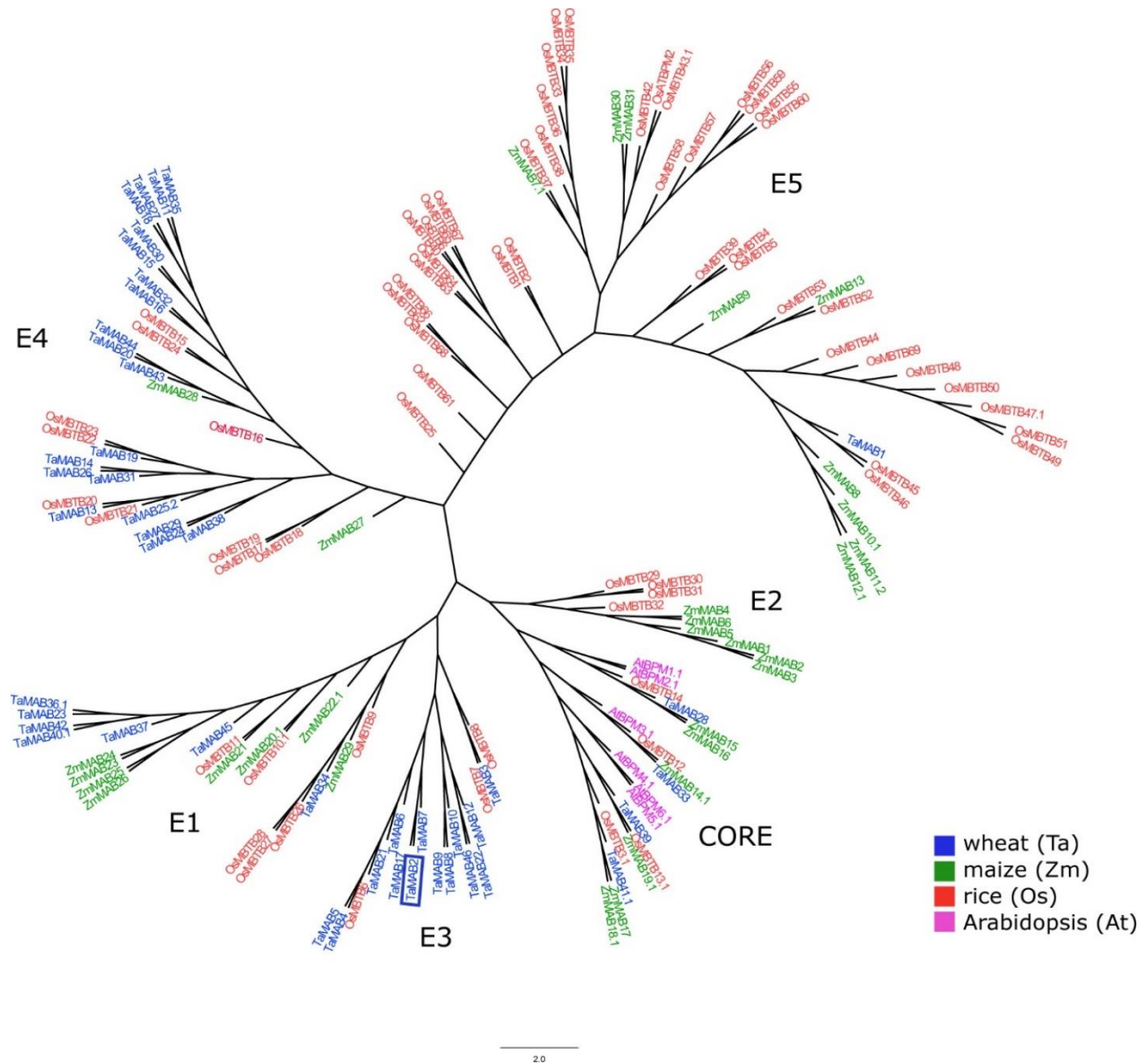


Figure 1. Unrooted phylogenetic tree of 152 MATH-BTB proteins from three monocotyledonous plants (*Triticum aestivum* (TaMAB), *Oryza sativa* (OsMBTB) and *Zea mays* (ZmMAB)), and a dicot *Arabidopsis thaliana* (AtBPM). Amino acid sequences of full-length MATH-BTB proteins were used to estimate maximum likelihood phylogeny. Proteins from each species are designated with a specific color. MATH-BTB proteins cluster into the core clade and five major subclades of the expanded clade (E1 to E5), which are specified correspondingly. In protein annotations, the number after the decimal point represents a splicing variant used for the analysis. TaMAB2 of subclade E3 is boxed in blue. For TaMAB sequence identifiers see **Table 2**. Rice, maize and *Arabidopsis* sequences were retrieved on July 11th, 2017. For statistical support of phylogenetic tree see **Figure 2**.

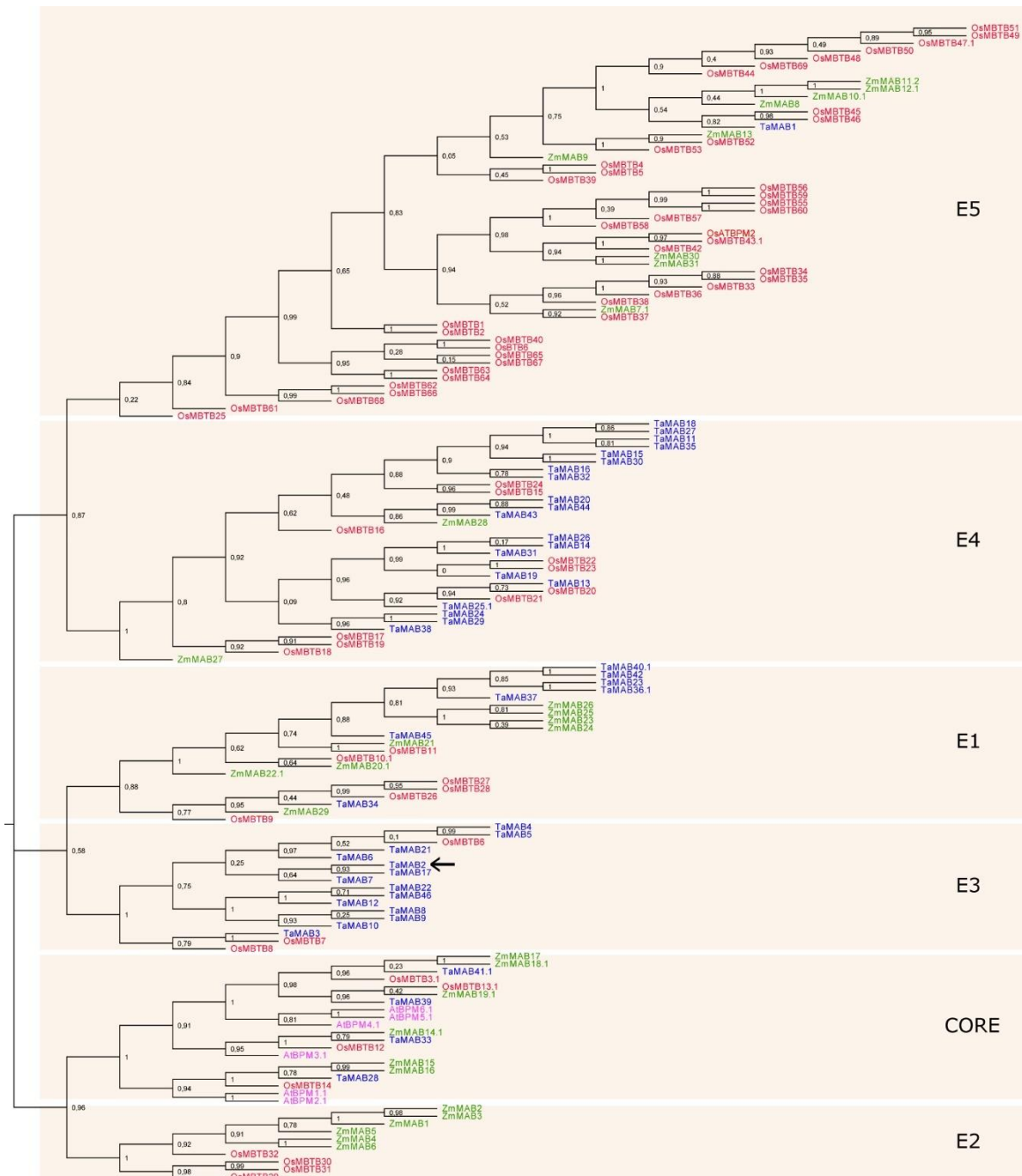


Figure 2. Phylogram of 152 MATH-BTB proteins from three monocotyledonous plants (*Triticum aestivum* (TaMAB), *Oryza sativa* (OsMTB) and *Zea mays* (ZmMAB)), and a dicot *Arabidopsis thaliana* (AtBPM). The tree is based on the same amino-acid sequence alignment used to build the tree shown in **Figure 1**. The number at each node represents the Shimodaira-Hasegawa index of branch support. Proteins from each species are designated with a specific color (see legend in **Figure 1**). MATH-BTB proteins cluster into the core clade and five major subclades of the expanded clade (E1 to E5), which are specified correspondingly. In protein annotations, the number after the decimal point represents a splicing variant used for the analysis. Arrow points to TaMAB2.

4.1.3. *Arabidopsis* BPM protein isoforms

The TAIR, Ensembl Plants and UniProt databases were searched for *BPM* gene and BPM protein annotations. According to data available in the Ensembl Plants database, the six known *BPM* genes of *Arabidopsis* encode 17 splicing variants: *BPM1* and *BPM6* each have three splicing variants, *BPM2* has five, *BPM3* has four and *BPM4* and *BPM5* each have one splicing variant (**Table 3**). These data correspond to data available in the TAIR database, with the exception of *BPM3*, which is reported to have only three splicing variants in the TAIR database. For this reason, Ensembl Plants database was considered as a more definitive source. The protein sequence of the BPM3.4 variant found only in Ensembl Plants database is identical to variant BPM3.3, but the two transcripts differ in predicted number of exons (Ensembl Plants database; **Table 3**). An additional protein isoform of BPM4 was found in the UniProt database, listed in **Table 3** as transcript *BPM4.2*, but without a specific transcript ID linking it to the Ensembl Plants or TAIR database. Because the full-length sequence could not be found using Ensembl Plants BLAST Tool, prediction of exon number was not available. Nevertheless, all 18 BPM protein isoforms were used for multiple sequence alignments of BPM proteins (section 4.1.4.).

Two *BPM* genes, *BPM1* and *BPM2*, were functionally analyzed in this work at the level of mRNA transcript abundance and/or protein stability and subcellular localization. Therefore, their splicing variants will be discussed in more detail. The *BPM1* gene encodes three splicing variants. The protein sequence of BPM1.1 is identical to protein variant BPM1.3, but the two transcripts differ in predicted number of exons (Ensembl Plants database; **Table 3**). The BPM1.2 variant differs from the other two variants by having a large segment of 35 amino acids within the BTB domain, while the rest of the sequence is identical in all three variants (see schematic diagram in **Appendix B1**). All three variants encode putative MATH, BTB and BACK domains (**Table 3**).

Table 3. Splicing variants of *Arabidopsis MATH-BTB (BPM)* genes. Listed in the table are each gene's and splicing variant symbol, gene or protein identifier (ID) from the Ensembl Plants or UniProt database, length of protein product as the number of amino acids (aa) and number of exons within the coding sequence as predicted in the Ensembl Plants database. Full-length protein sequences were searched using NCBI Protein BLAST and checked for presence of putative MATH, BTB and BACK domains in conserved domain databases. The databases were accessed and data retrieved on January 18th 2022.

GENE SYMBOL	SPLICING VARIANT SYMBOL	GENE/PROTEIN ID	LENGTH (aa)	NUMBER OF EXONS	PREDICTED DOMAINS
BPM1	<i>BPM1.1</i>	AT5G19000.1	407	4	MATH, BTB, BACK
	<i>BPM1.2</i>	AT5G19000.2	442	5	MATH, BTB, BACK
	<i>BPM1.3</i>	AT5G19000.3	407	5	MATH, BTB, BACK
BPM2	<i>BPM2.1</i>	AT3G06190.1	406	4	MATH, BTB, BACK
	<i>BPM2.2</i>	AT3G06190.2	295	4	MATH, BTB
	<i>BPM2.3</i>	AT3G06190.3	301	4	MATH, BTB
	<i>BPM2.4</i>	AT3G06190.4	298	5	MATH, BTB
	<i>BPM2.5</i>	AT3G06190.5	355	3	MATH, BTB, BACK
BPM3	<i>BPM3.1</i>	AT2G39760.1	408	4	MATH, BTB, BACK
	<i>BPM3.2</i>	AT2G39760.2	343	3	MATH, BTB, BACK
	<i>BPM3.3</i>	AT2G39760.3	344	5	MATH, BTB, BACK
	<i>BPM3.4</i>	AT2G39760.4	344	4	MATH, BTB, BACK
BPM4	<i>BPM4.1</i>	AT3G03740.1	465	4	MATH, BTB, BACK
	<i>BPM4.2</i>	A0A178V9U9	436	unknown	MATH, BTB, BACK
BPM5	<i>BPM5.1</i>	AT5G21010.1	410	4	MATH, BTB, BACK
BPM6	<i>BPM6.1</i>	AT3G43700.1	415	4	MATH, BTB, BACK
	<i>BPM6.2</i>	AT3G43700.2	363	3	MATH, BTB, BACK
	<i>BPM6.3</i>	AT3G43700.3	356	4	MATH, BTB, BACK

The *BPM2* gene encodes the largest number of splicing variants (five), which significantly differ in amino acid content, sequence length and domain content (**Table 3, Figure 3**). Alignment of cDNA sequences of *BPM2* splicing variants showed high similarity in UTR regions and 1st and 2nd exon between all five sequences, while significant differences exist in the 3rd and 4th exon (**Appendix B2**). According to sequences retrieved from the Ensembl Plants database, the *BPM2.1–2.5* splicing variants encode 406, 295, 301, 298 and 355 aa-long proteins, respectively. All splicing variants encode an identical MATH domain (134 aa) at the N-terminal end of the protein. However, only variants *BPM2.1* and *BPM2.5* contain a putative BTB domain (121 aa) and BACK domain (64 and 35 aa, respectively). Variants *BPM2.2*, *BPM2.3* and *BPM2.4* contain a truncated BTB

domain (59, 70 and 70 aa, respectively), recognized as part of a BTB domain in both the Pfam and CD database. In all three protein variants, the truncated BTB sequence is followed by a 49, 44 and 41 aa-long stretch, respectively, which is not recognized as part of either BTB or BACK domain in the Pfam or CD database. Overall, variants BPM2.3 and BPM2.4 share 95% sequence identity. To analyze whether the five BPM2 splicing variants would theoretically be able to bind CUL3, their BTB domain sequences were analyzed for presence of amino-acid residues presumed to mediate this interaction. The BTB domain sequences of *C. elegans* MEL-26 and *Schizosaccharomyces pombe* BTBP3, two MATH-BTB proteins acting as substrate adaptors of CUL3-based E3 ligases, were shown to contain eight specific residues important for interaction with CUL3 (Geyer et al., 2003; Xu et al., 2003). These eight residues were also found in the BPM1.1. sequence and are presumed to have the same function (Gingerich et al., 2007). Therefore, the BTB domain sequences of the five BPM2 variants were aligned with the BTB sequence of BPM1.1 (**Figure 4**). In the BPM1.1 sequence used for this alignment, the positions of the eight prominent residues were Asp-12, His-25, Ile-52, Ile-54, Asp-56, Asp-101, Tyr-103 and Leu-105. All eight residues were also found in the highly similar BPM1.2 variant (not shown here but visible in **Figure 5**). The alignment showed that all five BPM2 sequences contain the first four residues, albeit with two similar substitutions in the BPM2.2 sequence (Ile to Leu at position 52 and Ile to Val at position 54). At position 56, variant BPM2.2 underwent a non-similar substitution from negatively charged Asp to hydrophobic Ala, while all other BPM2 variants still contain the Asp residue. The remaining three residues are located at the very end of the BTB domain, at positions 101, 103 and 105. Of the two full-length BPM2 variants, both BPM2.1 and BPM2.5 contain the conserved residues. However, in variant BPM2.1, the Leu at position 105 was substituted for a similar amino acid residue, Phe. The truncated variants BPM2.2, BPM2.3 and BPM2.4 lack all three residues. To summarize, the BPM2.5 variant contains all eight fully conserved amino acid residues important for the interaction with CUL3, BPM2.1 contains seven, BPM2.3 and BPM2.4 contain five, and BPM2.2 only two.

```

BPM2.1 1 MDTIRVSKEVPGSSKSTAQSLTESTSRTETINGSHEFKISGYSLVKGMGIGKYVASDTFMVGGYSWAIFYFPDGKSPEDNSVYVSLFIALASEGADVRLFELTLVD 107
BPM2.2 1 MDTIRVSKEVPGSSKSTAQSLTESTSRTETINGSHEFKISGYSLVKGMGIGKYVASDTFMVGGYSWAIFYFPDGKSPEDNSVYVSLFIALASEGADVRLFELTLVD 107
BPM2.3 1 MDTIRVSKEVPGSSKSTAQSLTESTSRTETINGSHEFKISGYSLVKGMGIGKYVASDTFMVGGYSWAIFYFPDGKSPEDNSVYVSLFIALASEGADVRLFELTLVD 107
BPM2.4 1 MDTIRVSKEVPGSSKSTAQSLTESTSRTETINGSHEFKISGYSLVKGMGIGKYVASDTFMVGGYSWAIFYFPDGKSPEDNSVYVSLFIALASEGADVRLFELTLVD 107
BPM2.5 1 MDTIRVSKEVPGSSKSTAQSLTESTSRTETINGSHEFKISGYSLVKGMGIGKYVASDTFMVGGYSWAIFYFPDGKSPEDNSVYVSLFIALASEGADVRLFELTLVD 107

BPM2.1 108 QSGNERHKVHSHFGRTL ESGPYTLKYRGS MWG YKRFFKRS LLESSDYLKDNGLLVRCCVGVVKSRT EGPRCYNIPVPVSG LGQQFGK LLESGKGADVT FEVDGETFP 214
BPM2.2 108 QSGNERHKVHSHFGRTL ESGPYTLKYRGS MWG YKRFFKRS LLESSDYLKDNGLLVRCCVGVVKSRT EGPRCYNIPVPVSG LGQQFGK LLESGKGADVT FEVDGETFP 214
BPM2.3 108 QSGNERHKVHSHFGRTL ESGPYTLKYRGS MWG YKRFFKRS LLESSDYLKDNGLLVRCCVGVVKSRT EGPRCYNIPVPVSG LGQQFGK LLESGKGADVT FEVDGETFP 214
BPM2.4 108 QSGNERHKVHSHFGRTL ESGPYTLKYRGS MWG YKRFFKRS LLESSDYLKDNGLLVRCCVGVVKSRT EGPRCYNIPVPVSG LGQQFGK LLESGKGADVT FEVDGETFP 214
BPM2.5 108 QSGNERHKVHSHFGRTL ESGPYTLKYRGS MWG YKRFFKRS LLESSDYLKDNGLLVRCCVGVVKSRT EGPRCYNIPVPVSG LGQQFGK LLESGKGADVT FEVDGETFP 214

BPM2.1 215 AHKLVL AARS AVFRAQLFGPLRSENTNCII IEDVQAPIFKMLLHF IYWDEMPDMQDL IGTDLKWASTLVAQHLLAAADRYAFERLRTICESKLC EGISINTVATTLA 321
BPM2.2 215 AHKLVL AARS AVFRAQLFGPLRSENTNSLEVE ----- 244
BPM2.3 215 AHKLVL AARS AVFRAQLFGPLRSENTNCII IEDVQAPIFKDFLFTSV -----QSGTFSWGAAPVLKYYS P-GIRFNLS T--FLLDCMIVSISR MQ----- 301
BPM2.4 215 AHKLVL AARS AVFRAQLFGPLRSENTNCII IEDVQAPIFKDFLFTSV -----QSGTFSWGAAPVLKYYS P-GIRCCF IL-STGMKCLICKT ----- 298
BPM2.5 215 AHKLVL AARS AVFRAQLFGPLRSENTNCII IEDVQAPIFKMLLHF IYWDEMPDMQDL IGTDLKWASTLVAQHLLAAADRYALERLRTICESKLC EGISINTVATTLA 321

BPM2.1 322 LAEQHHCFQLKAACLKFIALPENL KAVMETDGF DYLKESCP SL LSELLEYVARLSEHSLTSSGHRKELFADGCDLNGRRVKQRLH 406
BPM2.2 245 -----AESCP SL LSELLEYVARLSEHSLTSSGHRKELFADGCDLNGRRVKQRLH 295
BPM2.3 -----
BPM2.4 -----
BPM2.5 322 LAEQHHCFQLKAACLKFIALPENLKGTE DHSLLV ----- 355

```

Figure 3. Putative MATH, BTB and BACK domains of protein isoforms encoded by *BPM2* splicing (BPM2.1-2.5). Full-length protein sequences were searched using NCBI Protein BLAST and putative MATH, BTB and BACK domains were extracted (highlighted in yellow, blue and pink, respectively). Broken lines represent areas where amino acids could not be aligned. Sequences were aligned in Clustal Omega v1.2.4 (Sievers et al., 2011) and displayed in Jalview v.2 (Waterhouse et al., 2009). Sequences were retrieved on January 18th, 2022.

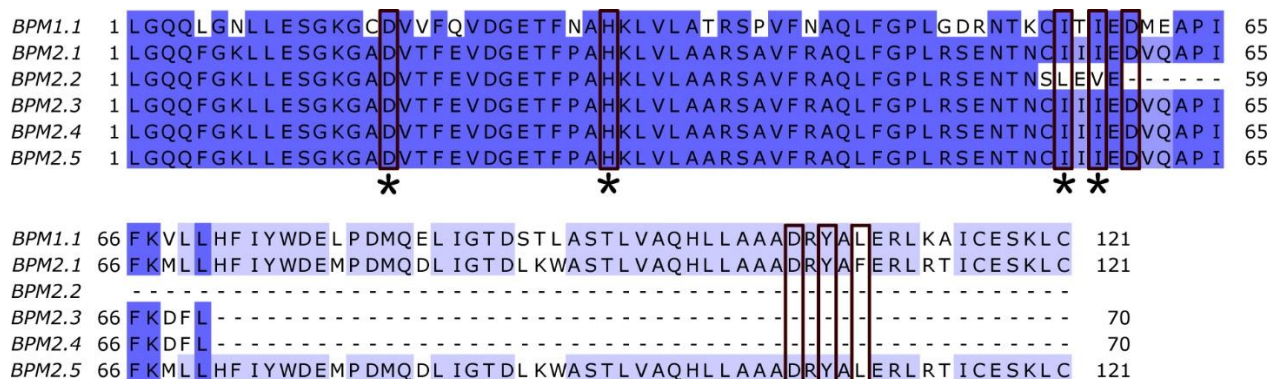


Figure 4. Multiple sequence alignments of BTB domains of *Arabidopsis* proteins BPM1.1 and BPM2.1-2.5. The five BPM2 sequences represent protein products of five known splicing variants encoded by the *BPM2* gene. In the protein name, the number after decimal point denotes the splicing variant. Identical and similar amino acids are shaded in blue, with darker shades indicating higher similarity. Black rectangles denote positions of amino acid residues important for interactions of MATH-BTB proteins *Caenorhabditis elegans* MEL-26 and *Schizosaccharomyces pombe* BTB3 with CUL3, and presumed to mediate CUL3 interactions of other MATH-BTB proteins (Geyer et al., 2003; Gingerich et al., 2005; Xu et al., 2003). The BPM1.1 sequence contains all eight conserved residues. Asterisks indicate amino acids conserved in all five BPM2 variants, either fully or with similar substitutions. Broken lines represent areas where amino acids could not be aligned. Sequences were aligned in ClustalX v.2.0 (Larkin et al., 2007) and displayed in Jalview v.2 (Waterhouse et al., 2009). Sequences were retrieved on January 18th, 2022.

To analyze whether expanded clade and core clade MATH-BTB proteins differ in their conservation status of the two respective domains, MATH and BTB, multiple sequence alignments of selected sequences were performed. To pool putative MATH and BTB domain sequences, the full-length protein sequence of each protein was searched in the NCBI database, and sequences with highest specificity (based on E value) in CD and Pfam databases were retrieved. Forty expanded clade TaMAB proteins were included in the analysis. According to the initial NCBI database search performed in July 2017, all TaMAB proteins contained a putative N-terminal MATH domain and a putative C-terminal BTB domain. Upon repeated NCBI Protein BLAST search performed in September 2021, a putative MATH domain was no longer reported for the TaMAB23 protein in any database. TaMAB23 was not omitted from the previously performed phylogenetic analysis, but it was omitted from the multiple sequence alignments of MATH and

BTB domain sequences. Additionally, TaMAB46 was omitted because it was predicted to contain two MATH and two BTB domains and there were no formal criteria for selection of either of the two copies. Calculation of sequence identity revealed that, on average, expanded clade MATH sequences of TaMAB proteins shared 35.94% identical amino acid residues (**Figure 5A**), while BTB sequences shared 56.32% identity (**Figure 5B**). In the expanded clade of wheat TaMAB proteins, the MATH domain is less conserved than the BTB domain.

To assess whether a different scenario occurs in the core clade, putative MATH and BTB sequences of all core clade proteins belonging to *Arabidopsis*, rice, maize and wheat, were aligned and their sequence identity was calculated. Here, the MATH sequences shared 75.22% identical amino acid residues (**Figure 6A**), while the BTB sequences shared 62.53% identity (**Figure 6B**), the opposite of what was found for expanded clade wheat proteins.

Finally, to assess the conservation status of the MATH and BTB domain of all known BPM protein isoforms, putative MATH and BTB domains were retrieved from the NCBI database and multiple sequence alignments were prepared (**Figure 7**). As expected for a family of exclusively core clade proteins, the MATH domain showed high identity (81.25%; **Figure 7A**), while the BTB domain showed high variability (48.13% identity; **Figure 7B**). Clearly, conservation of the MATH domain in the core clade is even more pronounced when only *Arabidopsis* MATH-BTB proteins are taken into consideration.

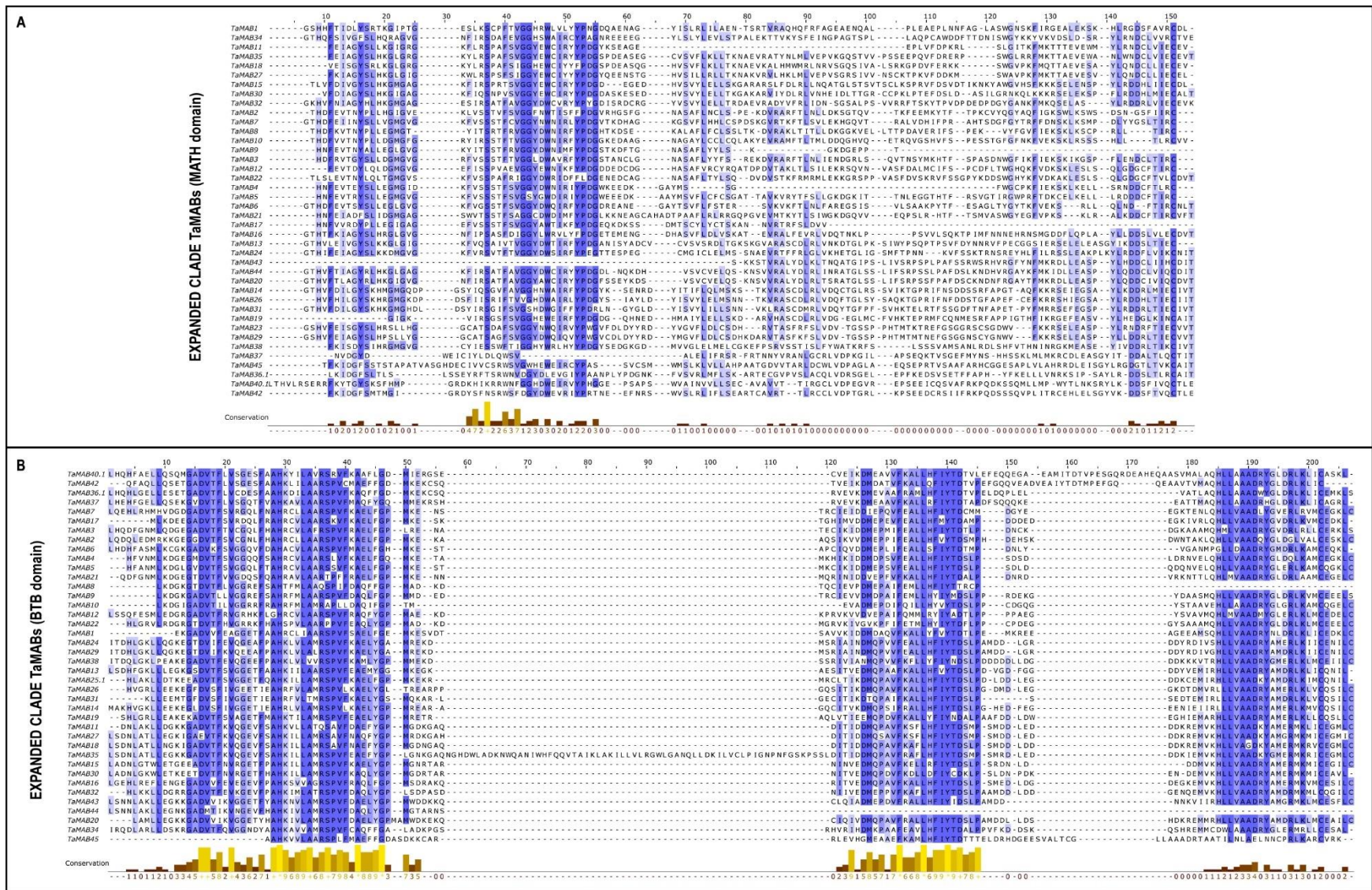


Figure 5. Multiple sequence alignments of (A) MATH and (B) BTB domains of expanded clade proteins of wheat (*Triticum aestivum*; TaMAB). Proteins were selected based on a phylogenetic analysis of MATH-BTB proteins from wheat, rice, maize and *Arabidopsis* (Figure 1 and 2).

Figure 5. – continued.

In the protein name, the number after decimal point denotes the splicing variant. Identical and similar amino acids are shaded in blue, with darker shades indicating higher similarity. Each amino acid is adjoined with its conservation status indicated by yellow bars at the bottom of the alignment and numbered 1 to 9, with higher numbers indicating more conserved amino acids. Asterisks denote 100% conserved amino acids. Broken lines represent areas where no amino acids could be aligned. Sequences were aligned in ClustalX v.2.0 (Larkin et al., 2007) and displayed in Jalview v.2 (Waterhouse et al., 2009). Sequences were retrieved on September 8th, 2021.

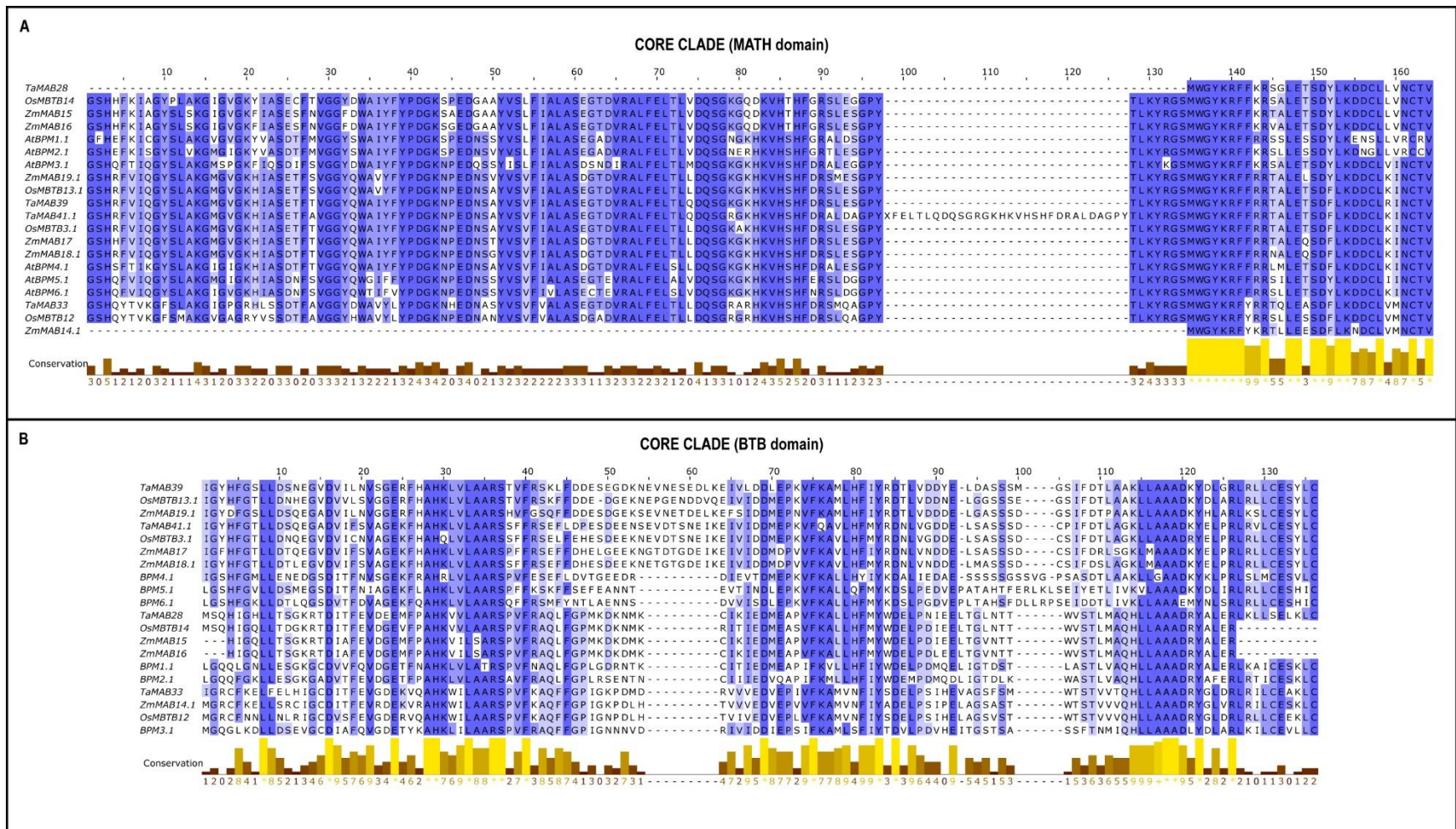


Figure 6. Multiple sequence alignments of (A) MATH and (B) BTB domains of 20 core clade proteins from *Triticum aestivum* (TaMAB), *Oryza sativa* (OsMBTB), *Zea mays* (ZmMAB) and *Arabidopsis thaliana* (AtBPM). Proteins were selected based on a phylogenetic analysis of all MATH-BTB proteins (Figure 1 and 2). All proteins were searched using NCBI Protein BLAST and putative MATH and BTB domains were retrieved. In the protein name, the number after LK denotes the splicing variant. Identical and similar amino acids are shaded in blue, with darker shades indicating higher similarity.

Figure 6. – continued.

Each amino acid is adjoined with its conservation status indicated by yellow bars at the bottom of the alignment and numbered 1 to 9, with higher numbers indicating more conserved amino acids. Asterisks denote 100% conserved amino acids. Broken lines represent areas where no amino acids could be aligned. Sequences were aligned in ClustalX v.2.0 (Larkin et al., 2007) and displayed in Jalview v.2 (Waterhouse et al., 2009). Sequences were retrieved on September 8th, 2021.

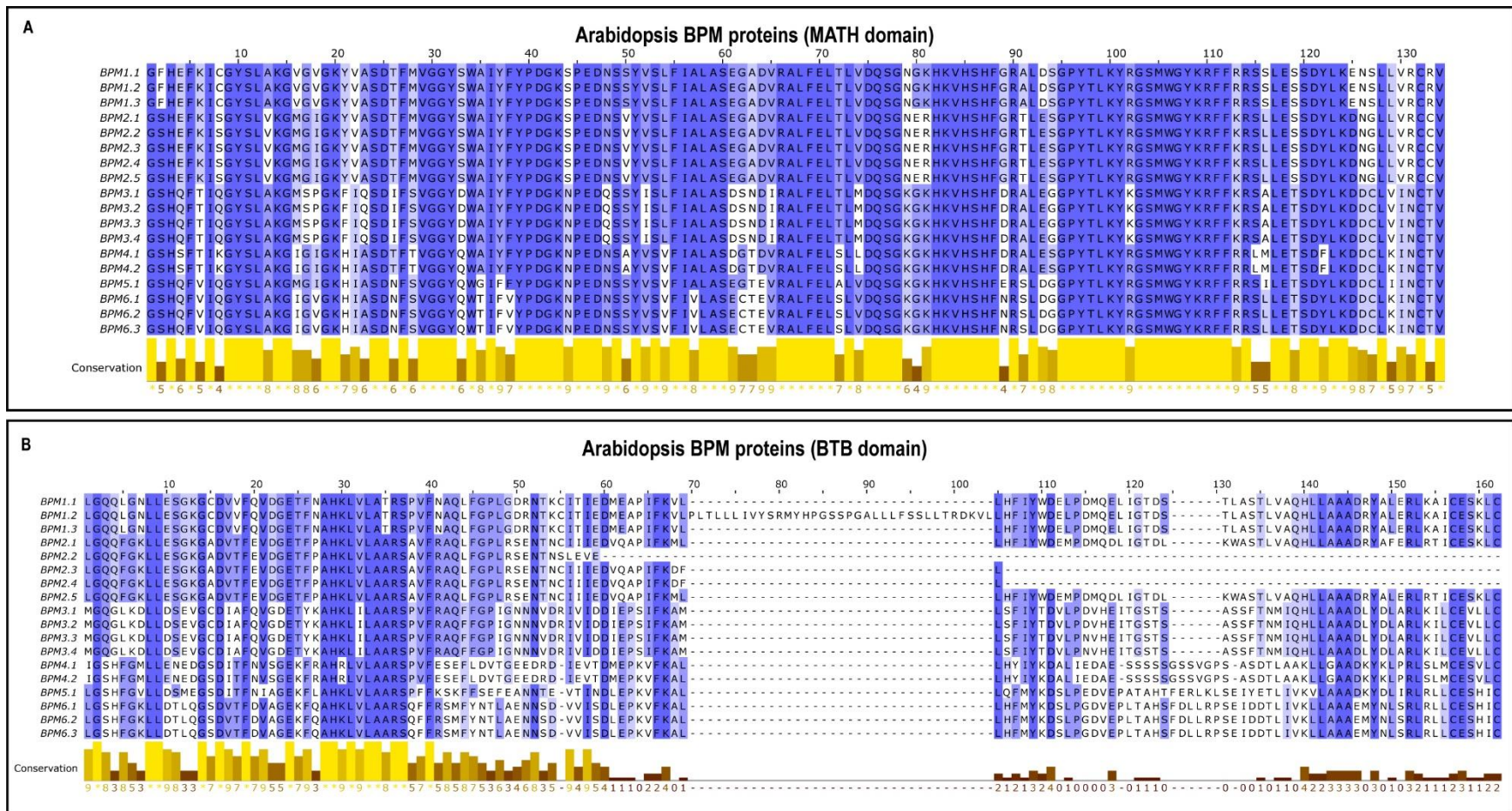


Figure 7. Multiple sequence alignments of (A) MATH and (B) BTB domains of 18 *Arabidopsis* MATH-BTB protein isoforms (BPM). All proteins were searched using NCBI Protein BLAST and putative MATH and BTB domains were retrieved. In the protein name, the number after decimal point denotes the splicing variant. Identical and similar amino acids are shaded in blue, with darker shades indicating higher similarity. Each amino acid is adjoined with its conservation status indicated by yellow bars at the bottom of the alignment and numbered 1 to 9, with higher numbers indicating more conserved amino acids. Asterisks denote 100% conserved amino acids. Broken lines represent areas where no amino acids could be aligned. Sequences were aligned in ClustalX v.2.0 (Larkin et al., 2007) and displayed in Jalview v.2 (Waterhouse et al., 2009). Sequences were retrieved on January 18th, 2022.

4.2. Functional analysis of wheat TaMAB2

4.2.1. Overexpression of TaMAB2 affects epidermal cell length

To elucidate possible roles of TaMAB2, a previously established transgenic *Arabidopsis* line overexpressing GFP-tagged TaMAB2 under control of the constitutive CaMV 35S promoter (Bauer et al., 2019) was used. To study whether constitutive overexpression of TaMAB2 affects longitudinal growth of *Arabidopsis* roots, 5-day-old seedlings were grown on MS medium in short-day conditions and subsequently analyzed. TaMAB2 overexpression did not cause a statistically significant change in primary root length (**Figure 8A**). However, root epidermal cells exhibited a significant change in longitudinal length, with average cell length of 230 μm in the transgenic line, compared to 200 μm in wild type (**Figure 8B**).

4.2.2. TaMAB2 colocalization and protein interaction analysis

To test whether TaMAB2 co-localizes with ubiquitin, a proximity ligation assay (PLA) was performed in *Arabidopsis* seedlings overexpressing GFP-tagged TaMAB2 (Bauer et al., 2019). To assess whether TaMAB2 associates with ubiquitin, protoplasts of 2-week-old seedlings overexpressing GFP-tagged TaMAB2 were incubated with anti-GFP and anti-ubiquitin primary antibodies. TaMAB2-GFP co-localized with ubiquitin in foci around the nucleus and possibly in the nucleus as well (**Figure 9A**), indicating that TaMAB2, like its maize and *Arabidopsis* orthologs, could be part of a CUL3-based E3 ubiquitin ligase complex.

To identify possible substrates of TaMAB2 as part of a putative CUL3-based E3 ligase complex, results of a tandem affinity purification (TAP) combined with mass spectrometry (MS) were used as a pool of proteins for which an interaction with TaMAB2 could be analyzed *in vivo*. The experiment was based on 7-day-old suspension cultures and 12-day-old *Arabidopsis* seedlings overexpressing TAP-tagged TaMAB2 (Bauer et al. 2019). Among others, subunit A of the translation initiation factor 4 (eIF4A1) and subunit G of the translation initiation factor 3 (eIF3G1) appeared as putative TaMAB2 interactors.

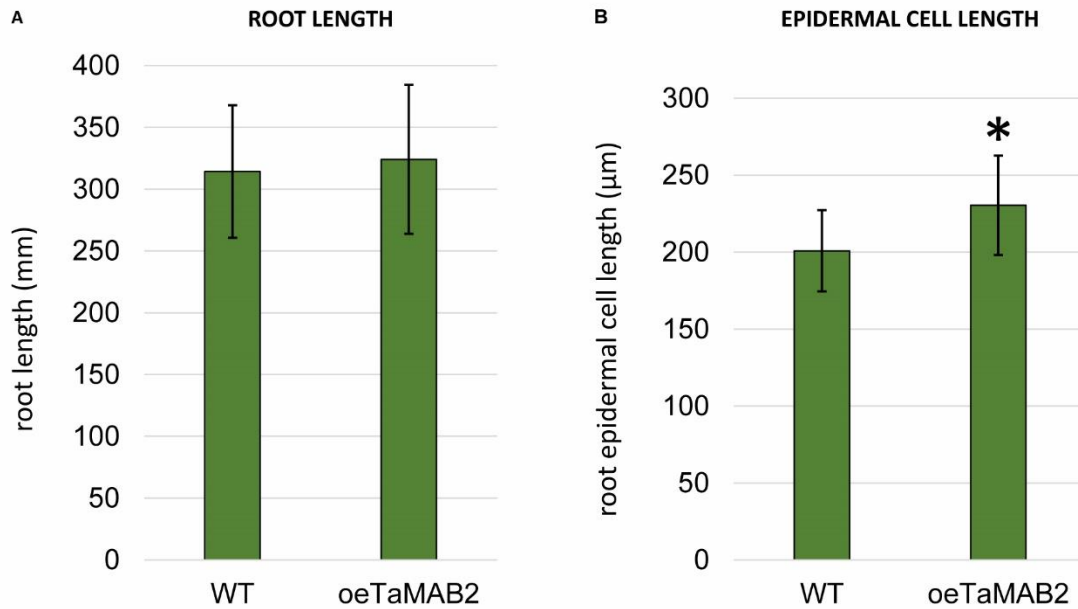


Figure 8. Root and root epidermal cell length in *Arabidopsis* seedlings overexpressing TaMAB2 (oeTaMAB2). **(A)** No difference in primary root length was observed between oeTaMAB2 and wild type (WT). **(B)** Epidermal cells in the root hair initiation zone are longer in oeTaMAB2 line compared to wild type. Both analyses were performed on five-day-old seedlings of wild type and oeTaMAB2 grown on MS medium in short day conditions. Results of one independent experiment are shown (for root length: n = 40, for cell length: n = 120), but similar trends were observed in a second independent experiment (for root length: n = 40, for cell length: n = 75). Bars show mean values ± SD. Asterisk denotes statistical significance between means of wild type and oeTaMAB2 (Student's T test, P < 0.05).

To investigate whether TaMAB2 is capable to directly interact with *Arabidopsis* eIF4A1, eIF3G1 and cytoskeleton-related protein Katanin from wheat (TaKAT), a Y2H assay was performed. Neither eIF4A1 nor eIF3G1 showed a direct interaction with TaMAB2 (**Figure 9B**). A positive result was obtained in the His prototrophy assay for interaction with TaKAT. However, TaKAT also interacted with empty vector control, indicating a false positive reaction (**Figure 9B**).

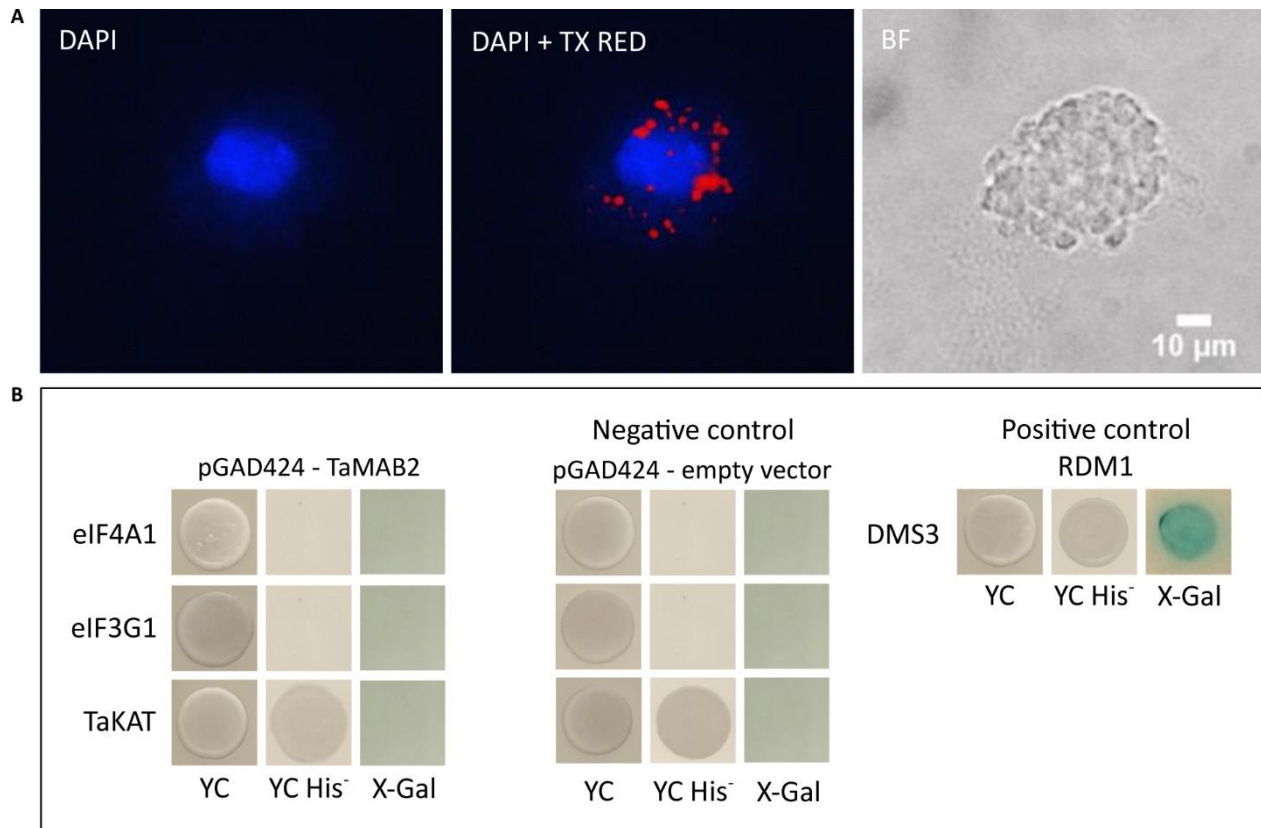


Figure 9. TaMAB2 colocalizes with ubiquitin but does not interact with putative targets in Y2H (A) TaMAB2-GFP and ubiquitin co-localize in cytoplasmic complexes in transgenic *Arabidopsis* protoplasts overexpressing TaMAB2. Duolink In Situ PLA was performed using primary antibodies against ubiquitin and GFP. When the antibodies are in close proximity, a Texas (TX) Red fluorescent signal is emitted through amplification of oligonucleotide probes attached to secondary antibodies. Protoplast nuclei were stained with DAPI and visualized under UV light (left) and merged with TX red signals (middle). Protoplast is shown in bright field (BF; right). Scale bar = 10 μ m. PLA signals were observed in three independent experiments. (B) Y2H protein interaction assay of TaMAB2 with *Arabidopsis* eukaryotic translation initiation factors 4 (subunit A; eIF4A1) and 3 (subunit G; eIF3G1), and wheat Katanin (TaKAT). Co-transformants were selected on solid dropout medium lacking Leu and Trp (YC) and protein-protein interaction was detected on dropout medium lacking Leu, Trp and His (YC His⁻). β -galactosidase assay was performed using X-Gal as substrate. RDM1-DMS3 interaction served as a positive control. TaMAB2 and RDM1 in the pGAD424 backbone (bait) were co-transformed with interaction partners in the pGBT9 backbone (prey). For negative controls, prey constructs were co-transformed with empty pGAD424 vector. TaMAB2 does not interact with eIF4A1 or eIF3G1. Interaction with TaKAT is a false positive. Three individual colonies of each co-transformant were analyzed.

4.3. Functional analysis of *Arabidopsis* BPM1

4.3.1 ABA and osmotic stress affect BPM1 protein turnover

To examine the role of BPM1 in stress response, wild type and BPM1-overexpressing lines were subjected to ABA, NaCl or mannitol treatment, which was followed by gene expression analysis of endogenous *BPM* genes in wild type, as well as analysis of germination rates, and BPM1-GFP protein stability and intracellular localization in overexpression lines. Preliminary experiments revealed the effective concentration range of ABA, NaCl and mannitol (unpublished results, courtesy of Nataša Bauer) and these concentrations were used for downstream assays.

To test whether ABA, mannitol or NaCl treatment affect the expression of endogenous *BPM* genes, a relative gene expression analysis was performed using RT-qPCR. Expression of the majority of endogenous *BPM* genes was unaffected by ABA, mannitol or NaCl treatment, the only exceptions being *BPM5* with slightly decreased expression after mannitol treatment, and *BPM6* with slightly increased expression after NaCl treatment (**Figure 10A**).

The results of Western blotting showed that 6 h exposure to mannitol and ABA treatment had no observable effect on BPM1 protein levels (**Figure 10B**). Conversely, exposure to NaCl correlated with a decrease in BPM1 protein levels (**Figure 10B**).

ABA and mannitol treatment caused changes in transgenic BPM1 subcellular localization in *Arabidopsis* roots. When seedlings were untreated, BPM1 predominantly localized in root cell nuclei, with a weaker fluorescent signal present along the root stele (**Figure 10C**). Treatment with ABA and mannitol caused a more prominent accumulation of BPM1 inside root cell nuclei, while NaCl treatment caused a more dispersed protein presence along the root stele (**Figure 10C**).

Here, ABA, mannitol and NaCl treatments were used to assess the germination rates of plants overexpressing BPM1. Seeds of wild type and BPM1-overexpressing lines (L003 and L104) were plated on MS-MES medium supplemented with different concentrations of NaCl (25, 50 and 100 mM), mannitol (100, 200 and 300 mM) or ABA (0.5 and 1 μ M). Seed germination rates were calculated based on observation of radicle protrusion. Generally, seeds of BPM1 overexpressors showed a slight delay in radicle protrusion compared to wild type but this discrepancy was no longer observable 48 h after imbibition (**Appendix B3**). Therefore, the 48-h time point was chosen for assessment of radicle protrusion. Similar to results of protein stability assays, a trend could be observed in BPM1 overexpressors' response to ABA and osmotic stress as opposed to salt stress

(**Figure 10D**). Germination rates were higher in seeds of BPM1 overexpressors than in wild type after exposure to ABA and mannitol. For instance, only 23% wild type seeds germinated when treated with 1 μ M ABA, while this number reached 39-58% for BPM1-overexpressing lines (**Figure 10D**). Therefore, transgenic protein stabilization and stable germination rates after ABA and mannitol treatment indicate that overexpression of BPM1 leads to increased resistance of transgenic plants to ABA and osmotic stress, implying a possible role of BPM1 in drought response. Conversely, no difference in germination was observed between wild type and transgenic lines after NaCl treatment (**Figure 10D**).

4.3.2. Temperature affects expression of *BPM* genes and BPM1 protein turnover

To test whether exposure to elevated temperature will induce the expression of all six endogenous *BPMs*, wild type plants were exposed to 3 h of incubation at 37 °C, followed by RNA extraction and RT-qPCR analysis (**Figure 11A**). Exposure to elevated temperature significantly induced the expression of endogenous *BPM1*, *BPM2* and *BPM3*, with the strongest increase measured for *BPM2*. Expression of *BPM4* was slightly decreased, while expression of *BPM5* and *BPM6* remained unchanged (**Figure 11A**). These results additionally indicate involvement of BPM proteins in heat stress response, and they also show that BPM1-3 might take on different, arguably more dominant roles than BPM4-6 in conditions of elevated temperature.

Protein stability of BPM1 was analyzed after exposure of 12-day-old seedlings to 37 °C using Western blotting and confocal fluorescence microscopy. Accumulation of BPM1-GFP was confirmed by fluorescence microscopy of transgenic seedlings' roots, where BPM1-GFP highly accumulated in root cell nuclei after 6 h of incubation at 37 °C (**Figure 11B**). Additionally, after 1 and 3 h of exposure to elevated temperature, overall BPM1-GFP protein levels increased compared to control (**Figure 11C**).

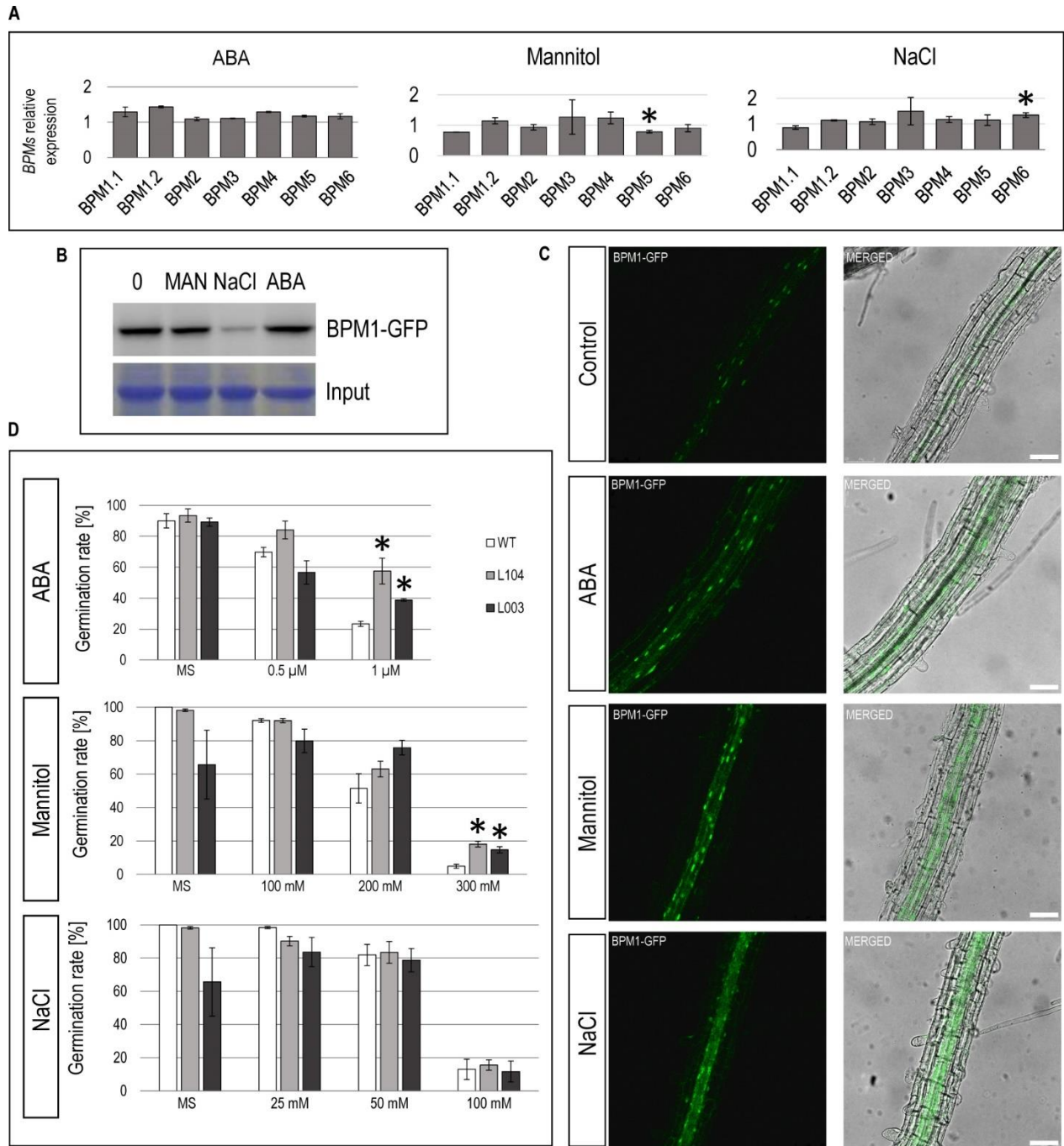


Figure 10. BPM1-GFP protein stability and germination rate of BPM1 overexpressors increase under ABA and osmotic stress. (A) Wild type seedlings were exposed for 3 h to either 50 μ M ABA, 300 mM mannitol, 150 mM NaCl or mock solution and sampled for *BPM* gene expression analysis using RT-qPCR. Expression of *BPM* genes was normalized to expression of *RHIP1*. For all treatments, expression of each individual *BPM* gene was calibrated to expression of that gene in untreated control. Endogenous *BPM5* expression decreased after treatment with mannitol (middle) and *BPM6* expression increased after treatment with NaCl (right). Other endogenous *BPM* genes did not significantly change in response to ABA (left), mannitol or NaCl treatment.

Figure 10. - continued.

Expression values are shown as mean fold change \pm SD of two biological replicates. Asterisks indicate statistical significance (Student's T test, $P < 0.05$). **(B)** Twelve-day old seedlings were exposed for 6 h to either 50 μ M ABA, 150 mM NaCl, 300 mM mannitol (MAN) or mock solution. Whole protein extracts were immunoblotted with anti-GFP antibody (top panel). For loading control, proteins were stained with Coomassie on PVDF membranes (bottom panel). BPM1 protein levels dropped after exposure to NaCl-induced salt stress but remained stable after ABA treatment and mannitol-induced osmotic stress. Similar results were obtained in at least three independent experiments. **(C)** Twelve-day old seedlings of BPM1 overexpression lines (L104 and L003) were exposed for 6 h to 50 μ M ABA, 150 mM NaCl, 300 mM mannitol or mock solution and at least three seedlings immediately analyzed by confocal microscopy. BPM1-GFP accumulated in root cell nuclei after exposure to ABA and osmotic stress but diminished and translocated to root vasculature after exposure to salt stress. Fluorescent and merged (bright field and BPM1-GFP signal) images of L104 are shown. Scale bar = 50 μ m. Similar results were obtained in at least three independent experiments. **(D)** Seeds of wild type (WT) and BPM1 overexpressors (L104 and L003) were germinated on MS medium supplemented with varying concentrations of ABA, mannitol or NaCl (denoted on the graphs) and germination rates were examined after 48 h. BPM1 overexpressors germinated better under ABA and mannitol-induced osmotic stress compared to wild type. BPM1 overexpressors and wild type are equally susceptible to NaCl-induced salt stress. Three independent experiments were performed ($n > 100$). Asterisks indicate statistical significance (Student's T test, $P < 0.05$).

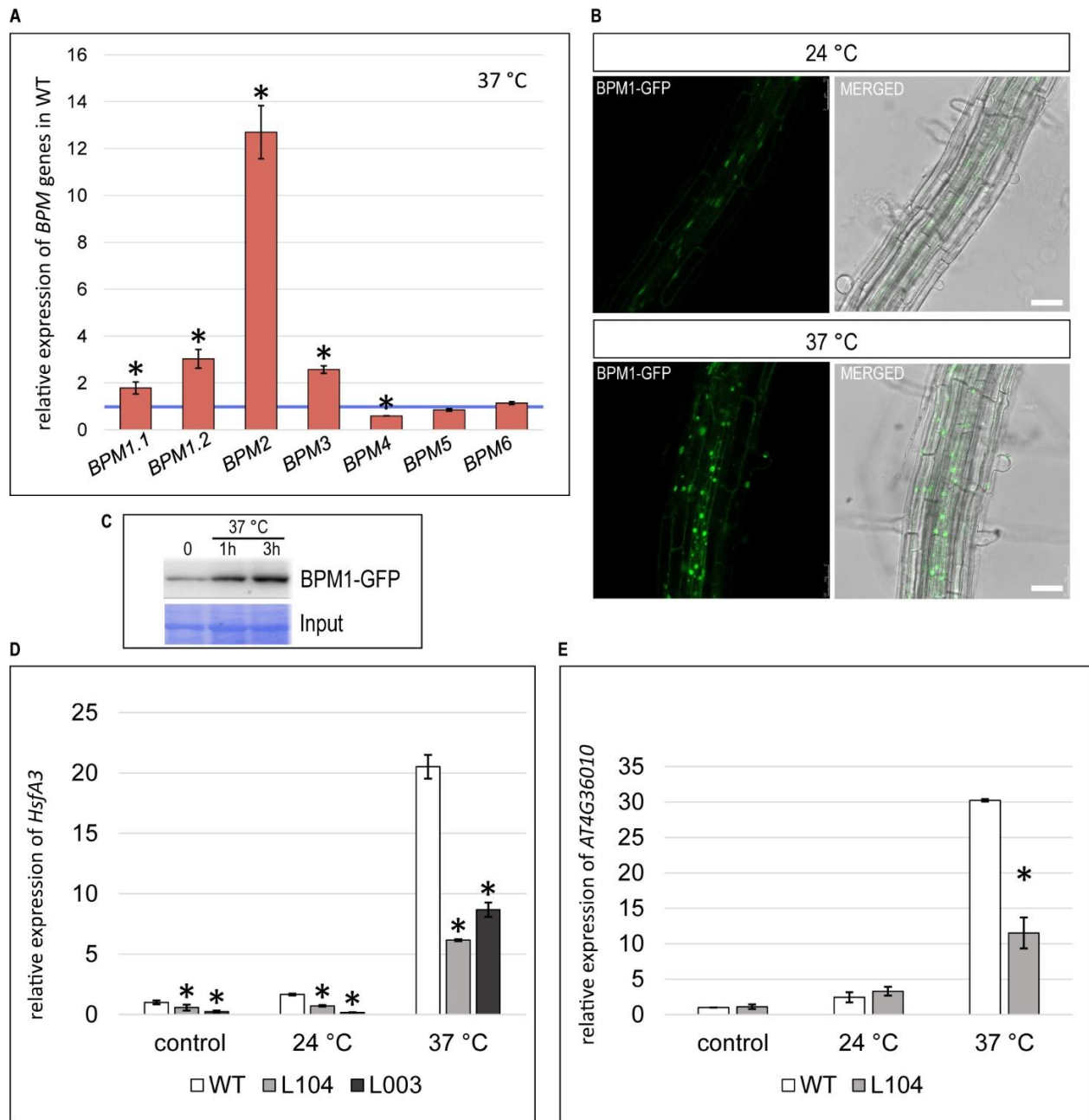


Figure 11. Endogenous *BPM* gene expression and BPM1-GFP protein levels increase at elevated temperatures. **(A)** Wild type seedlings were incubated for 3 h at 24 °C (control) or 37 °C and sampled for gene expression analysis using RT-qPCR. Expression levels of endogenous *BPM1*, *BPM2* and *BPM3* significantly increased after heat treatment, with the highest increase measured for *BPM2*. Expression of *BPM4* decreased. The blue line indicates expression in untreated control (calibrated to 1). **(B)** Twelve-day-old seedlings of *BPM1* overexpression lines (L104 and L003) were incubated for 6 h at 24 °C (control) and 37 °C in the dark and at least three seedlings were immediately analyzed by confocal microscopy. BPM1-GFP protein accumulated in root cell nuclei after exposure to 37 °C.

Figure 11. – continued.

Similar results were obtained in at least three independent experiments. Fluorescent and merged (bright field and BPM1-GFP signal) images of L104 are shown. Scale bar = 50 μ m. (C) Six-day-old seedlings were sampled before treatment (0) and 1 and 3 h after incubation at 37 °C in the dark. Whole protein extracts were immunoblotted with anti-GFP monoclonal antibody (top panel). BPM1-GFP accumulated after exposure to 37 °C. For loading control, proteins were stained with Coomassie on PVDF membranes (bottom panel). Similar results were obtained in at least three independent experiments. (D-E) Expression profiles of DREB2A downstream targets *HsfA3* (in D) and *AT4G36010* (in E) in BPM1-overexpression lines. Seedlings of wild type and BPM1-overexpressors (L104 and/or L003) were sampled for gene expression analysis prior to treatment (control), after 3 h at 24 °C or after 3 h at 37 °C. The increase in expression of *HsfA3* and *AT4G36010* in response to heat treatment was lower in BPM1 overexpression lines compared to wild type. In A, D, E, expression levels of *BPM* genes, *HsfA3* and *AT4G36010* were normalized to expression of *RHIP1* and calibrated to expression of tested gene in untreated wild type control. Expression values are shown as mean fold change \pm SD of two biological replicates. Asterisks indicate statistically significant differences between means of control and treated sample in A, or between means of wild type and BPM1-overexpression lines for each sample type (control, 24 °C and 37 °C) in D and E (Student's T test, $P < 0.05$).

To indirectly test whether overexpression of BPM1 will cause a comparable change in DREB2A levels, a gene expression analysis of a DREB2A downstream target, *HsfA3*, was performed. Seedlings of wild type and BPM1 overexpression lines (L104 and L003) were incubated at 37 °C for 3 h and *HsfA3* expression levels were estimated relative to wild type levels prior to heat treatment. As expected, in wild type plants *HsfA3* levels significantly increased (20-fold) after heat exposure (Figure 11D). The *HsfA3* levels also increased in BPM1 overexpression lines after heat treatment but this increase was significantly lower compared to wild type (only sixfold in L104 and eightfold in L003). Additionally, even when no heat treatment was applied (24 °C), *HsfA3* expression in BPM1 overexpressing lines was downregulated compared to wild type plants (Figure 11D). To additionally confirm the reduction of DREB2A activity in BPM1 overexpressors, expression of another downstream target of DREB2A (*AT4G36010*) was tested in line L104 in control and heat stress conditions. This gene encodes a pathogenesis-related thaumatin family protein and was shown to be upregulated in wild type after heat stress as well as in the amiBPM line (Morimoto et al., 2017; Sakuma et al., 2006b). A similar trend was obtained for *AT4G36010*, namely, the 30-fold increase in expression measured in wild type was reduced to an 11-fold increase in the BPM1 overexpressor (Figure 11E).

The BPM2 protein was highlighted by Morimoto et al. (2017) as a DREB2A interactor after exposure to heat stress. Interestingly, here the *BPM2* gene exhibited the most substantial (12-fold)

increase in gene expression after exposure to elevated temperature (**Figure 11A**). For this reason, *BPM2* was selected for analysis of splicing variant expression analysis. Once the *BPM2* gene is transcribed, the primary transcript can be processed into five different splicing variants, *BPM2.1* – *BPM2.5* (**Table 3**). To analyze possible differences in transcript abundance of individual *BPM2* splicing variants after exposure to heat, an RT-qPCR analysis was performed. Due to technical constraints, specific expression of splicing variants *BPM2.1* and *BPM2.2* could not be analyzed. For *BPM2.1*, a primer pair could not be designed due to sequence similarity with other splicing variants, and for *BPM2.2*, a single primer pair was designed but, a PCR product could not be obtained in these experimental conditions. The remaining three variants, however, showed distinct transcript abundance profiles after a 3 h exposure of 12-day-old wild type seedlings to 37 °C (**Figure 12A**). While *BPM2.3* and *BPM2.5* transcripts were highly abundant (5.2 and 13.5 fold change, respectively) compared to control, the abundance of *BPM2.4* transcript was significantly downregulated (0.27 fold change) (**Figure 12A**). These results indicate that individual splicing variants contributed differently to the overall 12-fold increase in *BPM2* expression, which was measured using a primer pair binding all five splicing variants (**Figure 11A**). Therefore, conditions of elevated temperature not only induce *BPM2* gene expression but influence differential splicing of the *BPM2* transcript. A slight difference in expression was also measured for *BPM1.1* (1.78 fold change) and *BPM1.2* (3.03 fold change) splicing variants (**Figure 11A**). However, the primers used for the *BPM1.1* variant also recognized the *BPM1.3* variant, therefore, the result is not specific for *BPM1.1*.

Transcript abundance of *BPM1* and *BPM2* splicing variants was also analyzed after exposure of 12-day-old seedlings for 3 h to low temperature (4 °C) (**Figure 12B and C**). Abundance of *BPM1.1* and *BPM1.3* transcripts (measured with a single primer pair) slightly increased, while abundance of *BPM1.2* decreased after cold treatment (**Figure 12B**). While there was no difference in transcript abundance of *BPM2.3* and *BPM2.4* after cold treatment, it increased 7.23 times for transcript *BPM2.5* (**Figure 12C**). It appears that, compared to other splicing variants, the *BPM2.5* splicing variant is most significantly upregulated by both heat and cold stress conditions.

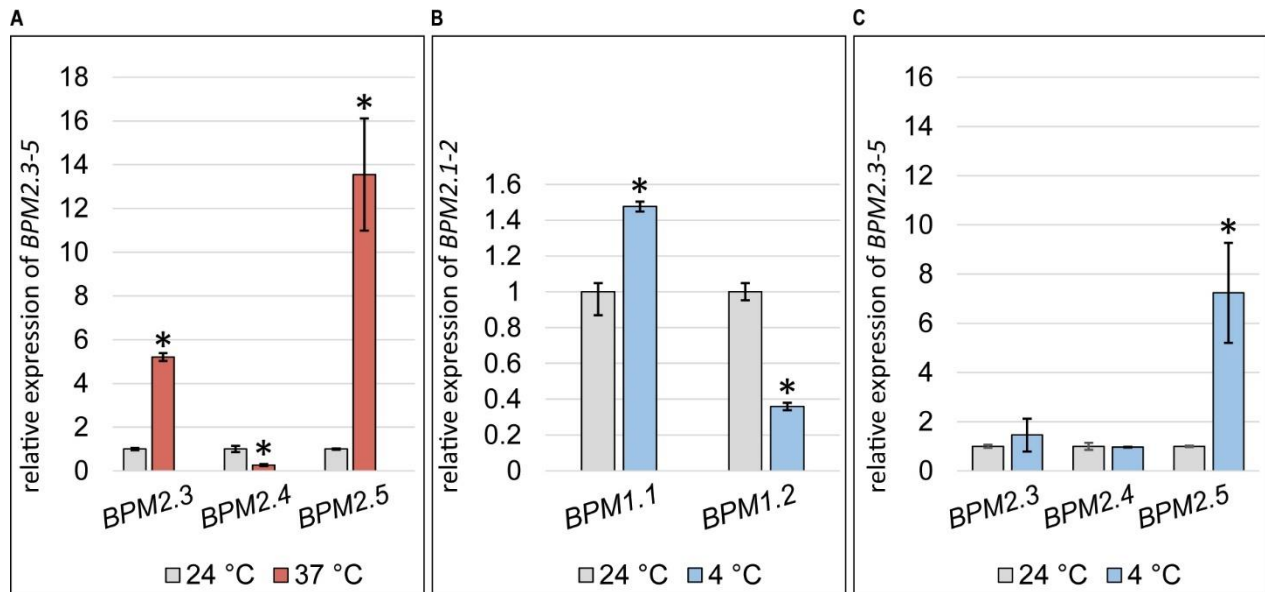


Figure 12. Transcript abundance of *BPM1* and *BPM2* splicing variants after exposure to elevated temperature and cold stress. (A) Wild type seedlings were incubated for 3 h at 24 °C (control) or 37 °C and gene expression was analyzed by RT-qPCR. *BPM2.3* and *BPM2.5* variants were significantly more abundant after exposure to elevated temperature compared to control. (B-C) Wild type seedlings were incubated for 3 h at 24 °C (control) or 4 °C and gene expression was analyzed by RT-qPCR. In B, abundance of transcripts *BPM1.1* and *BPM1.3* (measured using a single primer pair) slightly increased after cold treatment, while *BPM1.2* decreased. In C, splicing variant *BPM2.5* was the dominant variant after cold treatment. In A-C, expression levels of *BPM* genes were normalized to expression of *RHIP1* gene and calibrated to expression of tested gene in untreated control. Expression values are shown as mean fold change \pm SD of two biological replicates. Asterisks indicate statistical significance (Student's T test, $P < 0.05$). Fold change value (relative expression) represents transcript abundance.

4.3.3. Photoperiod affects transgenic *BPM1* protein stability

To test whether photoperiod affects expression of endogenous *BPM* genes, a relative gene expression analysis was performed on tissues harvested at different time points during the day. Wild type seedlings were sampled during the light period (at 12 p.m. and 5 p.m.) and at the end of the dark period (6 a.m.). Expression of each endogenous *BPM* gene was measured at each time point and fold change values were estimated relative to the 12 p.m. value. The expression of *BPM* genes remained stable during the day and showed a tendency to increase at the end of the dark period, but with statistical significance only for *BPM2* and *BPM6* (Figure 13A).

To assess whether BPM1 protein stability changes relative to photoperiod or duration of light exposure, 12-day old seedlings were grown in standard conditions and protein accumulation was analyzed at different time points during the day, or after continuous exposure to either light or dark for 6 or 15 h (**Figure 13B** and **C**). To test the effect of photoperiod, every four hours seedlings were harvested for Western blotting. BPM1-GFP consistently accumulated throughout the day and during the first hours of the night (between 10 a.m. and 10 p.m.), with an apparent reduction near the middle of the night (2 a.m.) and reaching a minimum at the end of the dark period, at 6 a.m. (**Figure 13B**).

Continuous exposure to light, regardless of treatment duration (6 or 15 h), caused a characteristic accumulation of BPM1-GFP in root epidermal cell nuclei of transgenic seedlings (**Figure 13C**). On the other hand, incubation in the dark first showed a dispersion of GFP signal (6 h), then translocation of signal into and along the root stele (15 h) (**Figure 13C**). Finally, prolonged incubation in the dark (24 h) resulted in a diffused BPM1-GFP signal along the xylem (**Appendix B4**).

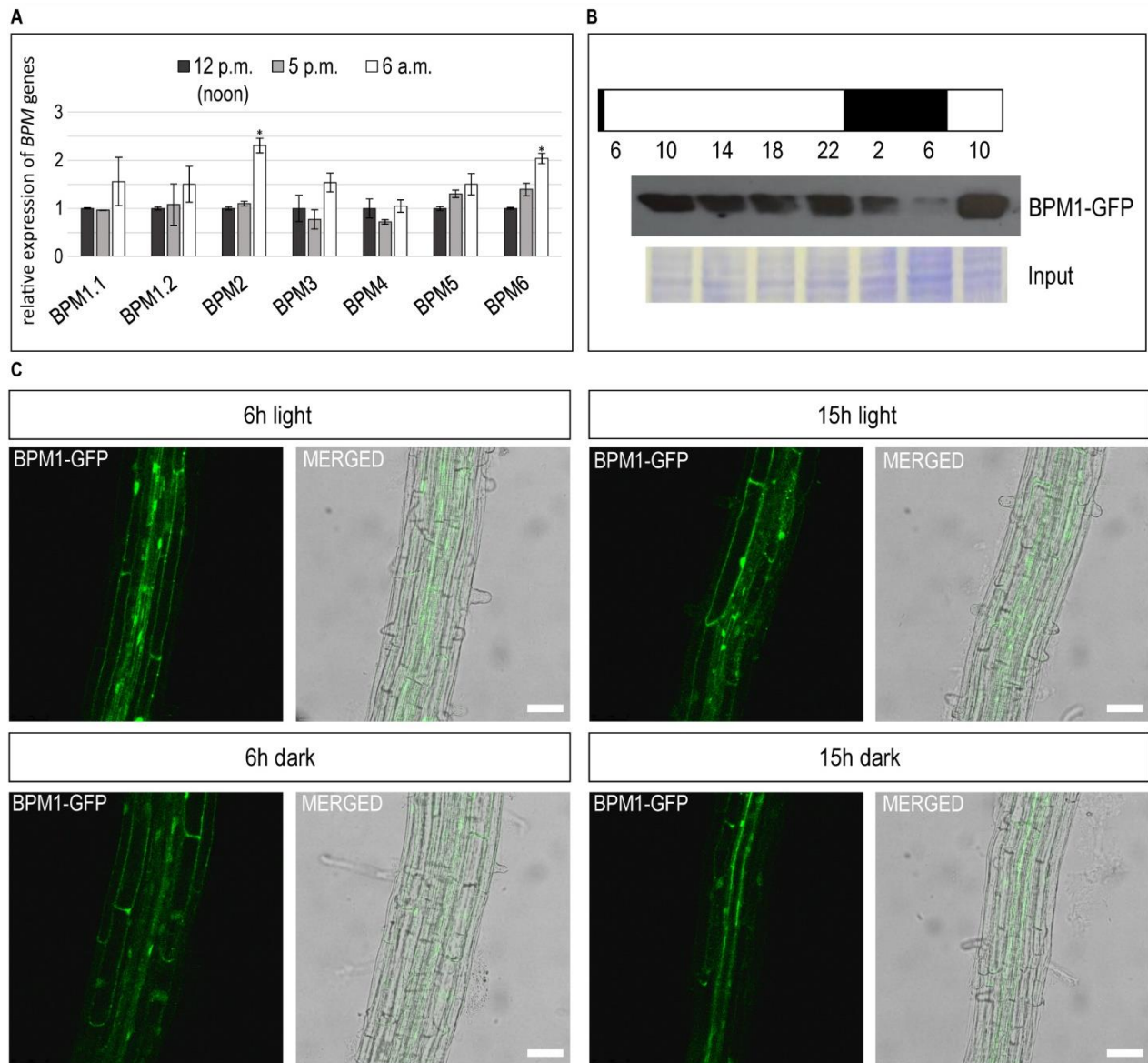


Figure 13. BPM1-GFP protein stability is susceptible to daily rhythm changes. **(A)** Wild type seedlings were grown in standard growth conditions and sampled for gene expression analysis at 12 p.m. (noon), 5 p.m. and 6 a.m. (near the end of the dark period). Expression levels of *BPM* genes were examined by RT-qPCR. Expression levels of endogenous *BPM2* and *BPM6* remained stable during the day and significantly increased at the end of the dark period. A similar trend was observed for other *BPM* genes. Expression of *BPM* genes was normalized to expression of *RHIP1* and expression at 5 p.m. and 6 a.m. was calibrated to expression at 12 p.m. Expression values are shown as mean fold change \pm SD of two biological replicates. Asterisks indicate statistical significance (Student's T Test, $P < 0.05$). **(B)** Seedlings of *BPM1* overexpression lines were cultivated in 16 h day/8 h night regime with the dark period beginning at 11 p.m. and ending at 7 a.m. (represented by black color in the schematic diagram). Seedlings were sampled every 4 h for protein extraction. Whole protein extracts were immunoblotted with anti-GFP antibody (top panel). *BPM1* protein levels dropped during the dark period. For loading control, proteins were stained with Coomassie on PVDF membranes (bottom panel).

Figure 13. – continued.

Similar results were obtained in two biological replicates of one independent experiment. (C) Seedlings of BPM1 overexpression lines were incubated in either dark or light for 6 h (left) or 15 h (right) and at least three seedlings were immediately analyzed by confocal microscopy. BPM1-GFP protein accumulated in root epidermal cell nuclei during light exposure and in stele during prolonged dark exposure. Similar results were obtained in at least three independent experiments. Fluorescent and merged (bright field and BPM1-GFP signal) images of L104 are shown. Scale bar = 50 μm .

4.4. Evaluation of reference genes for RT-qPCR gene expression analysis in *Arabidopsis*

4.4.1. Expression variation of candidate reference genes

Previous chapters showed results of various RT-qPCR experiments, most extensively used in the analysis of elevated temperature effects on *BPM* gene expression. According to available literature, no reference genes were systematically analyzed and validated for use in RT-qPCR experiments employing elevated temperature in *Arabidopsis*. Therefore, to procure a list of candidate reference genes with stable expression after exposure to non-optimal temperatures, publicly available microarray data as well as scientific literature was searched. Expression profiling data (ATH1 Genome Array datasets) obtained on several *Arabidopsis* tissues exposed to different temperature treatments (4 to 40 °C) were used to select candidate reference genes with minimum expression variation. This analysis yielded ten lists of 100 most stable genes (Top100 lists), from which ten candidate reference genes were selected for expression stability analysis. The criteria for selection of candidate reference genes from Top100 lists was the number of their appearances within all ten lists, with highest priority given to genes with the highest number of appearances. Additionally, available literature was searched for RT-qPCR reference genes adhering to the following criteria: they belonged to traditional reference genes (“housekeeping genes”) and/or they had already been identified as potential reference genes for experiments employing specific temperatures in *Arabidopsis* (Hong et al., 2010). The full protocol for microarray data processing and selection of candidate reference genes is described in Škiljaica et al. (2022). The ten selected candidate reference genes (*DWA1*, *OGIO*, *PUX7*, *TRAPPC6*, *GLR2*, *PP2AA3*, *MON1*, *RHIP1*, *TIP41* and *UBC21*) are listed in **Table 4**.

Table 4. RT-qPCR candidate reference genes selected for evaluation of gene expression stability in *Arabidopsis* exposed to elevated temperatures. Genes were selected after screening of publicly available microarray data and literature, as described in Škiljaica et al. (2022). The table lists each gene's symbol and identifier (ID) from the TAIR database, and protein name and function as described in TAIR or UniProt database.

GENE SYMBOL	GENE ID	PROTEIN NAME	PROTEIN FUNCTION
<i>TRAPPC6</i>	<i>AT3G05000</i>	Transport protein particle (TRAPP) component 6	Endoplasmic reticulum to Golgi vesicle-mediated transport, pollen tube development, regulation of GTPase activity, response to ABA
<i>PUX7</i>	<i>AT1G14570</i>	Plant UBX domain-containing protein 7	Encodes a nuclear UBX-containing protein that can bridge ubiquitin to AtCDC48A
<i>OGIO</i>	<i>AT5G51880</i>	2-oxoglutarate (2OG) and Fe(II)-dependent oxygenase superfamily protein	Oxidoreductase activity
<i>DWA1</i>	<i>AT2G19430</i>	DWD (DDB1-binding WD40 protein) hypersensitive to ABA 1	Gene silencing by RNA, negative regulation of ABA-activated signaling pathway, production of ta-siRNAs involved in RNA interference, protein ubiquitination
<i>GLR2</i>	<i>AT2G17260</i>	Glutamate receptor 2	Cellular calcium ion homeostasis, response to light stimulus, stomatal movement
<i>PP2AA3</i>	<i>AT1G13320</i>	Protein phosphatase 2A subunit A3	Subunit of protein phosphatase 2A (PP2A), regulation of phosphorylation
<i>RHIP1</i>	<i>AT4G26410</i>	RGS1-HXK1 interacting protein 1	Cellular response to glucose stimulus, regulation of glucose mediated signaling pathway
<i>TIP41</i>	<i>AT4G34270</i>	TIP41-like family protein	TOR signaling, regulation of phosphoprotein phosphatase activity, signal transduction
<i>MON1</i>	<i>AT2G28390</i>	Monensin sensitivity 1 - SAND family protein	Intracellular protein transport, late endosome to vacuole transport, plant organ development, vacuole organization
<i>UBC21/PEX4</i>	<i>AT5G25760</i>	Ubiquitin-conjugating enzyme 21/Peroxin 4	Fatty acid beta-oxidation, peroxisome organization, protein import into peroxisome matrix, protein ubiquitination

Gene expression stability of candidate reference genes was evaluated by RT-qPCR in three types of tissues: 12-day-old seedlings, rosette leaves and flower buds of 5-week-old plants. Seedlings and plants were exposed to a range of elevated temperatures (22 °C, 27 °C, 32 °C, 37 °C and 42 °C) for 3 h, followed by tissue harvesting and RNA extraction. The quality of total extracted RNA was verified before reverse transcription, with $A_{260/280}$ ratio of all RNA samples approximately 2 and the $A_{260/230}$ ratio 2.0-2.2. Additionally, electrophoresis showed distinct bands of 18S and 28S ribosomal RNA (**Appendix B5**). For each gene, primer pairs were designed to generate a qPCR

product not longer than 225 bp, the T_m of each primer was adjusted to $59\text{ }^\circ\text{C} \pm 1\text{ }^\circ\text{C}$ and GC content of each primer sequence was 40% to 60%. When possible, primers were designed to span an exon-exon junction. All primer sequences are listed in **Appendix A1**. Primers used for *DREB2A* were previously published in Morimoto et al. (2017). Successful primer design for ten candidate reference genes was tested with RT-qPCR. The presence of a single peak in a melting curve was taken to indicate amplification of a single PCR product and absence of primer dimer formation (**Appendix B6**). Furthermore, amplification of a PCR product of expected size was confirmed by agarose gel electrophoresis (**Appendix B6**).

Two biological replicates of each temperature-treated tissue were prepared, with two technical replicates in qPCR reactions. After averaging technical replicates, a dataset of 300 C_q values was obtained (**Appendix B7**). Based on the analysis of average C_q values, *UBC21* was the gene with highest expression in all three individual tissues (seedlings, leaves and buds) exposed to five different temperatures (**Figure 14A**). Two genes with lowest expression in individual tissues were *GLR2* (seedlings and buds) and *MON1* (leaves) (**Figure 14A**). When looking at all three tissues combined, average C_q values of candidate reference genes ranged from 21.95 to 25.82. Again, the gene with highest expression was *UBC21* (C_q mean = 21.95) and the lowest expressed gene was *GLR2* (C_q mean = 25.82) (**Figure 14B**). Beside lowest expression, *GLR2* and *MON1* had the highest overall C_q value dispersion (**Figure 14A and B**), indicating lower stability in different experimental conditions.

4.4.2. Evaluation of expression stability of candidate reference genes

To assess the expression stability of candidate reference genes in *Arabidopsis* seedlings, leaves and buds after temperature treatments, the obtained C_q data was analyzed with four validation algorithms: BestKeeper, geNorm, NormFinder and comparative ΔC_q method, according to the protocol described in Škiljaica et al. (2022). For each candidate reference gene, correlation coefficient (BestKeeper), M value (geNorm), stability value (NormFinder) and meanSD (comparative ΔC_q method) were calculated for individual tissue samples (seedlings, leaves, buds) and all three tissues combined (**Table 5**).

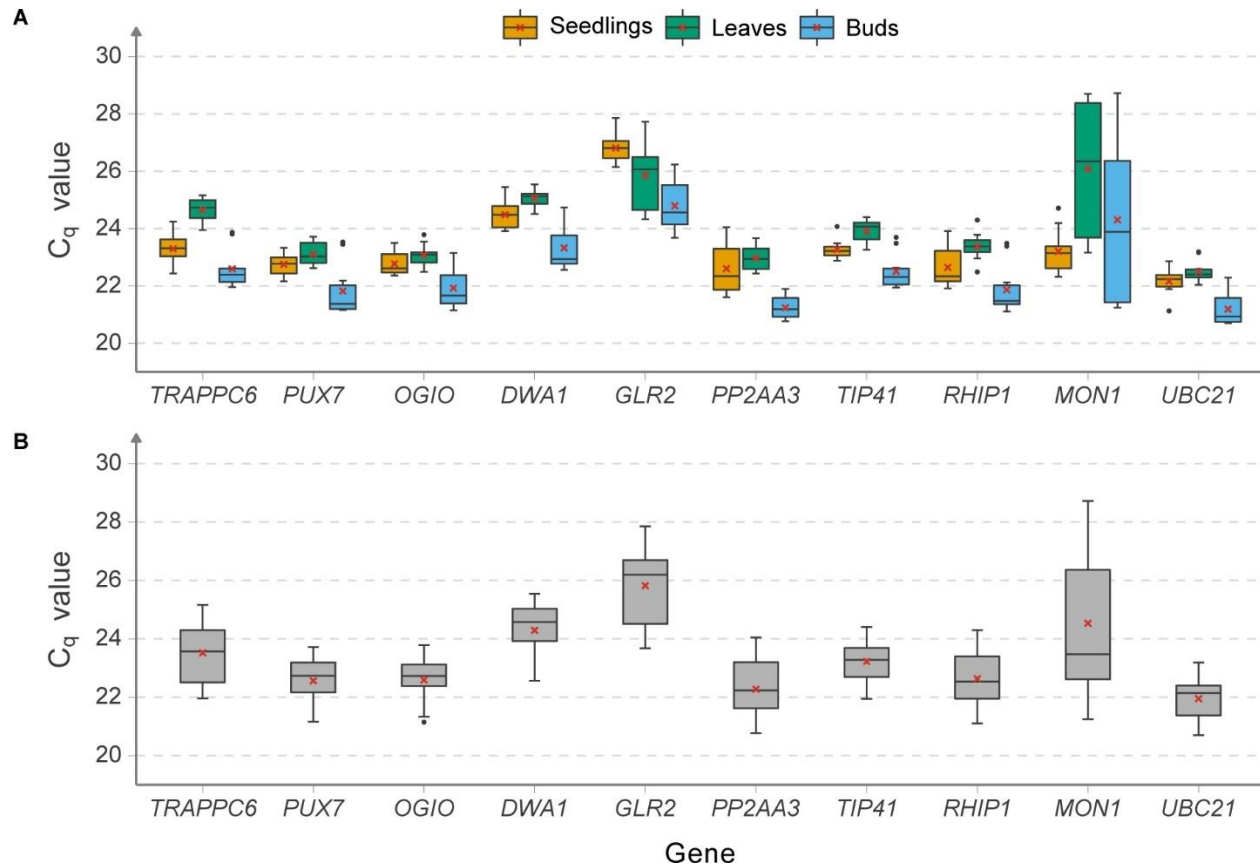


Figure 14. Expression profiles of ten candidate reference genes in *Arabidopsis* tissues exposed to elevated temperatures. *Arabidopsis* seedlings, leaves and flower buds were incubated for 3 h at different temperatures (22°C, 27°C, 32°C, 37°C and 42°C) and RT-qPCR analysis was performed. C_q value variation was calculated for (A) samples of individual tissues (N = 10 per gene/tissue) and in (B) samples of all tissues combined (N = 30 per gene). Boxes indicate the 25th/75th percentiles, the horizontal line in the box represents the median value and the vertical lines mark 5th and 95th percentiles. Outliers are marked with a dot and average values are marked with a red cross.

According to BestKeeper, the most stable gene was *DWA1* (0.98) in seedlings, *PP2A3* (0.964) in leaves and *RHIP1* (0.975) in buds. In all tissues combined, *DWA1* (0.959) was considered most stable (**Table 5**). The version of geNorm used in this work outputs a stability ranking list in which two genes share the position of the most stable gene. Therefore, according to geNorm, most stable genes were *OGIO/PUX7* (0.159) in seedlings, *UBC21/MON1* (0.167) in leaves and *TIP41/UBC21* (0.182) in buds. In all three tissues combined, *DWA1/PUX7* (0.271) was considered most stable. The stability value of the geNorm algorithm is the M value. Generally, genes with the M value

below 0.5 are considered to be of adequate stability and therefore suitable for use as reference genes (Hellemans et al., 2007). Here, all genes had M values below 0.5 in individual tissues and all tissues combined (**Table 5**). According to NormFinder, the most stable gene was *DWAI* (0.10) in seedlings, *UBC21* (0.14) in leaves and *TIP41* (0.13) in buds and all tissues combined (**Table 5**). When all genes were compared against one another using the comparative ΔC_q method and then ranked by mean SD values, the most stable gene was *TIP41* (0.645) in seedlings, *DWAI* (0.789) in leaves and *PP2AA3* (1.055) in buds (**Table 5**). In all three tissues combined, the most stable gene was *OGIO* (1.306). A comprehensive ranking based on outputs of the four algorithms was obtained using RankAggreg. In this ranking, the most stable candidate reference genes were *OGIO* and *PUX7* in seedlings, *UBC21* and *PUX7* in leaves and *TIP41* and *UBC21* in buds and all three tissues combined. These results confirm what was shown by individual algorithms, with the top-ranked genes appearing at least twice in the top three positions of the four algorithms. Interestingly, *PUX7* ranked in sixth place in the BestKeeper analysis for seedlings. However, its SD value was 0.34, which is still among the lowest SD values measured in the BestKeeper analysis (**Table 5**). Overall, genes which were consistently top-ranked were *OGIO*, *PUX7*, *UBC21* and *TIP41*, while *GLR2* and *MONI* were consistently lowest-ranked.

4.4.3. Validation of top-ranked reference genes

To evaluate the reliability of selected reference genes, single or multiple reference genes were used to normalize the expression of a heat-inducible gene *DREB2A*. Relative expression levels of *DREB2A* upon temperature treatment were evaluated in individual tissues (seedlings, leaves and buds) and all three tissues combined. Both for individual tissue analysis and group tissue analysis, data normalization was performed using two respective top-ranked and one lowest-ranked reference gene according to **Table 5**. The heat-induced rise in expression levels of *DREB2A* was most prominent during the highest temperature treatment (42 °C) in all three tissues, and was higher in seedlings than in leaves and buds (**Figure 15**). When either of the two top-ranked reference genes was used to normalize the data (*OGIO* or *PUX7* for seedlings, *UBC21* or *PUX7* for leaves and *TIP41* or *UBC21* for buds) the resulting expression levels of *DREB2A* were similar. On the other hand, using lowest-ranked reference genes for data normalization (*MONI* for seedlings and *GLR2* for leaves and buds) caused an increase in reported *DREB2A* expression levels (**Figure 15A**).

Table 5. Stability ranking of ten candidate reference genes in *Arabidopsis* tissues exposed to elevated temperatures. *Arabidopsis* seedlings, leaves and flower buds were incubated for 3 h at different temperatures (22°C, 27°C, 32°C, 37°C and 42°C) and RT-qPCR analysis was performed. Genes were ranked according to expression stability values ‘r’, ‘meanM’, ‘Stability’ and ‘MeanSD’, as implemented by BestKeeper, geNorm, NormFinder and comparative ΔC_q method, respectively. Comprehensive ranking derived from RankAggreg is based on individual rankings of the four algorithms. Protocols of all validation software are available in Škiljaica et al. (2022). Data are shown for individual tissues and all tissues combined.

TISSUE	RANK	BestKeeper		geNorm ^a		NormFinder		Comparative ΔC_q		Rank Aggreg
		GENE	r	GENE	meanM	GENE	Stability	GENE	MeanSD	GENE
SEEDLINGS	1	DWA1	0.980	OGIO/PUX7	0.159	DWA1	0.10	TIP41	0.645	OGIO
	2	MON1	0.964			OGIO	0.14	PUX7	0.672	PUX7
	3	OGIO	0.956	TIP41	0.184	PUX7	0.16	OGIO	0.674	DWA1
	4	RHIP1	0.884	DWA1	0.197	UBC21	0.18	UBC21	0.705	TIP41
	5	GLR2	0.875	UBC21	0.228	TIP41	0.19	GLR2	0.723	GLR2
	6	PUX7	0.873	GLR2	0.252	GLR2	0.23	DWA1	0.725	UBC21
	7	TIP41	0.828	TRAPPC6	0.264	RHIP1	0.27	TRAPPC6	0.768	RHIP1
	8	TRAPPC6	0.792	RHIP1	0.287	TRAPPC6	0.29	RHIP1	0.845	MON1
	9	PP2AA3	0.656	MON1	0.306	MON1	0.30	MON1	0.901	TRAPPC6
	10	UBC21	0.516	PP2AA3	0.340	PP2AA3	0.40	PP2AA3	0.993	PP2AA3
LEAVES	1	PP2AA3	0.882	UBC21/MON1	0.167	UBC21	0.14	DWA1	0.789	UBC21
	2	OGIO	0.679			TIP41	0.18	OGIO	0.815	PUX7
	3	TRAPPC6	0.570	PUX7	0.209	PUX7	0.19	UBC21	0.821	OGIO
	4	RHIP1	0.553	OGIO	0.283	MON1	0.22	TRAPPC6	0.824	PP2AA3
	5	PUX7	0.551	TIP41	0.316	PP2AA3	0.22	PUX7	0.826	TIP41
	6	UBC21	0.525	PP2AA3	0.337	OGIO	0.23	TIP41	0.829	TRAPPC6
	7	TIP41	0.428	TRAPPC6	0.353	TRAPPC6	0.25	PP2AA3	0.843	MON1
	8	DWA1	0.355	DWA1	0.367	DWA1	0.29	RHIP1	0.868	DWA1
	9	MON1	0.341	RHIP1	0.398	RHIP1	0.35	GLR2	1.383	RHIP1
	10	GLR2	0.084	GLR2	0.437	GLR2	0.41	MON1	2.414	GLR2
BUDS	1	RHIP1	0.975	TIP41/UBC21	0.182	TIP41	0.13	PP2AA3	1.055	TIP41
	2	DWA1	0.972			UBC21	0.16	UBC21	1.123	UBC21
	3	PUX7	0.970	RHIP1	0.235	RHIP1	0.20	TIP41	1.150	RHIP1
	4	UBC21	0.940	DWA1	0.258	TRAPPC6	0.21	TRAPPC6	1.186	DWA1
	5	TIP41	0.922	TRAPPC6	0.281	DWA1	0.23	OGIO	1.195	TRAPPC6
	6	MON1	0.881	PUX7	0.299	OGIO	0.32	DWA1	1.242	PUX7
	7	PP2AA3	0.870	MON1	0.318	MON1	0.33	GLR2	1.282	PP2AA3
	8	TRAPPC6	0.868	PP2AA3	0.352	PUX7	0.33	RHIP1	1.294	OGIO
	9	OGIO	0.851	OGIO	0.382	PP2AA3	0.34	PUX7	1.328	MON1
	10	GLR2	0.571	GLR2	0.430	GLR2	0.37	MON1	3.073	GLR2

^aThis version of geNorm does not differentiate between the top two positions within a ranking

Table 5. – continued.

ALL TISSUES	1	<i>DWA1</i>	0.959 *			<i>TIP41</i>	0.13	<i>OGIO</i>	1.306	<i>TIP41</i>	
	2	<i>RHIP1</i>	0.938 *	<i>DWA1/PUX7</i>	0.271	<i>UBC21</i>	0.14	<i>UBC21</i>	1.319	<i>UBC21</i>	
	3	<i>PUX7</i>	0.938 *		<i>TIP41</i>	0.295	<i>PUX7</i>	0.15	<i>TIP41</i>	1.324	<i>RHIP1</i>
	4	<i>TIP41</i>	0.919 *		<i>UBC21</i>	0.310	<i>DWA1</i>	0.16	<i>PUX7</i>	1.368	<i>DWA1</i>
	5	<i>OGIO</i>	0.914 *	<i>TRAPPC6</i>	0.327	<i>TRAPPC6</i>	0.18	<i>DWA1</i>	1.423		<i>TRAPP C6</i>
	6	<i>TRAPPC6</i>	0.893 *		<i>OGIO</i>	0.352	<i>OGIO</i>	0.18	<i>RHIP1</i>	1.426	<i>PUX7</i>
	7	<i>UBC21</i>	0.879 *		<i>RHIP1</i>	0.365	<i>MON1</i>	0.19	<i>PP2AA3</i>	1.452	<i>PP2AA3</i>
	8	<i>PP2AA3</i>	0.827 *		<i>MON1</i>	0.379	<i>PP2AA3</i>	0.20	<i>TRAPCC6</i>	1.490	<i>OGIO</i>
	9	<i>MON1</i>	0.609 *		<i>PP2AA3</i>	0.394	<i>RHIP1</i>	0.22	<i>GLR2</i>	1.612	<i>MON1</i>
	10	<i>GLR2</i>	0.499 *		<i>GLR2</i>	0.424	<i>GLR2</i>	0.22	<i>MON1</i>	2.687	<i>GLR2</i>

^aThis version of geNorm does not differentiate between the top two positions within a ranking

This deviation was most striking in leaves and buds, where bottom-ranked *GLR2* was used. For example, in buds at 42 °C, relative gene expression level of *DREB2A* was 31.02 and 32.6 when normalized with *TIP41* and *UBC21*, respectively, and 70.5 when normalized with *GLR2* (**Figure 15A**, right panel). The deviation in *DREB2A* expression levels was somewhat less apparent in seedlings, where *MON1* was used as a representative of a low-ranked gene (**Figure 15A**, left panel). The cause might be the relatively high stability values of *MON1*, which ranked eight but still had similar values to those of the first-ranked *OGIO*. This was especially evident in the BestKeeper analysis, where *MON1* and *OGIO* had a similarly high Pearson correlation coefficient ($r > 0.9$). For comparison, in buds, the r value of the first-ranked reference gene *TIP41* was 0.922 and the last-ranked *GLR2* was 0.571. A similar pattern of *DREB2A* expression was observed when a group analysis was performed for all three tissues combined (**Figure 15B**). Here, two top-ranked genes were *TIP41* and *UBC21* and the lowest-ranked gene was *GLR2*. Again, relative expression levels of *DREB2A* remained comparable when *TIP41* and *UBC21* were used for data normalization and deviated when *GLR2* was used.

Candidate reference genes used in this study were selected based on a microarray data analysis of experiments employing elevated temperatures. The analysis also included experiments employing low temperature treatments. Although expression stability of candidate reference genes was not analyzed by RT-qPCR after low temperature treatment, they still represent a pool of genes to validate for use in conditions of low temperature. Two candidate reference genes, the previously validated *RHIP1* and the unvalidated *DWA1* were selected for data normalization in an experiment where seedlings were incubated at both 37 °C and 4 °C (for experiment details, see section 4.3.3; expression analysis of *BPM2* splicing variants). While *RHIP1* was selected based on its previous

validation in the heat-based experiment, *DWAI* was selected because it was the second most stable gene in two large microarray datasets comprised of experiments employing both cold and heat stress (unpublished analysis, courtesy of Lucija Markulin). The first most stable gene in these arrays was *PP2AA3*, which was not used here because it ranked in the last place in the heat-based group ranking obtained for seedlings (**Table 5**). **Figure 16** shows expression levels of *BPM2.3*, *BPM2.4* and *BPM2.5* at 37 °C (**Figure 16A**) and 4 °C (**Figure 16B**). For each gene, expression data was normalized either to expression of *RHIP1* or to a geometric mean of expression of *RHIP1* and *DWAI*, and the obtained fold-change values are shown side by side. At 37 °C, normalization with *RHIP1* resulted in a relative expression increase of 5.2, 0.3 and 13.5 for *BPM2.3*, *BPM2.4* and *BPM2.5*, respectively. Surprisingly, when both reference genes were used, fold-change doubled, measuring 11.3, 0.6 and 29.4 for the three variants, respectively (**Figure 16A**).

Exposure of seedlings to 37 °C resulted in an increase in *DWAI* expression which was substantial enough to create a strong shift in relative expression of tested gene variants. The heat-induced shift in *DWAI* expression is clearly evident in a side-by-side comparison of C_q values of *RHIP1* and *DWAI* at 24 °C (control), 4 °C and 37 °C (**Figure 16C**). On the other hand, expression of *DWAI* did not change in the 4 °C experiment, where relative gene expression remained similar for all variants regardless of whether *RHIP1* was used alone or along with *DWAI* for data normalization (**Figure 16B**), and stable expression of both genes was evident by their average C_q values (**Figure 16C**).

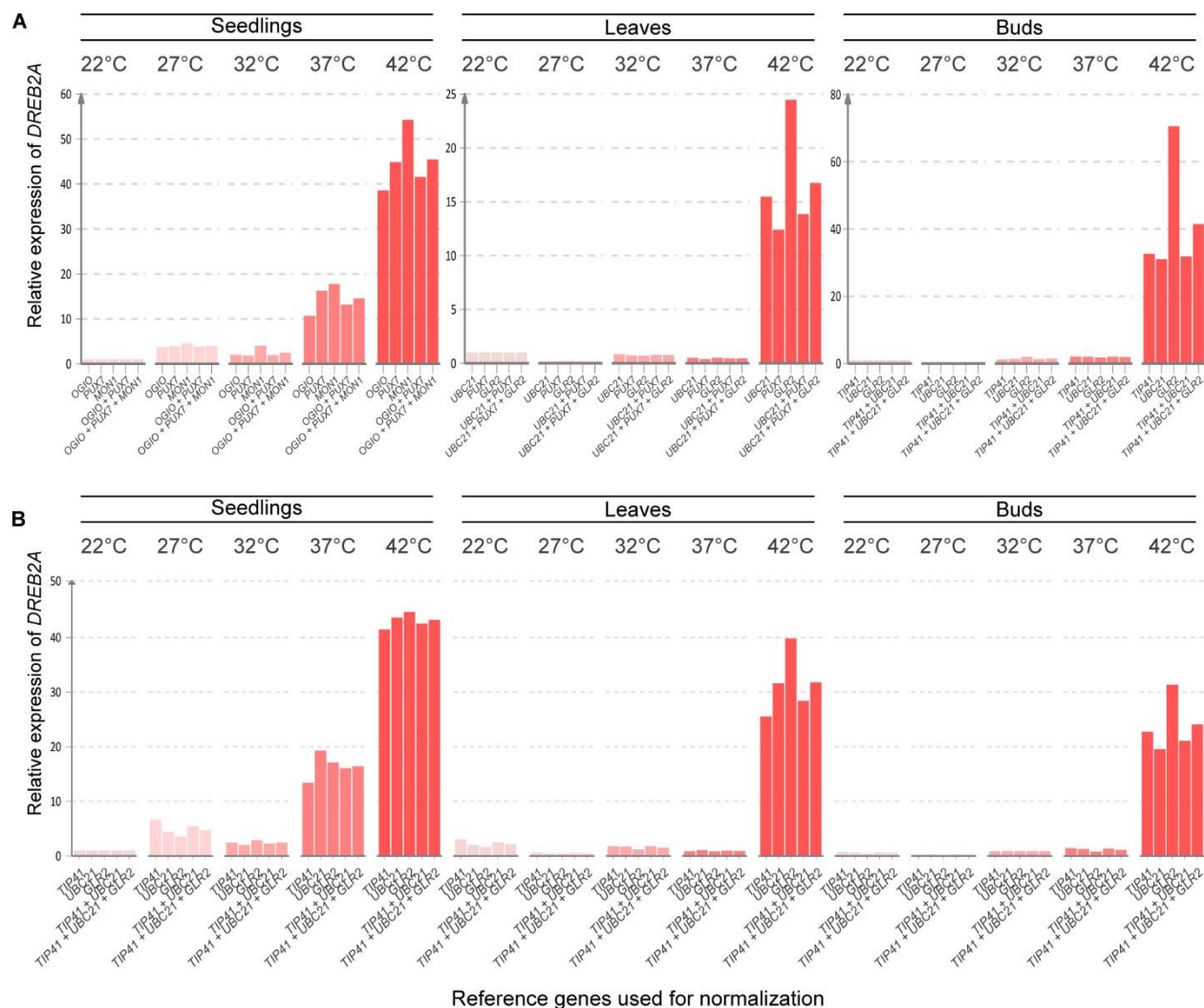


Figure 15. Validation of selected reference genes in individual *Arabidopsis* tissues exposed to elevated temperatures. *Arabidopsis* seedlings, leaves and flower buds were incubated for 3 h at different temperatures (22 °C, 27 °C, 32 °C, 37 °C and 42 °C) and expression levels of *DREB2A* were calculated using the $\Delta\Delta Cq$ method with single or multiple reference genes used for normalization. *DREB2A* expression was calculated (**A**) individually for each tissue, using their respective top- and bottom-ranked genes, and (**B**) in a group analysis, using the top- and bottom-ranked genes for all tissues combined. For gene rankings, see **Table 5**. The left, middle and right side of each panel show seedlings, leaves and buds, respectively. Results of one independent experiment are shown.

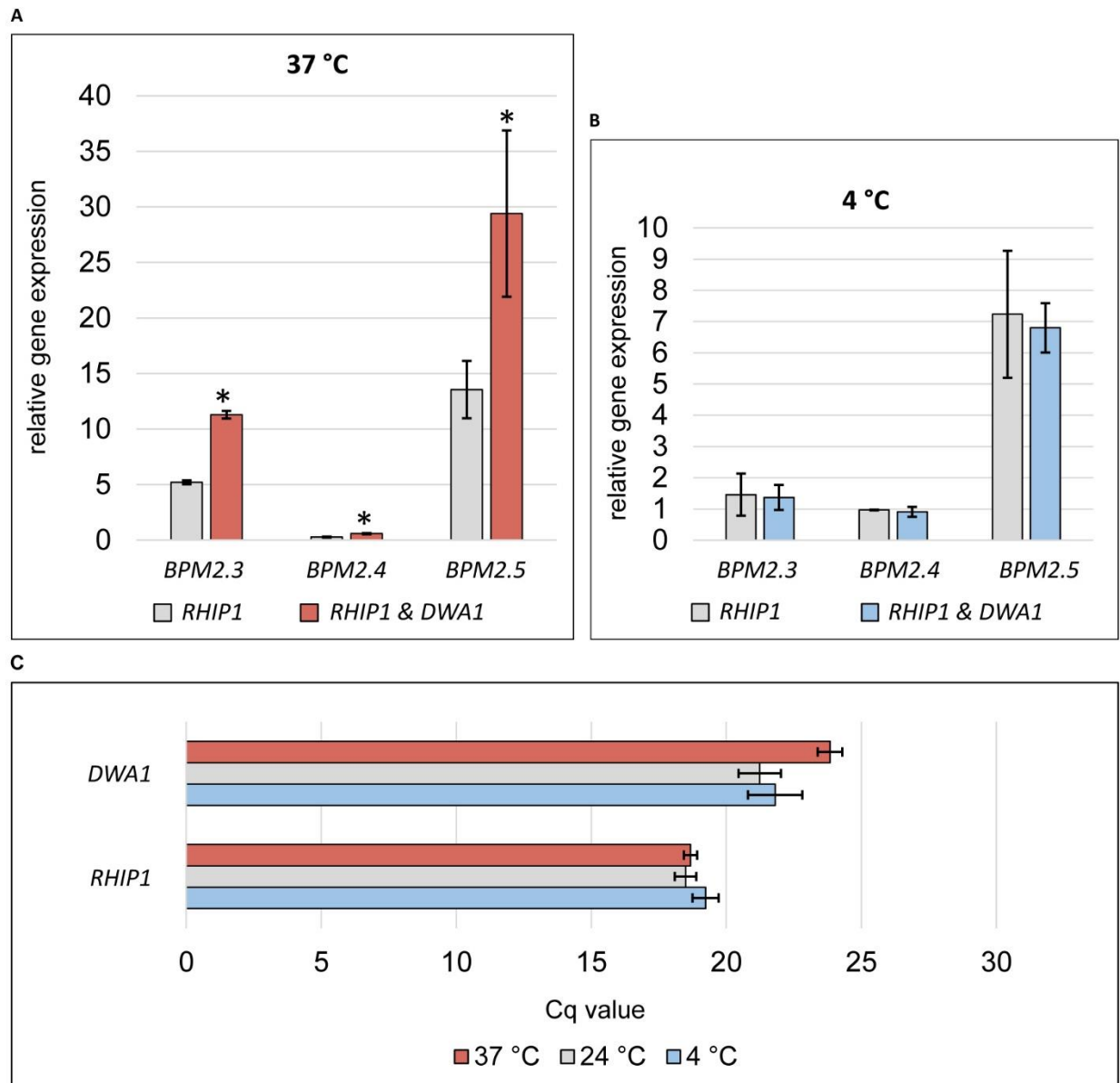


Figure 16. *RHIP1* is a suitable reference gene in experiments employing cold and heat treatments, and *DWA1* only in cold treatment. Wild type seedlings were incubated for 3 h at 4 °C, 24 °C and 37 °C and relative gene expression of *BPM2.3*, *BPM2.4* and *BPM2.5* was analyzed by RT-qPCR. *RHIP1* was used for data normalization either alone or in combination with *DWA1*. (A) When expression of *BPM2.3*, *BPM2.4* and *BPM2.5* after heat treatment is normalized to expression of *RHIP1*, fold change levels significantly differ from those obtained using both *RHIP1* and *DWA1* for normalization. (B) Fold change levels of *BPM2.3*, *BPM2.4* and *BPM2.5* after cold treatment are similar when *RHIP1* is used alone or in combination with *DWA1* for data normalization. (C) Expression of *DWA1* is less stable than expression of *RHIP1* at 4 °C, 24 °C and 37 °C. (A-C) Expression values are shown as mean fold change \pm SD of two biological replicates. Asterisks indicate statistical significance (Student's T test, $P < 0.05$).

5. DISCUSSION

5.1. Expansion of the MATH-BTB family in wheat

An Ensembl Plants database search against the wheat proteome using the TaMAB2 sequence as query revealed 46 putative MATH-BTB proteins in wheat *Triticum aestivum*. An earlier analysis of wheat MATH-BTB proteins revealed 49 putative proteins in total (Škiljaica, 2016). Additionally, the two analyses differed in the numbers of splicing variants predicted for *TaMAB* genes encoding the putative TaMAB proteins. In the first analysis, only one splicing variant was predicted for each gene (Škiljaica, 2016), while in the repeated analysis, four genes were predicted to contain two splicing variants. Nevertheless, both analyses indicate significant expansion of the MATH-BTB family in wheat. This result is in accordance with earlier reports of significant MATH-BTB expansion in several other grass species, such as rice, *Sorghum*, *Brachypodium* and maize (Gingerich et al., 2007; Juranić & Dresselhaus, 2014) as well as in the nematode *C. elegans* (Stogios et al., 2005). Out of 42 expanded clade *TaMAB* genes, 21 contain a single exon, while the other 21 genes contain two or more exons, with one member having as much as eight exons. This differs from results of an earlier study reporting that genes of the expanded clade, unlike the core clade, do not contain introns (Gingerich et al., 2007). This could be something specific to wheat MATH-BTB genes, as the aforementioned study did not include wheat, or it might simply reflect the development of sequence prediction software.

The process in which a gene family expands only in a select group of species, such as the expansion of the MATH-BTB family in wheat and other grasses, has been termed lineage-specific expansion (LSE) and it has been observed across all kingdoms of biological species (Lespinet et al., 2002). An early study of LSE events in five eukaryote species, including *A. thaliana*, showed that LSEs provide material for specific adaptations and for evolution of new functional systems in different eukaryotic taxa. LSEs were observed in gene families involved in pathogen and stress response, transcription regulation, controlled protein degradation mediated by the ubiquitin system, protein modification, signal transduction, chemoreception, and small molecule metabolism (Lespinet et al., 2002). Interestingly, in *Arabidopsis*, plant-specific kinases and plant-specific F-box proteins (substrate adaptors of E3 ligases) were the two most expanded gene families (Lespinet et al., 2002). A common denominator in LSE scenarios is a gene duplication event followed by retention in the

genome due to a functional adaptation (Lespinet et al., 2002). A preferential retention of gene duplicates was observed in species which underwent several rounds of whole genome duplication, such as *A. thaliana*, which was shaped by three distinct genome duplication events, termed α , β , and γ (Bowers et al., 2003). The genes which were retained after one round of duplication were more likely to remain in the genome as duplicates following the second round of duplication. This process was functionally biased, with genes involved in regulation of transcription being highly over-represented (Seoighe & Gehring, 2004). In general, proteins which require a stoichiometric balance due to interaction with other proteins are less likely to expand by single gene duplications, but are more easily retained in the genome following whole genome duplication. The reason for this phenomenon is that whole genome duplications result in balanced dosages of all proteins involved in the interaction (Birchler & Veitia, 2007). Interestingly, the *MATH-BTB* family did not expand in the *A. thaliana* genome which was duplicated three times (Gingerich et al., 2005, 2007), nor did it expand in the *Musa* lineage (banana), where three rounds of whole genome duplications occurred (D'hont et al., 2012). According to Juranić & Dresselhaus (2014), this indicates that expansion of the *MATH-BTB* family in maize, rice, *Brachypodium* and *Sorghum* was biased relative to grasses-specific functions (Juranić & Dresselhaus, 2014), and a similar bias likely played a role in retention of the *MATH-BTB* family in the wheat genome.

The phylogenetic analysis of MATH-BTB proteins of *Arabidopsis*, wheat, maize and rice, confirmed what was previously shown by Juranić & Dresselhaus (2014), i.e., the clustering of MATH-BTB proteins into two distinct clades, the smaller core clade containing all *Arabidopsis* proteins and the large, expanded clade containing predominantly MATH-BTB proteins of grasses. Expanded clade MATH-BTB proteins of wheat clustered into four out of five distinct subclades of the expanded clade, E1 to E5. Using multiple sequence alignments of core and expanded clade proteins, I analyzed the conservation status of their individual domains, the MATH and the BTB domain. This analysis showed that the MATH domain of wheat MATH-BTB proteins of the expanded clade is less conserved than the BTB domain, which agrees with previous indications that the MATH domain of expanded clade MATH-BTB proteins is becoming more diversified (Gingerich et al., 2007). A similar process seems to have shaped another family of E3 ligase adaptor proteins, namely the F-box family of proteins. F-box proteins cluster into two subclades, FBA and FBK, both of which underwent expansion but following different evolutionary patterns. While subclade FBK expanded near the beginning of land plant evolution, expansion of subclade FBA

occurred only in flowering plants and most intensely in the *Brassicaceae* family, with an average of 200 members in each species. The FBA subfamily evolved by waves of duplication, followed by sequence conservation of the F-box domain and sequence diversification of the target-recruiting domain (Navarro-Quezada et al., 2013), similar to what was found here for wheat MATH-BTB proteins of the expanded clade. The authors postulate that unlike FBK proteins, the majority of FBA proteins are not involved in basic developmental processes, but were important for adaptation of specific lineages to their respective environments (Navarro-Quezada et al., 2013). In an earlier study, Thomas (2006) hypothesized that in *C. elegans*, both the MATH-BTB and F-box family expanded to combat viral pathogens or bacterial protein toxins, and this view was shared for rice MATH-BTB proteins, which underwent similar expansion (Gingerich et al., 2007). Indeed, an extensive paleogenomic study revealed that the wheat genome, similar to four other grass species (rice, *Sorghum*, maize and barley) underwent fast evolution with very active episodes of genome rearrangements and gene mobility (Salse et al., 2009). The authors suggest that preferential retention of duplicated genes occurs as an adaptation to rapidly changing biotic and abiotic extrinsic factors (Salse et al., 2009), which is what most likely shaped the expanded MATH-BTB families of grasses. To summarize, it is highly likely that expansion of the wheat MATH-BTB family, combined with the diversification of the MATH-domain, occurred in response to environmental challenges placing specific constraints on the wheat lineage.

On the other hand, multiple sequence alignments indicated that the core clade MATH domain is highly conserved. Clearly, two distinct evolutionary processes are shaping the two major clades of the MATH-BTB family, and both are more pronounced in the MATH domain. Indeed, Gingerich et al. (2007) show that the core clade of *Arabidopsis* and rice MATH-BTB proteins undergoes a purifying selection, especially in its target-binding MATH domain, most likely to facilitate interaction with a highly specialized set of substrates. Salse et al. (2009) suggest that reversion to singleton status is more common for genes involved in stable biological processes, and this role has been most commonly attributed to *Arabidopsis* MATH-BTB proteins (Gingerich et al., 2007; Juranić & Dresselhaus, 2014).

5.2. Putative roles of TaMAB2 during wheat embryogenesis

One of the goals of this research was evaluation of effects that overexpression of TaMAB2 has on plant morphology and physiology. In the case of TaMAB2, earlier attempts at creating a wheat knockout mutant resulted in embryo lethal phenotype, indicating its crucial role during wheat embryogenesis (Bauer et al., 2019). Therefore, a transgenic *Arabidopsis* line overexpressing GFP-tagged TaMAB2 under control of the constitutive CaMV 35S promoter was regenerated. These plants exhibit mild to severe growth defects, such as reduced growth, rugose leaf blades, failed leaf stalk elongation and no flowering (Bauer et al., 2019). In protoplasts of TaMAB2 overexpressors, TaMAB2 colocalized with ubiquitin, indicating association with a CUL3-based E3 ligase mediating ubiquitination of target proteins, as reported previously for ZmMAB1 (Juranić et al., 2012). This agrees with the finding that TaMAB2 directly interacts with *Arabidopsis* CUL3 in Y2H (Bauer et al., 2019). TaMAB2 also strongly interacts with itself, which agrees with the proposed model of MATH-BTB proteins acting as dimers in CUL3-based E3 ligase complexes (Juranić et al., 2012; Zhuang et al., 2009). Additionally, root epidermal cell size measurements indicate an involvement of TaMAB2 in cell size regulation, possibly through an interaction with proteins of the cytoskeleton and/or its regulatory network. Although the increase in epidermal cell length in TaMAB2 overexpressors compared to wild type was relatively small, it agrees with a more pronounced increase in root and epidermal cell length observed in a different *Arabidopsis* line overexpressing TAP-tagged TaMAB2 (Bauer et al., 2019). Additionally, crossing of this line with a microtubule marker line caused disorganization of microtubule bundles in seedling roots (Bauer et al., 2019), and the TaMAB2 protein co-localized with microtubules in cells during mitosis (Bauer et al., 2019). Links between BTB-containing E3 ligase adaptors and cytoskeletal regulation were observed in various eukaryote species. In human cells, a BTB-Kelch substrate adaptor of a CUL3-based E3 ligase helps regulate mitotic progression and completion of cytokinesis by mediating degradation of Aurora B (Sumara et al., 2007). In *C. elegans*, the female germline-specific MATH-BTB protein MEL26 mediates degradation of a microtubule severing protein Katanin during the meiosis-to-mitosis transition, which enables formation of long microtubules necessary for proper anchoring of the spindle apparatus and chromosome segregation (Furukawa et al., 2003; Pintard et al., 2003). Similarly, in maize, a germline- and zygote-specific MATH-BTB protein ZmMAB1 interacts with the p60 unit of Katanin and regulates spindle length after the meiosis-to-mitosis transition in the male and female gametophyte. Although ZmMAB1 was shown to be essential for proper nuclei separation during germline development, it is unknown whether

interaction with Katanin is necessary for this process to occur (Juranić et al., 2012). Here, interaction of TaMAB2 with wheat Katanin was detected in the Y2H His prototrophy assay. However, Katanin also seems to interact with the activation domain of Gal4 (negative control), and therefore, true interaction with TaMAB2 in Y2H cannot be confirmed. Interaction of TaMAB2 with Katanin was also tested in a pull-down assay in our lab, but here as well, Katanin interacted with the empty GST tag (negative control), indicating that it might be a sticky protein (data not shown). A lack of interaction in a Y2H assay was also reported for actin11 and four different tubulin proteins (Bauer et al., 2019). Additionally, no interaction was found in Y2H for two translation initiation factors, eIF4A1 and eIF3G1, which were reported as putative TaMAB2 targets in a TAP-MS analysis (Bauer et al., 2019). Interestingly, a positive result in Y2H was obtained only for TaMAB2 interaction with CUL3 and itself, and the strongest interaction was its homodimerization (Bauer et al., 2019). Because all tested interaction partners so far were *Arabidopsis* proteins (except Katanin), there is a possibility that amino acid sequences of wheat and *Arabidopsis* homologs changed significantly enough for a lack of recognition in a heterologous system such as yeast. Additionally, these interactions might be conditioned by post-translational modifications which might not occur in yeasts, or the interaction partners are unable to enter yeast nuclei, which is where transcription of the reporter gene is induced. Interestingly, out of all TaMAB2 interactions studied to date, the previously reported TaMAB2-TaMAB2 interaction (Bauer et al., 2019) is the only one which could naturally occur, seeing how both interaction partners come from the same species. In the future, it would be interesting to repeat this experiment using wheat homologs. Moreover, other techniques for analysis of protein-protein interactions could be used to analyze possible interaction in vitro (e.g. pull-down, microscale thermophoresis) or in-vivo (e.g. bimolecular fluorescence complementation).

On a similar note, *Arabidopsis* represents a divergent host for a wheat protein, and overexpression of TaMAB2 in *Arabidopsis* does not come without caveats, as there is no assurance that the protein will behave in a physiologically relevant manner. *Arabidopsis* and wheat belong to families of eudicots and monocots, respectively, which diverged 140-150 million years ago (Chaw et al., 2004) and whose members have been shaped by distinct adaptive mechanisms to cope with changes in their respective environments. Firstly, *TaMAB2* is specifically expressed in the wheat zygote and two-celled proembryo, and is not observed in vegetative tissues (Leljak-Levanić et al., 2013). With this in mind, the results obtained on *Arabidopsis* seedlings overexpressing TaMAB2 cannot be

used to draw direct cause-and-effect relationships between the observed phenotypes and the true physiological roles of TaMAB2 in wheat embryos. Interestingly, analyses of *Arabidopsis* embryos overexpressing GFP-tagged TaMAB2 indicated no abnormalities in morphology or arrests in development (Škiljaica, 2016). However, this could have been due to inactivity of the CaMV 35S promoter during early embryogenesis, as a GFP signal could not be detected in embryos overexpressing GFP-tagged TaMAB2 during early embryogenesis (data not shown), similar to previous findings in cotton (Sunilkumar et al., 2002) and the *Arabidopsis* line overexpressing BPM1 (L104; from personal correspondence with Nataša Bauer).

Finally, following the previously proposed hypothesis that MATH-BTB proteins of grass species have expanded and diversified in response to diversification of their substrates and/or specific environmental constraints, a question arises on whether TaMAB2 will have true physiological targets in a species which did not undergo this type of expansion and diversification. However, based on results obtained in the TAP-MS analysis (Bauer et al., 2019), putative TaMAB2 interactors seem to be proteins involved in fundamental biological processes, such as cytoskeletal regulation and translation, which are usually conserved across eukaryotes (Erickson, 2007; Sonenberg & Dever, 2003), and thus contain components which are likely to be recognized by orthologous interactors. On the very opposite end lies the possibility that precisely the lack of physiological targets caused a bias of TaMAB2 towards less specific targets in *Arabidopsis*. At least in part, the latter hypothesis is discouraged by the fact that maize ZmMAB1 was shown to have a role in cytoskeletal regulation, in an experiment performed in a homologous system, i.e., in maize plants (Juranić et al., 2012), and that a direct interaction was reported between wheat TaMAB2 and *Arabidopsis* CUL3 (Bauer et al., 2019). In the future, additional efforts will need to be made to design homologous systems more suitable for investigation of direct protein-protein interactions of TaMAB2 and its putative targets in wheat.

5.3. Environmental cues affect BPM1 turnover

5.3.1. BPM1 is involved in drought and heat stress response

ABA and mannitol treatment caused accumulation of BPM1-GFP protein in root cell nuclei, but did not affect its protein stability. Additionally, BPM1 overexpressors exhibited higher germination

rates than wild type when treated with ABA and mannitol. These results indicate that BPM1 has important roles during drought response, and that its stable nuclear localization might have protective roles in this process. On the other hand, NaCl treatment destabilized BPM1, presumably through protein degradation, and decreased its nuclear localization. These results indicate that BPM1 is not required for salt stress response in *Arabidopsis*. The diffused fluorescent signal along the root stele might even indicate that the transgenic protein was being actively pushed out of root cells into the stele, perhaps due to a change in cellular requirements during conditions of salt stress. Different subcellular localization patterns of BPM1 could also indicate changes in BPM1 stability in different cell types in the root. Since whole seedlings are used for Western blot analyses, the information regarding protein stability in different cells is lost, but results of fluorescence microscopy analysis indicate that BPM1 stability might be cell type-dependent. A more sensitive *in situ* assay of root cells exposed to different stressors would be helpful in clarifying the exact cellular fate of BPM1 in different parts of the root. Furthermore, the striking changes in intracellular localization of BPM1 in different environmental conditions might be connected to two types of localization signals present in the BPM1 protein sequence, a nuclear localization signal at the very C-terminal end, which is sufficient to drive the protein into the nucleus and nucleolus, as well as two nuclear export signals present within the BTB and BACK domains of BPM1 (Leljak Levanić et al., 2012).

The observed stress-tolerant effect of BPM1 overexpressors in the germination assay was generally more pronounced in line L104 than line L003, which is in accordance with the previously described differences between the two lines. Namely, line L104 accumulates more transgenic mRNA and protein than line L003, and has a more pronounced phenotype, i.e. smaller rosettes, exaggerated flower opening, shorter siliques and early flowering (Škiljaica et al., 2020), which might explain the observed differences in the abiotic stress assays. Interestingly, the differences were least pronounced after treatment with NaCl, where results obtained for BPM1 overexpressors were similar to wild type, additionally indicating no involvement of BPM1 in salt stress response.

The results of the protein stability and germination assays agree with previous findings linking BPM proteins to drought response. Namely, BPM proteins mediate proteolysis of ATHB6, a transcription factor which is upregulated in response to conditions of water deficit and ABA treatment, and has been proposed to function as a regulator of growth and development in response to limited water availability (Henriksson et al., 2005; Himmelbach et al., 2002; Söderman et al.,

1999). *ATHB6* is a negative regulator of drought response, inhibiting expression of three drought- and ABA-responsive genes, *RESPONSIVE TO ABA 18 (RAB18)*, *RESPONSIVE TO DESICCATION 29B (RD29B)* and *RD22*. By mediating *ATHB6* proteolysis, *BPMs* positively regulate drought response (Lechner et al., 2011). Here, plants overexpressing *BPM1* were less sensitive to drought conditions, exhibiting higher germination rates than wild type. The results of the protein stability assays indicate that this was possibly mediated by the stable *BPM1* protein level in germinating seeds. However, higher resistance to ABA and/or drought was also shown for several plant lines with downregulated *BPM* genes. For example, the amiR-*bpm* line with downregulated *BPM1*, 4, 5, and 6 is tolerant to ABA (Lechner et al., 2011). Similarly, the double *bpm3 bpm5* mutant line with loss-of-function of *BPM3* and *BPM5* is more tolerant to ABA, while plants overexpressing *BPM3* and *BPM5* are more sensitive to ABA (Julian et al., 2019). On the other hand, the ami*BPM* line with downregulated *BPM1*, 2, 3, 4 and 5 exhibits less tolerance to drought (Morimoto et al., 2017). These results indicate complex dynamics of individual *BPM* proteins during drought response. In the future, it would be interesting to see whether downregulation of several *BPM* genes would lead to increased gene expression and/or protein stabilization of other family members, and, vice versa, if overexpression of selected *BPM* genes would cause downregulation of other genes and/or destabilization of their protein products.

Elevated temperature caused stabilization of transgenic *BPM1* protein. Relative expression levels of *BPM1-GFP* transgene remain unchanged at 37 °C, indicating no induction of the 35S promoter at elevated temperatures (Škiljaica et al., 2020). Additionally, the protein remains abundant at 37 °C even after treatment with protein synthesis inhibitor cycloheximide (Škiljaica et al., 2020). These results corroborate the hypothesis that accumulation of *BPM1* is a consequence of protein stabilization and not induced transgene expression. Additionally, elevated temperature treatment caused upregulation of *BPM1-3* in wild type plants. This is interesting in light of the recently described role of *BPMs* in degradation of *DREB2A*, a major transcription factor involved in dehydration and heat stress response (Morimoto et al., 2017). Although all six *BPM* proteins are able to interact with *DREB2A*, based on the constitutive nuclear localization of *BPM2*, this member was studied in more detail, and it was shown that it forms a complex with *DREB2A* after exposure to heat (Morimoto et al., 2017). The authors hypothesize that *DREB2A* levels need to be quickly fine-tuned in order to achieve optimal levels of available protein relative to external conditions. This enables plants to adapt to the changing environment but at the same time minimizes the

possible negative effects of overly abundant DREB2A on plant growth and productivity (Morimoto et al., 2017). The apparent stabilization of transgenic BPM1 in conditions of elevated temperature indicates that BPM proteins might be regulated in a similar fashion, with fast stabilization after exposure to heat stress in order to ensure steady levels of available protein, which can then quickly and efficiently mediate degradation of DREB2A. Protein levels of DREB2A markedly increase immediately after exposure to heat stress (0.5 – 1 h), and begin to drop after five hours of continuous heat stress (Morimoto et al., 2013). This could indicate the time frame in which the accumulated and stabilized BPM1 and/or other BPMs (especially BPM2) mediate DREB2A degradation. The link between heat-induced stabilization of BPM1 and degradation of DREB2A was further corroborated by the downregulation of DREB2A downstream targets *HsfA3* and *AT4G36010* in plants overexpressing BPM1. These results strongly suggest that overexpression of BPM1 leads to a decrease in DREB2A protein levels, presumably due to BPM1-mediated proteolysis of excess DREB2A in all conditions, but particularly during heat stress when BPM1 is additionally stabilized, which then affects the expression of its downstream targets. Combined with the increase in *BPM1-3* gene expression after exposure to elevated temperature, it appears that BPM1 might be regulated both transcriptionally and post-translationally in response to heat stress, and similar regulatory mechanisms might be employed in regulation of other BPM proteins.

5.3.2. Photoperiod and light signaling affect BPM1 stability

Besides water availability and temperature, light is another environmental signal which triggers a variety of cellular and systemic responses in plants. Plants with functional green chloroplasts capture light and use it as a source of energy via the process of photosynthesis. Light also serves as a trigger in signal transduction pathways which mediate adaptive responses such as phototropism (orientation of shoot growth towards a light source) and shade avoidance, and developmental transitions such as germination and flowering (Kami et al., 2010). Transgenic BPM1 was shown to be stabilized during the light period and degraded during the night period. Additionally, prolonged exposure to light led to a characteristic nuclear localization of transgenic protein, whereas prolonged exposure to dark caused diffusion of the BPM1 signal and, eventually, translocation to the stele. The diffusion of the BPM1 signal after incubation in the dark correlates

with the drop in BPM1 levels measured during normal photoperiod, indicating roles related to light signaling.

Results of gene expression analysis do not show significant perturbations in expression of *BPM* genes during photoperiod, but the slight increase in expression of *BPM* genes at the end of the dark period might suggest a negative feedback mechanism regulating *BPM* gene expression. Hypothetically, if protein levels of *BPM* genes drop during the night and rise up again at daylight, there would indeed be an increased need for synthesis of BPM proteins at the end of the dark period, reflected by a rise in gene expression. However, only *BPM2* and *BPM6* exhibited statistically significant increase in expression at the end of night period, in an experiment where three points of measurement were considered. Nevertheless, the two genes make interesting candidates for further and more detailed research of light-mediated changes in stability and function of BPM proteins.

BPM proteins have been associated with light signaling via interaction with several transcription factors belonging to different protein families. For instance, BPMs induce degradation of the transcriptional inhibitor MYB56, which negatively regulates the expression of FT, a major activator of flowering. Thus, BPMs act as a positive regulator of flowering (Chen et al. 2015). The relationship between MYB56 and FT is illustrated by their photoperiod-dependent expression patterns. While *FT* expression has two peaks, one around 10 a.m. and one around 6 p.m., with drops in between (Suárez-López et al., 2001; Chen et al., 2015), expression of *MYB56* is highest at 8 a.m. (when *FT* expression is still low) and lowest at 6 p.m. (Chen et al., 2015). Clearly, intrinsic levels of *MYB56* and *FT* transcripts fluctuate depending on time of day. MYB56 protein levels are stable throughout the day and drop around 6 p.m. (Chen et al., 2015), which follows the course of *MYB56* expression, but could also be induced by BPM-mediated degradation. Here, transgenic BPM1 levels remained stable at 6 p.m., indicating that its activity is physiologically required at this time of day, possibly to maintain MYB56 levels low. Additionally, BPM1 was specifically shown to mediate degradation of another MYB transcription factor and a negative regulator of *FT* expression, MYB106 (Hong et al., 2021). The link between MYB transcription factors, BPMs and regulation of flowering was also found in the flowering phenotypes of different transgenic plants. Firstly, null mutants of both *MYB56* and *MYB106* exhibit an early flowering phenotype (Chen et al., 2015; Hong et al., 2021). Next, plants overexpressing BPM1 also exhibit an early flowering phenotype, with a number of growth defects related to inflorescence (Škiljaica et al., 2020). Finally,

6xamiBPM plants with reduced *BPM* expression have a late-flowering phenotype (Chen et al., 2013). All modified plants studied to date indicate that low levels of MYB TFs and high levels of BPMs positively correlate with promotion of flowering.

Additionally, MYC2, MYC3, and MYC4 are described as interactors of BPM proteins (Chico et al., 2020). Protein levels of these transcription factors are fine-tuned during the day/night cycles to optimize the balance between growth and defense (Shin et al., 2012). However, photoperiod-dependent MYC2 stability is regulated by the activity of a RING-finger E3 ubiquitin ligase called CONSTITUTIVE PHOTOMORPHOGENIC1 (COP1) (Chico et al., 2014), while BPM proteins were specifically shown not to be involved in photoperiod-dependent degradation of MYC2 (Chico et al., 2020). This agrees with results of the present work, seeing how both BPM1 (this work) and MYC2 (Chico et al., 2014) are significantly destabilized in the dark.

BPM1 was also shown to interact with RAP2.4 (Weber & Hellmann, 2009), a transcription factor involved in ethylene and light signaling. RAP2.4 expression is down-regulated by light and overexpression of RAP2.4 causes defects in multiple developmental processes regulated by light and ethylene (Lin et al., 2008). However, involvement of BPM1-mediated regulation of RAP2.4 has not been investigated in more detail.

5.3.3 Transcriptional and post-translational regulation of BPM proteins

BPM proteins act as adaptors of CUL3-based E3 ligases to induce degradation of several transcription factors. Many of these transcription factors can be simultaneously involved in multiple processes, for instance, DREB2A is involved in drought and heat stress response, ATHB6 is involved in ABA and light signaling, RAP2.4 in light, salt and drought stress responses and MYC proteins are involved in light signaling and JA response (Henriksson et al., 2005; Lin et al., 2008; Lechner et al., 2011; Morimoto et al., 2017; Chico et al., 2020). All of these processes are related to environmental signaling. Here, BPM proteins most likely play a role in regulating levels of available transcription factors during stress response, with the aim of avoiding negative consequences of their overaccumulation (Julian et al., 2019; Morimoto et al., 2017). In turn, BPM proteins can be simultaneously involved in regulation of multiple processes, and they can target different proteins involved in the same process. For instance, BPM proteins target ATHB6 and DREB2A, which have conflicting roles in drought response. While DREB2A positively regulates

drought response, *ATHB6* is a negative regulator of ABA signaling as part of drought response (Lechner et al., 2011; Morimoto et al., 2017). In *amiR-bpm* plants, the negative effect of *ATHB6* accumulation outweighs the positive effect of *DREB2A* accumulation in drought conditions, with plants exhibiting drought sensitivity despite the upregulation of *DREB2A* gene targets involved in drought response, illustrating the importance of BPM proteins in regulating the strength of stress response (Morimoto et al., 2017).

In order to maintain optimal levels of all transcription factors necessary for a certain type of stress response, plant cells need to maintain optimal levels of their regulators, such as BPM proteins. One possible mode of regulation of BPM proteins is at the level of protein stability. BPM protein stability differed in response to varying stress conditions, remaining unchanged in drought stress, increasing in response to elevated temperature and decreasing in response to salt stress. To date, stability of individual BPM proteins has been the focus of only one research study. Chico et al. (2020) showed that 1 h and especially 3 h of JA treatment stabilizes BPM3, similar to the stabilization of BPM1 in response to elevated temperature. Interestingly, although both BPM3 and BPM6 were described as regulators of MYC2, MYC3 and MYC4 as part of the JA signaling pathway, JA treatment did not stabilize BPM6, indicating individual physiological responses of the two proteins. BPM3 and BPM6 additionally differ in their intrinsic stability, with BPM3, unlike BPM6, being highly unstable and short-lived (Chico et al., 2020). Despite their sequence conservation and constitutive gene expression, BPM proteins seem to possess individual differences, possibly to ensure a more varied stress response. Further research should reveal whether BPM2-6 are stabilized by drought and elevated temperature as shown here for BPM1. At least with regards to elevated temperature, increased protein stability of BPM2 would be expected, based on the significant *BPM2* gene expression increase in response to elevated temperature, but also considering the stable BPM2-DREB2A complex which forms during heat-stress (Morimoto 2017). An important question remains to be answered – how is BPM protein stability regulated? Treatment with MG132, an inhibitor of 26S proteasome, indicated that BPM3 is degraded by the proteasome (Chico et al., 2020; Lechner et al., 2011), and a similar result was obtained for BPM1 (Škiljaica et al., 2020), but the exact regulatory mechanism is still unknown. Additional studies should reveal whether specific post-translational modifications are necessary for the BPM proteins to be stabilized, or whether an increase in stability is achieved by a decrease in protein levels of an unknown negative regulator. A Cul3-based E3 ligase might mediate BPM1 degradation, as

indicated by significant stabilization of recombinant BPM1 after treatment of transgenic plants with the rubylation inhibitor MLN4924 (Škiljaica et al., 2020).

The second possible mode of BPM regulation is at the level of gene expression. Chico et al. (2020) show that *BPM* genes are not transcriptionally regulated by JA (Chico et al., 2020), which is similar to the results of relative gene expression analyses of endogenous *BPM* genes after ABA and mannitol treatment, but different from results of elevated temperature treatment, which did show significant perturbations in expression of several *BPM* members. To date, regulation of *BPM* gene expression has not been extensively studied. However, a recent study demonstrated that an RNA-binding protein ARABIDOPSIS PUMILIO PROTEIN 24 (APUM24) directly reduces stability of *BPM3* and *BPM6* mRNAs via binding of Pumilio response elements in their 3'UTRs (Huang et al., 2021). BPM proteins mediate degradation of transcription factor WRI1, affecting seed maturation and fatty acid biosynthesis (Chen et al., 2013), and regulation of *BPM* expression via APUM24 has direct consequences on these developmental processes (Huang et al., 2021). It would be interesting to investigate whether this type of regulation might be involved in environmental responses as well, especially during heat stress response which seems to invoke differential expression of *BPM* genes.

A third possible mode of BPM regulation is at the level of RNA splicing, as shown here for *BPM2* gene in conditions of elevated temperature and cold stress. In eukaryotes, a gene can be transcribed into a full-length transcript which is later translated into a fully functional protein, but it can also give rise to a transcript which contains an in-frame premature termination codon, which can either be targeted for degradation by nonsense-mediated decay, or translated into a truncated protein with no or limited activity (Mastrangelo et al., 2012). This process plays an important role in plant biotic and abiotic stress responses. Interestingly, alternative splicing events in conditions of abiotic stress have been mostly described for genes with regulatory roles, such as E3 ubiquitin ligases, protein kinases involved in phosphorylation cascades, transcription factors and others (Mastrangelo et al., 2012 and references cited therein). To date, specific splicing events in *BPM* genes, or other plant *MATH-BTB* genes, have not been investigated in relation to environmental conditions. However, the fact that the *BPM2.5* transcript becomes highly abundant in conditions of elevated temperature and cold stress indicates that this protein variant plays a more dominant role in this type of stress response. This role is most likely related to the known function of MATH-BTB proteins as part of the CUL3-E3 ligase, as the protein contains full-length MATH and BTB domains, including all eight amino-acid residues within the BTB domain shown to mediate CUL3-binding of *C. elegans*

MEL-26 and *S. pombe* BTB3, and most likely other MATH-BTB proteins (Geyer et al., 2003; Gingerich et al., 2005; Xu et al., 2003). The other two splice variants analyzed here are *BPM2.3* and *BPM2.4*. Remarkably, after elevated temperature treatment (but not cold stress), the *BPM2.3* transcript was five times more abundant and the *BPM2.4* transcript was significantly less abundant compared to control. The *BPM2.4* transcript might be undergoing nonsense-mediated decay, to prevent accumulation of the truncated protein, but in that case, a similar course of action would be expected for *BPM2.3*, as their lengths and amino acid sequences are nearly identical (95% pairwise identity). The different profiles present a challenging question with regards to post-transcriptional regulation of different splicing variants. Nevertheless, temperature-induced alternative splicing offers an additional layer of gene expression regulation, equipping plants with an even more nuanced stress response. One possible role of alternative splicing is auto-regulation. For instance, alternative splicing induced by heat stress was found in *HsfA2*, a gene which encodes a key regulator of heat stress response in *Arabidopsis* (Sugio et al., 2009). Another study revealed that exposure to severe heat generates a cryptic 5' splice site in the intron of the *HsfA2* gene, creating the HsfA2-III splice variant, and the resulting protein product promotes self-regulation of *HsfA2* expression (Liu et al., 2013). Juranić & Dresselhaus (2014) propose that the number of splicing variants is related to the number of genes in a family. For instance, the total number of maize *MATH-BTB* genes is lower compared to rice, *Sorghum* and *Brachypodium*, but maize *MATH-BTB* genes contain a higher number of splicing variants, which were speculated to have a role in exerting regulatory effects on full-length variants (Juranić & Dresselhaus, 2014). Moreover, of the two human *SPOP* genes, one was estimated to have as much as 23 splicing variants (Juranić & Dresselhaus, 2014). Following this hypothesis, the small family of six *MATH-BTB* genes in *Arabidopsis* is even more likely to use its 17 splicing variants for regulatory functions, however, this is yet to be tested. Perhaps the most interesting finding of the transcript abundance analysis in conditions of elevated temperature was the highest increase measured for the truncated *BPM2.3* and the full-length *BPM2.5* variant. The *BPM2.3* variant lacks the BACK domain and three conserved amino acid residues presumed to be important for interaction with CUL3. Therefore, the *BPM2.3* variant is most likely incapable of a fully functional interaction with CUL3. Why would this variant be predominantly expressed during heat stress? It is tempting to speculate that BPM proteins have additional roles, which require their ability to bind protein substrates (i.e. the presence of a functional MATH domain) but not in a CUL3-dependent manner and therefore

possibly not related to proteasomal degradation. The existence of different forms of BPM proteins would allow plants to exert both functions simultaneously, and therefore to combat environmental stress on multiple fronts.

It appears that BPM proteins can be regulated on multiple levels, either transcriptionally (at the level of gene expression), post-transcriptionally (at the level of differential splicing), or post-translationally (at the level of protein stability), and that different environmental cues can induce some or none of these modes of regulation, depending on the gene or protein member. The results of this work present the possibility of a fourth mode of BPM regulation, via changes in subcellular localization. While higher BPM1 protein stability positively correlated with nuclear accumulation, lower protein stability (such as after salt stress and in the dark) correlated with weaker nuclear signal and eventually translocation to the root stele. However, it is unclear whether dispersion of this signal was a consequence of transgenic protein degradation and accumulation in the root stele. Nevertheless, subcellular localization of BPM1 presents an intriguing topic, seeing how the protein variant BPM1.1, which was used for generation of BPM1-overexpressing plants (Škiljaica et al., 2020), possesses both a nuclear localization signal and two nuclear export signals (NES) in its sequence (Leljak Levanić et al., 2012). The BPM1.2 protein variant contains additional 35 amino acids in the BTB domain, and within it are two additional putative NES sequences (Leljak Levanić et al., 2012), which indicates subtle differences in the roles of the two variants at the level of their subcellular localizations.

This work gives novel insights into different levels of BPM regulation in response to different external stimuli. Because changes in environmental conditions are “sensed” on the outside and communicated to the inside through various channels, depending on the type of environmental cue, one of the most challenging questions for future research is the point at which all these responses converge to ultimately affect BPM proteins in a way that ensures optimal levels for all of its various functions. This is especially important with regards to different environmental stressors, which in nature often affect plants simultaneously, and which are, with progression of climate change, becoming leading concerns for scientists in various areas of plant biology.

5.4. Evaluation of RT-qPCR candidate reference genes

Changes in environmental temperature significantly affect fundamental plant processes such as photosynthesis, respiration and metabolite synthesis, consequently influencing biomass yield, seed ripening and germination, as well as shifts between plant developmental programs (Lawlor, 2005). The currently accepted global climate change model predicts increases in overall temperature in the upcoming years (Meehl et al., 2007). With the aim of generating more resistant crop species, the scientific community responded with various gene expression analyses of potential regulators and other major players in the molecular cascades of plant heat stress response. Many of these studies use RT-qPCR, a medium-scale gene expression analysis method which offers both speed and sensitivity. The reliability of RT-qPCR results largely depends on proper implementation of the method, which, among other procedural requirements, demands the use of suitable reference genes. Inaccurate normalization of RT-qPCR data can cause misinterpretation of gene expression results and, ultimately, false conclusions (Bustin et al., 2009).

RT-qPCR was extensively used throughout this work to assess expression of different genes under various circumstances, including elevated temperature. In these experiments, a single reference gene, *RHIP1*, was used for normalization of expression data. *RHIP1* was selected based on previous empirical validation in specific laboratory settings. However, when literature was searched for more reference genes validated for use in experiments employing elevated temperatures, detailed validation studies were found for numerous plant species (Gao et al., 2017; Janská et al., 2013; Jin et al., 2019; Liu et al., 2020; Paolacci et al., 2009), but not for *Arabidopsis*. Czechowski et al. (2005) completed the first detailed study based on microarray data, in which several reference genes suitable for use in RT-qPCR experiments on *Arabidopsis* are identified and validated. The study includes data from different developmental stages, abiotic and biotic stresses, hormone stress and nutrient stress (Czechowski et al., 2005). Another extensive validation study includes data on seedlings exposed to 16 °C and 23 °C (Hong et al., 2010). In both papers, the results are based on a single tissue and no more than two temperatures (Hong et al., 2010), or only cold (4 °C) stress (Czechowski et al., 2005). Moreover, in Czechowski et al. (2005), to validate reference gene stability, cold stress samples were pooled together with 19 other samples obtained from different plant tissues, stresses or growth conditions, and no reference genes were proposed specifically for cold treatment.

Here, the recommended gene combinations for use in gene expression normalization of RT-qPCR data in experiments employing elevated temperature treatments were as follows: *OGIO* and *PUX7*

in seedlings, *UBC21* and *PUX7* in leaves, *TIP41* and *UBC21* in flower buds, and *TIP41* and *UBC21* in all three tissues combined. Interestingly, *UBC21*, a traditional reference gene, was shown as the optimal reference gene in three out of four cases. Similar results were shown previously, as in the case of stable expression of *GAPDH* in seedlings of *Arabidopsis pumila* exposed to 40 °C and 4 °C and *TUBα* and *EF1α* in seedlings of strawberry exposed to 38 °C and 4 °C, respectively (Jin et al., 2019; Liu et al., 2020). Moreover, expression of *MON1*, *PP2AA3*, *RHIP1* and *TIP41* is proposed to be stable in the analysis which comprises data from more than one tissue, namely rosette leaves and flowers (Hong et al., 2010), which implies expression stability of these genes not only across different temperatures but also across different temperature-treated tissues. Out of the ten analyzed candidate reference genes, five appear on stability rankings provided by Klepikova et al. (2016) in an RNA-seq analysis, namely *TIP41*, *MON1*, *PP2AA3*, *PUX7* and *UBC21*. This analysis, however, did not include temperature-treated tissues other than leaves at 42 °C but did include various others developmental stages exposed to different abiotic stresses (Klepikova et al., 2016).

To validate the reliability of top-ranked reference genes, a *DREB2A*-based relative gene expression analysis was performed. When geometric mean data of expression of two most stable genes was used for normalization of *DREB2A* expression data, relative gene expression levels were more accurately represented than when only a single gene was used. However, the provided correction was subtle, probably due to both genes being of similarly high stability. The importance of using multiple reference genes and the corrective effect of highly stable genes was more apparent in combination with least stable genes. When the low-ranked gene was individually used for normalization, *DREB2A* expression appeared artificially enhanced but when it was used in combination with top-ranked genes, this deviation was largely corrected, with expression levels pulled back toward the range provided by top-ranked genes. On the other hand, in the experiment where *DWAI* and *RHIP1* were used for normalization of expression in samples of seedlings exposed to 37 °C and 4 °C, addition of the less stable *DWAI* in the heat-based experiment resulted in a substantial shift in reported expression, which was absent when only *RHIP1* was used for normalization. This indicates that a single reference gene of high stability will give more reliable results than two genes of which one has more unstable expression in a given set of experimental conditions.

All RT-qPCR experiments described in the first part of this dissertation (analyzing *BPM* genes, *HsfA3* and *AT4G36010*) were performed on seedlings. The list of reference genes validated for use in two additional tissues, leaves and flowers, provides a wide choice of reference genes for use in further functional analyses of BPM proteins in these tissues. These experiments would be of great importance for better understanding of the various roles BPM proteins play in specific *Arabidopsis* tissues. Flowers might be especially interesting, considering the high expression of endogenous *BPM* genes in floral buds and open flowers compared to other tissues (Lechner et al., 2011), as well as the highest accumulation of BPM1 protein in flowers of BPM1-overexpressing plants compared to other tissues (Škiljaica et al., 2020).

Furthermore, although this work was focused on validation of reference genes in conditions of elevated temperature (22 – 42 °C), microarray data obtained from experiments using both low and elevated temperature treatments was used for selection of candidate reference genes (Škiljaica et al., 2022). Two genes were indeed shown to have stable expression in an experiment employing 4 °C treatment, *DWA1* and *RHIP1*, indicating that the list of candidate reference genes could be used as a pool of reference genes for further validation studies in experiments employing cold treatment. Finally, orthologs of the ten reference genes validated in this work could serve as candidate reference genes in other plant species. This has already been demonstrated in seeds of *A. thaliana* and *Solanum lycopersicum*, where six out of seven reference genes previously confirmed as stable in *A. thaliana* were also stable in *S. lycopersicum* (Dekkers et al., 2012). Similarly, in different developmental stages and in the cambial region of *A. thaliana* and hybrid aspen, two out of four reference genes considered stable in *A. thaliana* were also found to be stable in hybrid aspen (Gutierrez et al., 2008). Preliminary research in our laboratory showed that *OGIO* and *PUX7* are adequate reference genes for use in experiments employing elevated temperatures in *Brassica rapa* and that *OGIO* is stable in *Brassica oleracea* var. *acephala*, while neither gene is highly stable in *S. lycopersicum* (unpublished data, courtesy of Nataša Bauer and Mirta Tokić).

Reference genes validated for use in *Arabidopsis* RT-qPCR experiments employing non-optimal temperatures provide a valuable source of data for better implementation of the RT-qPCR method. Whether they are used for research performed in *Arabidopsis*, or in studies performed in closely related crop species, suitable reference genes could contribute to the fast-growing field studying both the consequences of heat stress on plant growth and development, but also the adaptive capabilities of economically important plants faced with climate change.

6. CONCLUSIONS

1. Forty-six putative *MATH-BTB* genes in the wheat genome indicate a significant expansion of the *MATH-BTB* family in wheat. While *Arabidopsis* BPM proteins cluster into the smaller core clade, wheat TaMAB proteins cluster into the grasses-specific expanded clade.
2. The MATH domain of expanded clade wheat TaMAB proteins is less conserved than the BTB domain. The opposite is true for core clade MATH-BTB proteins, indicating different evolutionary processes shaping the two clades of the *MATH-BTB* family.
3. TaMAB2 might be part of a CUL3-based E3 ubiquitin ligase complex, with possible roles in cytoskeletal regulation.
4. The BPM family is regulated on various levels and with dependence on environmental conditions:
 - a) Involvement of BPM1 protein in drought response is possibly mediated by nuclear localization and maintained protein stability, but not through changes in gene expression.
 - b) Involvement of BPM1 protein in heat stress response is possibly mediated through strong nuclear accumulation and increased protein stability.
 - c) Elevated temperature causes upregulation of *BPM1*, *BPM2* and *BPM3*, indicating regulation at the level of gene expression. The *BPM2.5* splicing variant is significantly more abundant after exposure to both elevated temperature and cold stress compared to control, indicating a dominant role of this protein variant as well as regulation at the level of RNA splicing.
 - d) BPM1 protein stability is sensitive to photoperiod and light exposure, with stabilization and preferential nuclear localization during the day and degradation during the night.
5. Overexpression of BPM1 results in downregulation of two DREB2A-regulated genes, confirming a previously shown role of BPM proteins in DREB2A degradation.
6. The recommended reference genes for normalization of expression data in RT-qPCR experiments employing elevated temperature treatments of *Arabidopsis* tissues are as follows:

OGIO and *PUX7* in seedlings, *UBC21* and *PUX7* in leaves, *TIP41* and *UBC21* in flower buds, and *TIP41* and *UBC21* in all three tissues combined.

7. REFERENCES

- Al-Saharin R., Hellmann H., Mooney S. (2022). Plant E3 ligases and their role in abiotic stress response. *Cells* 11, 890. doi:10.3390/cells11050890
- Agatep, R., Kirkpatrick, R. D., Parchaliuk, D. L., Woods, R. A., and Gietz, R. D. (1988). Transformation of *Saccharomyces cerevisiae* by the lithium acetate/single-stranded carrier DNA/polyethylene glycol protocol. *Tech. Tips Online* 3, 133–137. doi:10.1016/S1366-2120(08)70121-1.
- Bauer, N., Škiljaica, A., Malenica, N., Razdorov, G., Klasić, M., Juranić, M., et al. (2019). The MATH-BTB protein TaMAB2 accumulates in ubiquitin-containing foci and interacts with the translation initiation machinery in *Arabidopsis*. *Front. Plant Sci.* 10, 1469. doi:10.3389/fpls.2019.01469.
- Beathard, C., Mooney, S., Al-Saharin, R., Goyer, A., and Hellmann, H. (2021). Characterization of *Arabidopsis thaliana* R2R3 S23 MYB transcription factors as novel targets of the ubiquitin proteasome-pathway and regulators of salt stress and abscisic acid response. *Front. Plant Sci.* 12, 629208. doi:10.3389/FPLS.2021.629208/BIBTEX.
- Birchler, J. A., and Veitia, R. A. (2007). The gene balance hypothesis: From classical genetics to modern genomics. *Plant Cell* 19, 395–402. doi:10.1105/tpc.106.049338.
- Bostick, M., Lochhead, S. R., Honda, A., Palmer, S., and Callis, J. (2004). Related to ubiquitin 1 and 2 are redundant and essential and regulate vegetative growth, auxin signaling, and ethylene production in *Arabidopsis*. *Plant Cell* 16, 2418–2432. doi:10.1105/tpc.104.024943.
- Bowers, J. E., Chapman, B. A., Rong, J., and Paterson, A. H. (2003). Unravelling angiosperm genome evolution by phylogenetic analysis of chromosomal duplication events. *Nature* 422, 433–438. doi:10.1038/nature01521.
- Bustin S. (2002). Quantification of mRNA using real-time reverse transcription PCR (RT-PCR): trends and problems. *J. Mol. Endocrinol.* 29, 23–39.
- Canning, P., Cooper, C., Krojer, T., Murray, J. W., Pike, A., Chaikuad, A., et al. (2013). Structural basis for Cul3 protein assembly with the BTB-Kelch family of E3 ubiquitin ligases. *J. Bio. Chem.* 288, 7803–7814. doi:10.1074/jbc.M112.437996.
- Chaw, S. M., Chang, C. C., Chen, H. L., and Li, W. H. (2004). Dating the monocot-dicot divergence and the origin of core eudicots using whole chloroplast genomes. *J. Mol. Evol.* 58, 424–441. doi:10.1007/s00239-003-2564-9.
- Chen, L., Bernhardt, A., Lee, J., and Hellmann, H. (2015). Identification of *Arabidopsis* MYB56 as a novel substrate for CRL3BPM E3 ligases. *Mol. Plant* 8, 242–250. doi:10.1016/J.MOLP.2014.10.004.
- Chen, L., and Hellmann, H. (2013). Plant E3 ligases: Flexible enzymes in a sessile world. *Mol. Plant* 6, 1388–1404. doi:10.1093/mp/sst005.
- Chen, L., Lee, J. H., Weber, H., Tohge, T., Witt, S., Roje, S., et al. (2013). *Arabidopsis* BPM proteins function as substrate adaptors to a cullin3-based E3 ligase to affect fatty acid metabolism in plants. *Plant Cell* 25, 2253–64. doi:10.1105/tpc.112.107292.
- Chen, M. H., Wilson, C. W., Li, Y. J., Law, K. K. Lo, Lu, C. S., Gacayan, R., et al. (2009). Cilium-independent regulation of Gli protein function by Sufu in Hedgehog signaling is evolutionarily conserved. *Genes Dev.* 23, 1910–1928. doi:10.1101/gad.1794109.

- Chico, J. M., Fernández-Barbero, G., Chini, A., Fernández-Calvo, P., Díez-Díaz, M., and Solano, R. (2014). repression of jasmonate-dependent defenses by shade involves differential regulation of protein stability of MYC transcription factors and their JAZ repressors in Arabidopsis. *Plant Cell* 26, 1967–1980. doi:10.1105/TPC.114.125047.
- Chico, J. M., Lechner, E., Fernandez-Barbero, G., Canibano, E., García-Casado, G., Franco-Zorrilla, J. M., et al. (2020). CUL3BPM E3 ubiquitin ligases regulate MYC2, MYC3, and MYC4 stability and JA responses. *Proc. Natl. Acad. Sci.* 117, 6205–6215. doi:10.1073/PNAS.1912199117.
- Clark, A., and Burleson, M. (2020). SPOP and cancer: a systematic review. *Am. J. Cancer Res.* 10, 704–726.
- Cutler, S. R., Rodriguez, P. L., Finkelstein, R. R., and Abrams, S. R. (2010). Abscisic acid: Emergence of a core signaling network. *Annu. Rev. Plant Biol.* 61, 651–679. doi:10.1146/annurev-arplant-042809-112122.
- Czechowski, T., Stitt, M., Altmann, T., Udvardi, M. K., and Scheible, W.-R. D. (2005). Genome-wide identification and testing of superior reference genes for transcript normalization in Arabidopsis. *Genome Anal.* 139, 5–17. doi:10.1104/pp.105.063743.
- D’hont, A., Denoeud, F., Aury, J. M., Baurens, F. C., Carreel, F., Garsmeur, O., et al. (2012). The banana (*Musa acuminata*) genome and the evolution of monocotyledonous plants. *Nature* 488, 213–217. doi:10.1038/nature11241.
- Dekkers, B. J. W., Willems, L., Bassel, G. W., van Bolderen-Veldkamp, R. P., Ligterink, W., Hilhorst, H. W. M., et al. (2012). Identification of reference genes for RT-qPCR expression analysis in Arabidopsis and tomato seeds. *Plant Cell Physiol.* 53, 28–37. doi:10.1093/pcp/pcr113.
- Dieterle, M., Thomann, A., Renou, J. P., Parmentier, Y., Cognat, V., Lemonnier, G., et al. (2005). Molecular and functional characterization of Arabidopsis Cullin 3A. *Plant J.* 41, 386–399. doi:10.1111/J.1365-313X.2004.02302.X.
- Erickson H.P. (2007). Evolution of the cytoskeleton. *BioEssays* 29, 668-77. doi:10.1002/bies.20601.
- Errington W.J., Khan M.Q., Bueler S.A., Rubinstein J.L., Chakrabartty A. and Privé G.G. (2012). Adaptor protein self-assembly drives the control of a cullin-RING ubiquitin ligase. *Structure* 20, 1141–1153. doi:10.1016/j.str.2012.04.009.
- Feilotter, H. E., Hannon, G. J., Ruddell, C. J., and Beach, D. (1994). Construction of an improved host strain for two hybrid screening. *Nucleic Acids Res.* 22, 1502–1503. doi:10.1093/nar/22.8.1502.
- Figuroa, P., Gusmaroli, G., Serino, G., Habashi, J., Ma, L., Shen, Y., et al. (2005). Arabidopsis has two redundant Cullin3 proteins that are essential for embryo development and that interact with RBX1 and BTB proteins to form multisubunit E3 ubiquitin ligase complexes in vivo. *Plant Cell* 17, 1180–1195. doi:10.1105/tpc.105.031989.
- Finkelstein, R. R., Gampala, S. S. L., and Rock, C. D. (2002). Abscisic acid signaling in seeds and seedlings. *Plant Cell* 14 (Issue Supplement), S15–45. doi:10.1105/tpc.010441.
- Furukawa, M., He, Y. J., Borchers, C., and Xiong, Y. (2003). Targeting of protein ubiquitination by BTB-Cullin 3-Roc1 ubiquitin ligases. *Nat. Cell Biol.* 5, 1001–1007. doi:10.1038/ncb1056.
- Gao, M., Liu, Y., Ma, X., Shuai, Q., Gai, J., and Li, Y. (2017). Evaluation of reference genes for normalization of gene expression using quantitative RT-PCR under aluminum, cadmium, and heat stresses in soybean. *PLoS One* 12, e0168965. doi:10.1371/journal.pone.0168965.

- Genschik, P., Sumara, I., and Lechner, E. (2013). The emerging family of CULLIN3-RING ubiquitin ligases (CRL3s): cellular functions and disease implications. *EMBO J.* 32, 2307–2320. doi:10.1038/emboj.2013.173.
- Geyer, R., Wee, S., Anderson, S., Yates, J., & Wolf, D. A. (2003). BTB/POZ domain proteins are putative substrate adaptors for cullin 3 ubiquitin ligases. *Molecular Cell* 12, 783–790. https://doi.org/10.1016/s1097-2765(03)00341-1.
- Gingerich, D. J., Gagne, J. M., Salter, D. W., Hellmann, H., Estelle, M., Ma, L., et al. (2005). Cullins 3a and 3b assemble with members of the Broad Complex/Tramtrack/Bric-a-Brac (BTB) protein family to form essential ubiquitin-protein ligases (E3s) in Arabidopsis. *J. Biol. Chem.* 280, 18810–18821. doi:10.1074/jbc.M413247200.
- Gingerich, D. J., Hanada, K., Shiu, S.-H., and Vierstra, R. D. (2007). Large-scale, lineage-specific expansion of a bric-a-brac/tramtrack/broad complex ubiquitin-ligase gene family in rice. *Plant Cell* 19, 2329–2348. doi:10.1105/tpc.107.051300.
- Gouy, M., Guindon, S., and Gascuel, O. (2010). SeaView version 4: A multiplatform graphical user interface for sequence alignment and phylogenetic tree building. *Mol. Biol. Evol.* 27, 221–224. doi:10.1093/molbev/msp259.
- Gutierrez, L., Mauriat, M., Gunin, S., Pelloux, J., Lefebvre, J.-F., Louvet, R., et al. (2008). The lack of a systematic validation of reference genes: a serious pitfall undervalued in reverse transcription-polymerase chain reaction (RT-PCR) analysis in plants. *Plant Biotechnol. J.* 6, 609–618. doi:10.1111/j.1467-7652.2008.00346.x.
- Hara, T., Ishida, H., Raziuddin, R., Dorkhom, S., Kamijo, K., and Miki, T. (2004). Novel Kelch-like Protein, KLEIP, is involved in actin assembly at cell-cell contact sites of Madin-Darby canine kidney cells. *Mol. Biol. Cell* 15, 1172–1184. doi:10.1091/MBC.E03-07-0531.
- Hatfield, P.M., Gosink, M.M., Carpenter, T.B., Vierstra, R.D. (1997). The ubiquitin-activating enzyme (E1) gene family in Arabidopsis thaliana. *Plant J. Cell Mol. Biol.* 11, 213–226. doi:10.1046/j.1365-313x.1997.11020213.x
- Hellemans, J., Mortier, G., De Paepe, A., Speleman, F., and Vandesompele, J. (2007). qBase relative quantification framework and software for management and automated analysis of real-time quantitative PCR data. *Genome Biol.* 8, R19. doi:10.1186/gb-2007-8-2-r19.
- Henriksson, E., Olsson, A. S. B., Johannesson, H., Johansson, H., Hanson, J., Engström, P., et al. (2005). Homeodomain leucine zipper class I genes in Arabidopsis. Expression patterns and phylogenetic relationships. *Plant Physiol.* 139, 509–518. doi:10.1104/pp.105.063461.
- Hershko, A., and Ciechanover, A. (1998). The ubiquitin system. *Annu. Rev. Biochem.* 67, 425–479. doi:10.1146/annurev.biochem.67.1.425.
- Himmelbach, A., Hoffmann, T., Leube, M., Höhener, B., and Grill, E. (2002). Homeodomain protein ATHB6 is a target of the protein phosphatase ABI1 and regulates hormone responses in Arabidopsis. *EMBO J.* 21, 3029–3038. doi:10.1093/emboj/cdf316.
- Hong, S. M., Bahn, S. C., Lyu, A., Jung, H. S., and Ahn, J. H. (2010). Identification and testing of superior reference genes for a starting pool of transcript normalization in Arabidopsis. *Plant Cell Physiol.* 51, 1694–1706. doi:10.1093/pcp/pcq128.
- Hong, L., Niu, F., Lin, Y., Wang, S., Chen, L., and Jiang, L. (2021). MYB106 is a negative regulator and a substrate for CRL3BPM E3 ligase in regulating flowering time in Arabidopsis thaliana. *J. Integr. Plant Biol.* 63, 1104–1119. doi:10.1111/JIPB.13071.

- Huang, R., Liu, M., Gong, G., Wu, P., Patra, B., Yuan, L., et al. (2021). The Pumilio RNA-binding protein APUM24 regulates seed maturation by fine-tuning the BPM-WRI1 module in Arabidopsis. *J. Integr. Plant Biol.* 63, 1240–1259. doi: 10.1111/jipb.13092.
- Janská, A., Hodek, J., Svoboda, P., Zámečník, J., Prášil, I. T., Vlasáková, E., et al. (2013). The choice of reference gene set for assessing gene expression in barley (*Hordeum vulgare* L.) under low temperature and drought stress. *Mol. Genet. Genomics* 288, 639–649. doi:10.1007/s00438-013-0774-4.
- Jin, Y., Liu, F., Huang, W., Sun, Q., and Huang, X. (2019). Identification of reliable reference genes for qRT-PCR in the ephemeral plant *Arabidopsis pumila* based on full-length transcriptome data. *Sci. Rep.* 9, 1–11. doi:10.1038/s41598-019-44849-1.
- Julian, J., Coego, A., Lozano-Juste, J., Lechner, E., Wu, Q., Zhang, X., et al. (2019). The MATH-BTB BPM3 and BPM5 subunits of Cullin3-RING E3 ubiquitin ligases target PP2CA and other clade A PP2Cs for degradation. *Proc. Natl. Acad. Sci. U. S. A.* 116, 15725–15734. doi:10.1073/pnas.1908677116.
- Juranić, M., and Dresselhaus, T. (2014). Phylogenetic analysis of the expansion of the MATH-BTB gene family in the grasses. *Plant Signal. Behav.* 9, e28242. doi:10.4161/psb.28242.
- Juranić, M., Srilunchang, K., Krohn, N. G., Leljak-Levanic, D., Sprunck, S., and Dresselhaus, T. (2012). Germline-specific MATH-BTB substrate adaptor MAB1 regulates spindle length and nuclei identity in maize. *Plant Cell* 24, 4974–91. doi:10.1105/tpc.112.107169.
- Kami, C., Lorrain, S., Hornitschek, P., and Fankhauser, C. (2010). Light-regulated plant growth and development. *Curr. Top. Dev. Biol.* 91, 29–66. doi:10.1016/S0070-2153(10)91002-8.
- Klepikova, A. V., Kasianov, A. S., Gerasimov, E. S., Logacheva, M. D., and Penin, A. A. (2016). A high resolution map of the *Arabidopsis thaliana* developmental transcriptome based on RNA-seq profiling. *Plant J.* 88, 1058–1070. doi:10.1111/tpj.13312.
- Komander, D., and Rape, M. (2012). The ubiquitin code. *Annu. Rev. Biochem.* 81, 203–229. doi:10.1146/annurev-biochem-060310-170328.
- Kraft, E., Stone, S.L., Ma, L., Su, N., Gao, Y., Lau, O.S., Deng, X.W., Callis, J. (2005). Genome analysis and functional characterization of the E2 and RING-type E3 ligase ubiquitination enzymes of *Arabidopsis*. *Plant Physiol.* 139, 1597–1611. doi:10.1104/pp.105.067983
- Kushwaha, H. R., Joshi, R., Pareek, A., and Singla-Pareek, S. L. (2016). MATH-domain family shows response toward abiotic stress in *Arabidopsis* and rice. *Front. Plant Sci.* 7, 923. doi:10.3389/fpls.2016.00923.
- Larkin, M. A., Blackshields, G., Brown, N. P., Chenna, R., McGettigan, P. A., McWilliam, H., et al. (2007). Clustal W and Clustal X version 2.0. *Bioinformatics* 23, 2947–2948. doi:10.1093/bioinformatics/btm404.
- Lawlor D.W. (2005). “Plant responses to climate change: impacts and adaptation.” in *Plant Responses to Air Pollution and Global Change (Springer Japan)*, 81–88.
- Lechner, E., Leonhardt, N., Eisler, H., Parmentier, Y., Alioua, M., Jacquet, H., et al. (2011). MATH/BTB CRL3 receptors target the homeodomain-leucine zipper ATHB6 to modulate abscisic acid signaling. *Dev. Cell* 21, 1116–1128. doi:10.1016/j.devcel.2011.10.018.
- Leljak Levanić D., Horvat T., Martinčić J. and Bauer N. (2012). A novel bipartite nuclear localization signal guides BPM1 protein to nucleolus suggesting its Cullin3 independent function. *PLoS One*

- 7, 1–10. doi:10.1371/journal.pone.0051184.
- Leljak-Levanić, D., Juranić, M., and Sprunck, S. (2013). De novo zygotic transcription in wheat (*Triticum aestivum* L.) includes genes encoding small putative secreted peptides and a protein involved in proteasomal degradation. *Plant Reprod.* 26, 267–285. doi:10.1007/s00497-013-0229-4.
- Lespinet, O., Wolf, Y. I., Koonin, E. V., and Aravind, L. (2002). The role of lineage-specific gene family expansion in the evolution of eukaryotes. *Genome Res.* 12, 1048–1059. doi:10.1101/gr.174302.
- Li, J., Meng, Y., Zhang, K., Li, Q., Li, S., Xu, B., et al. (2021). Jasmonic acid-responsive RRTF1 transcription factor controls DTX18 gene expression in hydroxycinnamic acid amide secretion. *Plant Physiol.* 185, 369–384. doi:10.1093/PLPHYS/KIAA043.
- Li, J., Su, X., Wang, Y., Yang, W., Pan, Y., Su, C., et al. (2018). Genome-wide identification and expression analysis of the BTB domain-containing protein gene family in tomato. *Genes Genomics* 40, 1–15. doi:10.1007/s13258-017-0604-x.
- Lin, R. C., Park, H. J., and Wang, H. Y. (2008). Role of Arabidopsis RAP2.4 in regulating light and ethylene-mediated developmental processes and drought stress tolerance. *Mol. Plant* 1, 42–57. doi:10.1093/mp/ssm004.
- Liu, D., Huang, X., Lin, Y., Wang, X., Yan, Z., Wang, Q., et al. (2020). Identification of reference genes for transcript normalization in various tissue types and seedlings subjected to different abiotic stresses of woodland strawberry *Fragaria vesca*. *Sci. Hort.* 261, 108840. doi:10.1016/j.scienta.2019.108840.
- Liu, J., Sun, N., Liu, M., Liu, J., Du, B., Wang, X., et al. (2013). An autoregulatory loop controlling Arabidopsis HsfA2 expression: Role of heat shock-induced alternative splicing. *Plant Physiol.* 162, 512–521. doi:10.1104/PP.112.205864.
- Marshall, O. J. (2004). PerlPrimer: cross-platform, graphical primer design for standard, bisulphite and real-time PCR. *Bioinformatics* 20, 2471–2472. doi:10.1093/bioinformatics/bth254.
- Mastrangelo, A. M., Marone, D., Laidò, G., De Leonardis, A. M., and De Vita, P. (2012). Alternative splicing: enhancing ability to cope with stress via transcriptome plasticity. *Plant Sci.* 185–186, 40–49. doi:10.1016/J.PLANTSCI.2011.09.006.
- Masuda, H. P., Cabral, L. M., Veylder, L. De, Tanurdzic, M., Engler, J. de A., Geelen, D., et al. (2008). ABAP1 is a novel plant Armadillo BTB protein involved in DNA replication and transcription. *EMBO J.* 27, 2746–2756. doi:10.1038/EMBOJ.2008.191.
- Mazzucotelli, E., Belloni, S., Marone, D., de Leonardis, A., Guerra, D., di Fonzo, N., Cattivelli, L., Mastrangelo, A. (2006). The e3 ubiquitin ligase gene family in plants: Regulation by degradation. *Curr. Genom.* 7, 509–522. doi:10.2174/138920206779315728
- Meehl G.A., Stocker T.F., Collins W.D., Friedlingstein P., Gaye A.T., Gregory J.M., et al. (2007). “Global climate projections.” in *Climate Change 2007: The Physical Science Basis. Working Group I Contribution to the Fourth Assessment Report of the Intergovernmental Panel on Climate Change (Cambridge University Press)*, 747–846.
- Morimoto, K., Mizoi, J., Qin, F., Kim, J.-S., Sato, H., Osakabe, Y., et al. (2013). Stabilization of Arabidopsis DREB2A is required but not sufficient for the induction of target genes under conditions of stress. *PLoS One* 8, e80457. doi:10.1371/journal.pone.0080457.
- Morimoto, K., Ohama, N., Kidokoro, S., Mizoi, J., Takahashi, F., Todaka, D., et al. (2017). BPM-CUL3 E3 ligase modulates thermotolerance by facilitating negative regulatory domain-mediated

- degradation of DREB2A in Arabidopsis. *Proc. Natl. Acad. Sci. U. S. A.* 114, E8528–E8536. doi:10.1073/pnas.1704189114.
- Murashige, T., and Skoog, F. (1962). a revised medium for rapid growth and bio assays with tobacco tissue cultures. *Physiol. Plant.* 15, 473–497. doi:10.1111/j.1399-3054.1962.tb08052.x.
- Narahara, S., Sakai, E., Kadowaki, T., Yamaguchi Y., Narahara H., Okamoto K., et al. (2019). KBTBD11, a novel BTB-Kelch protein, is a negative regulator of osteoclastogenesis through controlling Cullin3-mediated ubiquitination of NFATc1. *Sci. Rep.* 9, 3523. doi:10.1038/s41598-019-40240-2.
- Navarro-Quezada, A., Schumann, N., and Quint, M. (2013). Plant F-Box protein evolution is determined by lineage-specific timing of major gene family expansion waves. *PLoS One* 8, e68672. doi:10.1371/journal.pone.0068672.
- Oelmuller, R., Peskan-Berghofer, T., Shahollari, B., Trebicka, A., Sherameti, I., and Varma, A. (2005). MATH domain proteins represent a novel protein family in Arabidopsis thaliana, and at least one member is modified in roots during the course of a plant-microbe interaction. *Physiol. Plant.* 124, 152–166. doi:10.1111/j.1399-3054.2005.00505.x.
- Paolacci, A. R., Tanzarella, O. A., Porceddu, E., and Ciaffi, M. (2009). Identification and validation of reference genes for quantitative RT-PCR normalization in wheat. *BMC Mol. Biol.* 10, 11. doi:10.1186/1471-2199-10-11.
- Perez-Torrado, R., Yamada, D., and Defosse, P.-A. (2006). Born to bind: the BTB protein–protein interaction domain. *BioEssays* 28, 1194–1202. doi:10.1002/bies.20500.
- Pintard, L., Willems, A., and Peter, M. (2004). Cullin-based ubiquitin ligases: Cul3-BTB complexes join the family. *EMBO J.* 23, 1681–1687. doi:10.1038/sj.emboj.7600186.
- Pintard, L., Willis, J. H., Willems, A., Johnson, J.-L. F., Srayko, M., Kurz, T., et al. (2003). The BTB protein MEL-26 is a substrate-specific adaptor of the CUL-3 ubiquitin-ligase. *Nature* 425, 311–316. doi:10.1038/nature01959.
- Ramakers, C., Ruijter, J. M., Deprez, R. H. L., and Moorman, A. F. M. (2003). Assumption-free analysis of quantitative real-time polymerase chain reaction (PCR) data. *Neurosci. Lett.* 339, 62–66. doi:10.1016/s0304-3940(02)01423-4.
- Risseuw, E. P., Daskalchuk, T. E., Banks, T. W., Liu, E., Cotelesage, J., Hellmann, H., et al. (2003). Protein interaction analysis of SCF ubiquitin E3 ligase subunits from Arabidopsis. *Plant J.* 34, 753–767. doi:10.1046/j.1365-313X.2003.01768.x.
- Romero-Barrios N., Vert G. (2018). Proteasome-independent functions of lysine-63 polyubiquitination in plants. *New Phytol.* 217, 995–1011. doi:10.1111/nph.14915
- Sakuma, Y., Maruyama, K., Osakabe, Y., Qin, F., Seki, M., Shinozaki, K., et al. (2006a). Functional analysis of an Arabidopsis transcription factor, DREB2A, involved in drought-responsive gene expression. *Plant Cell* 18, 1292–1309. doi:10.1105/tpc.105.035881.
- Sakuma, Y., Maruyama, K., Qin, F., Osakabe, Y., Shinozaki, K., and Yamaguchi-Shinozaki, K. (2006b). Dual function of an Arabidopsis transcription factor DREB2A in water-stress-responsive and heat-stress-responsive gene expression. *Proc. Natl. Acad. Sci. U. S. A.* 103, 18822–18827. doi:10.1073/pnas.0605639103.
- Salse, J., Abrouk, M., Bolot, S., Guilhot, N., Courcelle, E., Faraut, T., et al. (2009). Reconstruction of monocotyledonous proto-chromosomes reveals faster evolution in plants than in animals. *Proc. Natl. Acad. Sci. U. S. A.* 106, 14908–14913. doi:10.1073/pnas.0902350106.

- Sasaki T., Lorković Z.J., Liang S.-C., Matzke A.J.M., and Matzke M. (2014). The ability to form homodimers is essential for RDM1 to function in RNA-directed DNA methylation. *PloS one*, 9, e88190. doi: 10.1371/journal.pone.0088190.
- Schneider, C. A., Rasband, W. S., and Eliceiri, K. W. (2012). NIH Image to ImageJ: 25 years of image analysis. *Nat. Methods* 9, 671–675. doi:10.1038/nmeth.2089.
- Schwechheimer, C., and Mergner, J. (2014). The NEDD8 modification pathway in plants. *Front. Plant Sci.* 5, 103. doi:10.3389/fpls.2014.00103.
- Seoighe, C., and Gehring, C. (2004). Genome duplication led to highly selective expansion of the *Arabidopsis thaliana* proteome. *Trends Genet.* 20, 461–464. doi:10.1016/j.tig.2004.07.008.
- Sharma, B., Joshi, D., Yadav, P. K., Gupta, A. K., and Bhatt, T. K. (2016). Role of ubiquitin-mediated degradation system in plant biology. *Front. Plant Sci.* 7, 806. doi:10.3389/fpls.2016.00806.
- Shin, J., Heidrich, K., Sanchez-Villarreal, A., Parker, J. E., and Davis, S. J. (2012). TIME FOR COFFEE represses accumulation of the MYC2 transcription factor to provide time-of-day regulation of jasmonate signaling in *Arabidopsis*. *Plant Cell* 24, 2470–2482. doi:10.1105/TPC.111.095430.
- Sievers, F., Wilm, A., Dineen, D., Gibson, T. J., Karplus, K., Li, W., et al. (2011). Fast, scalable generation of high-quality protein multiple sequence alignments using Clustal Omega. *Mol. Syst. Biol.* 7, 539. doi:10.1038/msb.2011.75.
- Siggs, O., and Beutler, B. (2012). The BTB-ZF transcription factors. *Cell Cycle* 11, 3358–3369. doi:10.4161/CC.21277.
- Smalle, J., and Vierstra, R. D. (2004). The ubiquitin 26S proteasome proteolytic pathway. *Annu. Rev. Plant Biol.* 55, 555–590. doi:10.1146/annurev.arplant.55.031903.141801.
- Söderberg, O., Gullberg, M., Jarvius, M., Ridderstråle, K., Leuchowius, K.-J., Jarvius, J., et al. (2006). Direct observation of individual endogenous protein complexes in situ by proximity ligation. *Nat. Methods* 3, 995–1000. doi:10.1038/nmeth947.
- Söderman, E., Hjellström, M., Fahleson, J., and Engström, P. (1999). The HD-Zip gene *ATHB6* in *Arabidopsis* is expressed in developing leaves, roots and carpels and up-regulated by water deficit conditions. *Plant Mol. Biol.* 40, 1073–1083. doi:10.1023/A:1006267013170.
- Sonenberg, N. and Dever, T.E. (2003). Eukaryotic translation initiation factors and regulators. *Curr. Opin. Struct. Biol.* 13, 56–63. doi:10.1016/S0959-440X(03)00009-5.
- Sreenivasulu, N., Harshvardhan, V. T., Govind, G., Seiler, C., and Kohli, A. (2012). Contrapuntal role of ABA: Does it mediate stress tolerance or plant growth retardation under long-term drought stress? *Gene* 506, 265–273. doi:10.1016/J.GENE.2012.06.076.
- Stogios, P. J., Downs, G. S., Jauhal, J. J., Nandra, S. K., and Privé, G. G. (2005). Sequence and structural analysis of BTB domain proteins. *Genome Biol.* 6, R82. doi:10.1186/gb-2005-6-10-r82.
- Stogios P.J. and Privé G.G. (2004). The BACK domain in BTB-kelch proteins. *Trends Biochem. Sci.* 29, 634–637. doi: 10.1016/j.tibs.2004.10.003.
- Stothard, P. (2000). The sequence manipulation suite: JavaScript programs for analyzing and formatting protein and DNA sequences. *Biotechniques* 28, 1102–1104. doi:10.2144/00286ir01.
- Suárez-López, P., Wheatley, K., Robson, F., Onouchi, H., Valverde, F., and Coupland, G. (2001). *CONSTANS* mediates between the circadian clock and the control of flowering in *Arabidopsis*. *Nature* 410, 1116–1120. doi:10.1038/35074138.

- Sugio, A., Dreos, R., Aparicio, F., and Maule, A. J. (2009). The cytosolic protein response as a subcomponent of the wider heat shock response in Arabidopsis. *Plant Cell* 21, 642–654. doi:10.1105/TPC.108.062596.
- Sumara, I., Quadroni, M., Frei, C., Olma, M. H., Sumara, G., Ricci, R., et al. (2007). A Cul3-based E3 ligase removes Aurora B from mitotic chromosomes, regulating mitotic progression and completion of cytokinesis in human cells. *Dev. Cell* 12, 887–900. doi:10.1016/j.devcel.2007.03.019.
- Sunilkumar, G., Mohr, L. A., Lopata-Finch, E., Emani, C., and Rathore, K. S. (2002). Developmental and tissue-specific expression of CaMV 35S promoter in cotton as revealed by GFP. *Plant Mol. Biol.* 50, 463–479. doi:10.1023/A:1019832123444.
- Szostkiewicz, I., Richter, K., Kepka, M., Demmel, S., Ma, Y., Korte, A., et al. (2010). Closely related receptor complexes differ in their ABA selectivity and sensitivity. *Plant J.* 61, 25–35. doi:10.1111/j.1365-313X.2009.04025.x.
- Škiljaica, A. (2016). Wheat MATH-BTB proteins and their role in early embryogenesis. Graduation Thesis, University of Zagreb, Faculty of Science.
- Škiljaica, A., Jagić, M., Vuk T., Leljak Levanić D., Bauer N., and Markulin L. (2022) Evaluation of reference genes for RT-qPCR gene expression analysis in Arabidopsis thaliana exposed to elevated temperatures. *Plant Biol. J.* 367–379. doi:10.1111/plb.13382.
- Škiljaica, A., Lechner, E., Jagić, M., Majsec, K., Malenica, N., Genschik, P., et al. (2020). The protein turnover of Arabidopsis BPM1 is involved in regulation of flowering time and abiotic stress response. *Plant Mol. Biol.* 102, 359–372. doi:10.1007/s11103-019-00947-2.
- Thomann, A., Brukhin, V., Dieterle, M., Gheyeselink, J., Vantard, M., Grossniklaus, U., et al. (2005). Arabidopsis CUL3A and CUL3B genes are essential for normal embryogenesis. *Plant J.* 43, 437–448. doi:10.1111/j.1365-313X.2005.02467.x.
- Thomann, A., Lechner, E., Hansen, M., Dumbliauskas, E., Parmentier, Y., Kieber, J., et al. (2009). Arabidopsis CULLIN3 genes regulate primary root growth and patterning by ethylene-dependent and -independent mechanisms. *PLoS Genet.* 5, e1000328. doi:10.1371/journal.pgen.1000328.
- Thomas, J. H. (2006). Adaptive evolution in two large families of ubiquitin-ligase adapters in nematodes and plants. *Genome Res.* 16, 1017–1030. doi:10.1101/gr.5089806.
- Tuteja, N. (2007). Abscisic acid and abiotic stress signaling. *Plant Signal. Behav.* 2, 135–138. doi:10.4161/psb.2.3.4156.
- Vandesompele, J., De Preter, K., Pattyn, F., Poppe, B., Van Roy, N., De Paepe, A., et al. (2002). Accurate normalization of real-time quantitative RT-PCR data by geometric averaging of multiple internal control genes. *Genome Biol.* 3, 0034.1. doi:10.1186/gb-2002-3-7-research0034.
- Vierstra, R. D. (2009). The ubiquitin–26S proteasome system at the nexus of plant biology. *Nat. Rev. Mol. Cell Biol.* 10, 385–397. doi:10.1038/nrm2688.
- Vishal, B., and Kumar, P. P. (2018). Regulation of seed germination and abiotic stresses by gibberellins and abscisic acid. *Front. Plant Sci.* 9, 838. doi:10.3389/FPLS.2018.00838/BIBTEX.
- Vogel, C., Bashton, M., Kerrison, N. D., Chothia, C., and Teichmann, S. A. (2004). Structure, function and evolution of multidomain proteins. *Curr. Opin. Struct. Biol.* 14, 208–216. doi:10.1016/J.SBI.2004.03.011.

- Wasternack, C., and Hause, B. (2013). Jasmonates: biosynthesis, perception, signal transduction and action in plant stress response, growth and development. An update to the 2007 review in *Annals of Botany*. *Ann. Bot.* 111, 1021–1058. doi:10.1093/AOB/MCT067.
- Waterhouse, A. M., Procter, J. B., Martin, D. M. A., Clamp, M., and Barton, G. J. (2009). Jalview Version 2—a multiple sequence alignment editor and analysis workbench. *Bioinformatics* 25, 1189–1191. doi:10.1093/bioinformatics/btp033.
- Weber, H., Bernhardt, A., Dieterle, M., Hano, P., Mutlu, A., Estelle, M., et al. (2005). Arabidopsis AtCUL3a and AtCUL3b form complexes with members of the BTB/POZ-MATH protein family. *Plant Physiol.* 137, 83–93. doi:10.1104/pp.104.052654.
- Weber, H., and Hellmann, H. (2009). Arabidopsis thaliana BTB/ POZ-MATH proteins interact with members of the ERF/AP2 transcription factor family. *FEBS J.* 276, 6624–6635. doi:10.1111/j.1742-4658.2009.07373.x.
- Wimuttisuk, W., and Singer, J. D. (2007). The Cullin3 ubiquitin ligase functions as a Nedd8-bound heterodimer. *Mol. Biol. Cell* 18, 899–909. doi:10.1091/mbc.e06-06-0542.
- Xie, Z., Nolan, T. M., Jiang, H., and Yin, Y. (2019). AP2/ERF transcription factor regulatory networks in hormone and abiotic stress responses in Arabidopsis. *Front. Plant Sci.* 10, 228. doi:10.3389/fpls.2019.00228.
- Xu, L., Wei, Y., Reboul, J., Vaglio, P., Shin, T.-H., Vidal, M., Elledge, S. J., & Harper, J. W. (2003). BTB proteins are substrate-specific adaptors in an SCF-like modular ubiquitin ligase containing CUL-3. *Nature* 425, 316–321. doi:10.1038/nature01985.
- Yoshida, T., Ohama, N., Nakajima, J., Kidokoro, S., Mizoi, J., Nakashima, K., et al. (2011). Arabidopsis HsfA1 transcription factors function as the main positive regulators in heat shock-responsive gene expression. *Mol. Genet. Genomics* 286, 321–332. doi:10.1007/s00438-011-0647-7.
- Zapata, J. M., Martínez-García, V., and Lefebvre, S. (2007). Phylogeny of the TRAF/MATH Domain. *Adv. Exp. Med. Biol.* 597, 1–24. doi:10.1007/978-0-387-70630-6_1.
- Zhai, Z., Jung, H., and Vatamaniuk, O. K. (2009). Isolation of protoplasts from tissues of 14-day-old seedlings of Arabidopsis thaliana. *J. Vis. Exp.* 30, E1149. doi:10.3791/1149.
- Zhang, Q., Zhang, L., Wang, B., Ou, C. Y., Chien, C. T., and Jiang, J. (2006). A Hedgehog-induced BTB protein modulates Hedgehog signaling by degrading Ci/Gli transcription factor. *Dev. Cell* 10, 719–729. doi:10.1016/j.devcel.2006.05.004.
- Zhao, L., Huang, Y., Hu, Y., He, X., Shen, W., Liu, C., et al. (2013). Phylogenetic analysis of Brassica rapa MATH-domain proteins. *Curr. Genomics* 14, 214–223. doi:10.2174/1389202911314030007.
- Zhuang, M., Calabrese, M. F., Liu, J., Waddell, M. B., Nourse, A., Hammel, M., et al. (2009). Structures of SPOP-substrate complexes: Insights into molecular architectures of BTB-Cul3 ubiquitin ligases. *Mol. Cell* 36, 39–50. doi:10.1016/j.molcel.2009.09.022.

Online sources:

- Duolink® in situ – Fluorescence User Guide. *Olink, Sigma-Aldrich, Merck*. Available at: <https://www.sigmaaldrich.com/HR/en/technical-documents/protocol/protein-biology/protein-and-nucleic-acid-interactions/duolink-fluorescence-user-manual>
- In-Fusion® HD Cloning Kit User Manual (2011). version no. PR133833, *Clontech Laboratories, Inc., Takara Bio Inc.* Available at: <https://www.takara.co.kr/file/manual/pdf/pt5162-1.pdf>

MagMAX™ Plant RNA Isolation Kit User Guide (2016). version no. MAN0016311 Revision A.0,
Applied Biosystems, Thermo Fisher Scientific. Available at:
https://www.thermofisher.com/document-connect/document-connect.html?url=https%3A%2F%2Fassets.thermofisher.com%2FTFS-Assets%2FLSG%2Fmanuals%2FMAN0016311_MagMAX_PlantRNA_Isol_UG.pdf

Yeast Protocols Handbook (2009). version no. PR973283, *Clontech Laboratories, Inc., Takara Bio Inc.*
Available at: <https://www.takara.co.kr/file/manual/pdf/PT3024-1.pdf>

APPENDIX

APPENDIX A

Appendix A1. Primer sequences used for RT-qPCR. Listed are gene symbol and identifier (ID) from the TAIR database, forward (top) and reverse (bottom) primer sequence, average primer efficiency, amplicon size in base pairs (bp), and number of transcript variants bound by the primer pair (if applicable). For primer pairs that were used in multiple RT-qPCR experiments, a representative primer efficiency value is indicated (marked with asterisk). The downstream application is stated in the topmost cell above each subset of primer pairs.

GENE SYMBOL & ID	FORWARD AND REVERSE PRIMER SEQUENCE	AVERAGE PRIMER EFFICIENCY	AMPLICON SIZE (bp)	NUMBER OF TRANSCRIPTS
<i>Expression profiling under abiotic stress and elevated temperature</i>				
<i>BPM1</i> (AT5G19000.1, AT5G19000.3)	CCCGGTTGCACTGAATGGGA ACGATTCATTGTACTTGCTAGATCCGATT	1.95*	106	2 of 3
<i>BPM1.2</i> (AT5G19000.2)	TGCATAACGATAGAAGACATGG AATGGAGCAATACCTTATCCCG	1.96*	157	1 of 3
<i>BPM2</i> (AT3G06190)	TCTATCCGGGTAATAAGATCGAAGA CCTTGAAACCCTAATTGTGTC	1.99*	101	all (5)
<i>BPM3</i> (AT2G39760)	AGTGATAGACGACATCGAACCT CAAGGTCATAGAGGTCAGCA	1.90*	161	all (3)
<i>BPM4</i> (AT3G03740)	GAAGTTACTGACATGGAGCCT CACTGACTCGCACATTAGAC	1.84*	201	all (2)
<i>BPM5</i> (AT5G21010)	AAAGGCGTATCAGTCAAATCC TGTTGGTAAGCGTCTGTCTC	1.85*	137	all (1)
<i>BPM6</i> (AT3G43700)	GAACAACAGCGACGTAGTGA CGGACGGCCTTAATAGGTCA	1.95*	137	all (3)
<i>HsfA3</i> (AT5G03720)	GTCAGACAGCTTAACACTTATG GCAAGTTTGGTTGGATTGTGG	1.95	141	all (2)
<i>AT4G36010</i>	TTACGTCATCACTTTCTGTCCT CGTTTGGAGATGCCTTAGAG	1.97	101	all (2)
<i>Expression profiling of BPM2 splicing variants under elevated temperature</i>				
<i>BPM2.3</i> (AT3G06190.3)	TCAAGGATTTTCTGTTTACGAGTG AGTAGAAAGATTAAACCTTATCCCG	1.75	112	1
<i>BPM2.4</i> (AT3G06190.4)	TCAAGGATTTTCTGTTTACGAGTG AAATGAAGCAACATCTTATCCCG	1.84	100	1
<i>BPM2.5</i> (AT3G06190.5)	CCTGAAAGGTACAGAAGATCAC CCATCACAGCTAAAGAAATTACAG	1.91	114	1
<i>Data normalization (for experiments above)</i>				
<i>RHIP1</i> (AT4G26410)	GAGCTGAAGTGCTTCAATGAC GGTCCGACATACCCATGATCC	1.94*	81	all (1)

Appendix A1. – continued.

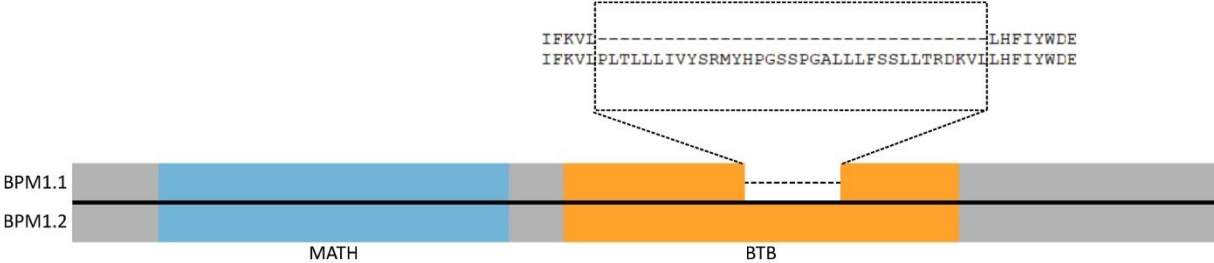
<i>Selection and validation of candidate reference genes</i>				
<i>TRAPPC6</i> (AT3G05000)	CTGAGAATGAAACCCAAGATCC TGACCCGAATCACGAAAGAG	1.80	180	all (1)
<i>PUX7</i> (AT1G14570)	GTTTCTCAGACTATCAAAGCCA ATCAATTACAAGCACACGG	1.93	120	all (4)
<i>OGIO</i> (AT5G51880)	ATCCAAGAGCAGTTCAAGCAAG GAGAGCCATACCTTCCACTG	1.92	130	all (1)
<i>DWA1</i> (AT2G19430)	AGTTGTGGTGATGATGGTAGAG ACAGACATGGCATTGATCTCAG	1.93	176	all (1)
<i>GLR2</i> (AT2G17260)	AGCGATTGTTGATGAACGTCC TCTCCAGTTTCGGATAGACCA	1.92	172	all (1)
<i>PP2AA3</i> (AT1G13320)	CATGTTCCAAACTCTTACCTGC GGTCTTCACTTAGCTCCACC	1.92	164	all (4)
<i>RHIP1</i> (AT4G26410)	CTATTGGGATTGGTGTGCT AGAATTGTGCCTCTCGCTC	1.92	105	all (1)
<i>TIP41</i> (AT4G34270)	GCAGCACAATGGAAATTCAGG GCCTCAACCGTTTCTTTGTC	1.93	122	all (1)
<i>MON1</i> (AT2G28390)	TGTCTTCTCATCTCTGTGCCA AGTAGAAGCAAGTCATCGGG	1.89	225	all (1)
<i>UBC21/PEX4</i> (AT5G25760)	TGCAGTTGACAATTCGTTCTC CGGTCCATTTGAATATGTTGGT	1.93	151	all (2)
<i>DREB2A</i> [†] (AT5G05410)	CAGTGTGCCAACGGTTCAT AAACGGAGGTATTCCGTAGTTGAG	1.92	88	all (2)

[†] *DREB2A* primers were originally published in Morimoto et al. (2017)

Appendix A2. Primer sequences used for cloning into plasmid pGBT9. Primers were designed using the online In-Fusion Primer Design Tool (Takara Bio Inc.; <https://takara.teselagen.com/#/DesignPage>). Listed in the table are gene symbol and identifier (ID) from the TAIR database, forward and reverse primer sequence and the restriction sites embedded within the primer sequence which were used for cloning into corresponding sites in the vector backbone. For each primer set, the table lists annealing temperature (Ta) and elongation time (ELONG.) used for standard PCR reactions.

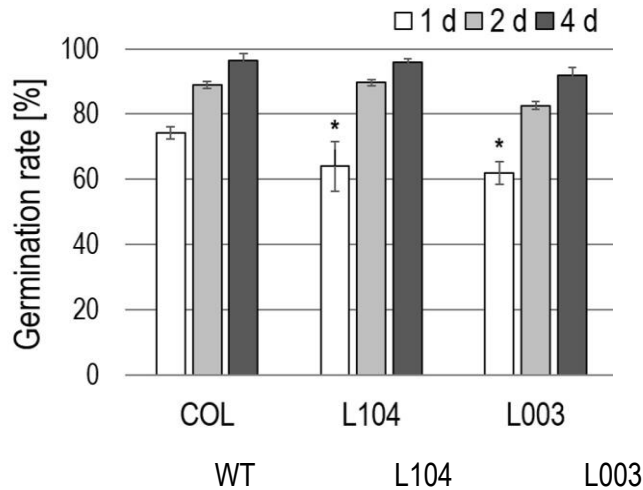
GENE SYMBOL	GENE ID	PRIMER SEQUENCE		RESTRICTION SITE	Ta, ELONG.
<i>eIF4A1</i>	AT4G11420	FW	TGTATCGCCGGAATTCATGGCAGGATCTGCACCAGA	EcoRI	58 °C, 3 min
		REV	GCAGGTCGACGGATCCCTAGTACGGCAGAGCAAACACA	BamHI	
<i>eIF3G1</i>	AT3G11400	FW	TGTATCGCCGGAATTCATGACGATCGATTGCAGC	EcoRI	60 °C, 3 min
		REV	GCAGGTCGACGGATCCCTAGGTTGGTCTTGGAGTTGCC	BamHI	

APPENDIX B

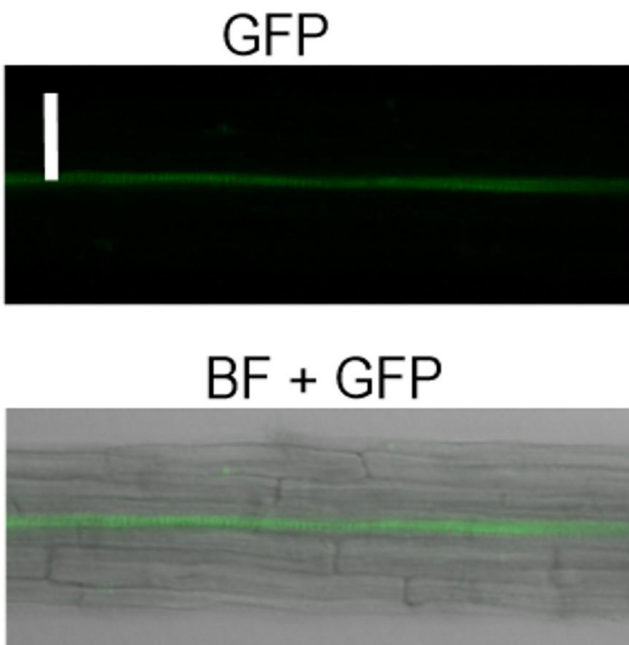


Appendix B1. Schematic representation of *Arabidopsis* BPM1.1 and BPM1.2 protein sequences, with a detailed view of 35 amino acids within the BTB domain present exclusively in the BPM1.2 variant.

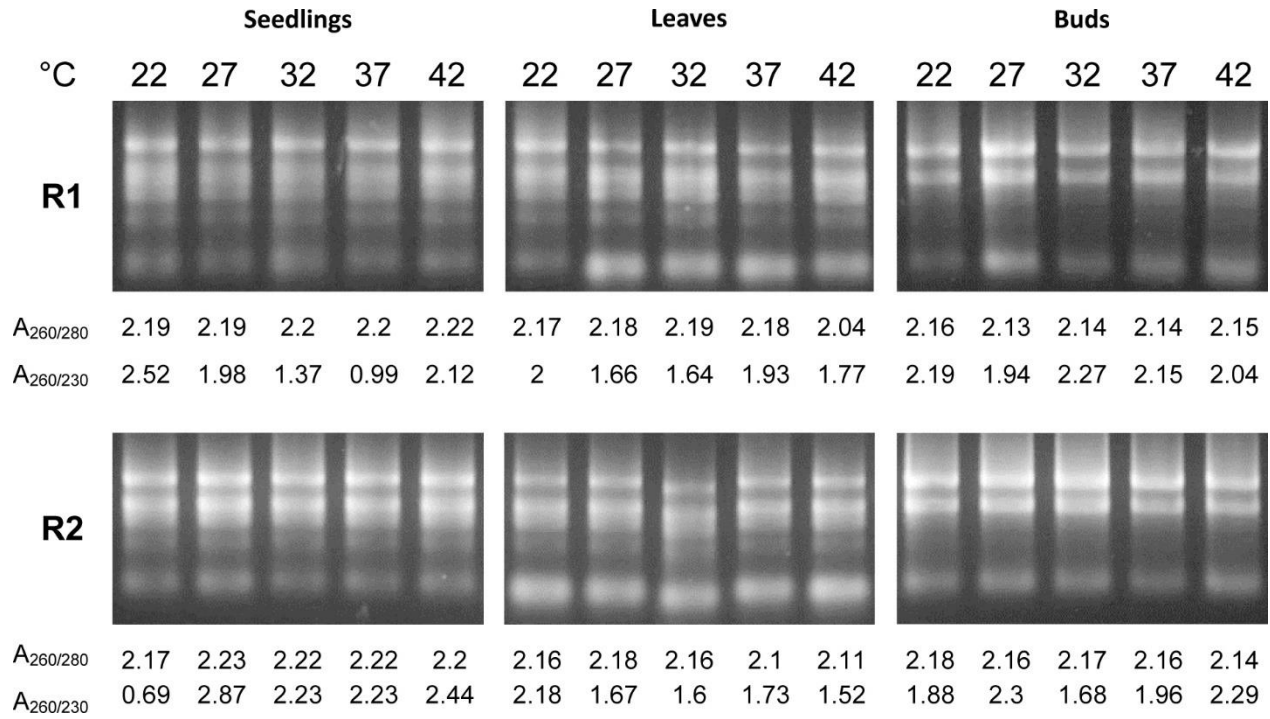
Appendix B2. Multiple sequence alignments of cDNA sequences of *BPM2* splicing variants. Putative 5' UTR, exons and 3' UTR regions were delineated according to estimates available in the Phytozome database (genome ID: 447). Yellow squares mark the first three nucleotides of each exon (E1-E4) and red squares mark the STOP codons. Green and orange arrows mark the beginning of 5' UTR and 3' UTR, respectively. Identical and similar nucleotides are shaded in blue, with darker shades indicating higher similarity. Broken lines represent areas where no nucleotides could be aligned. Sequences were aligned in ClustalX v.2.0 (Larkin et al., 2007) and displayed in Jalview v.2 (Waterhouse et al., 2009). Sequences were retrieved on January 18th, 2022.



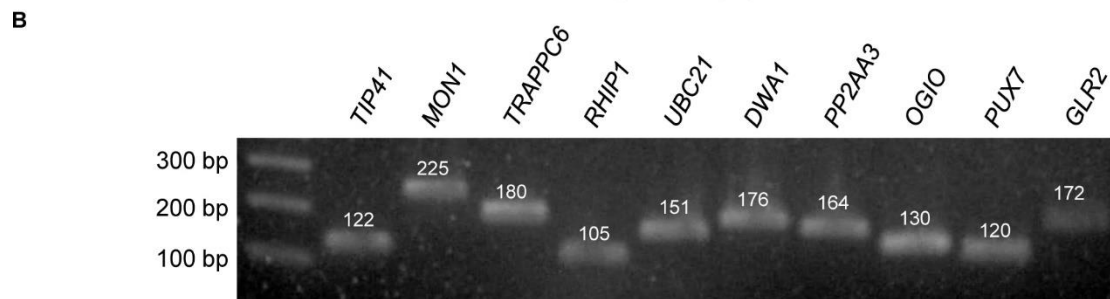
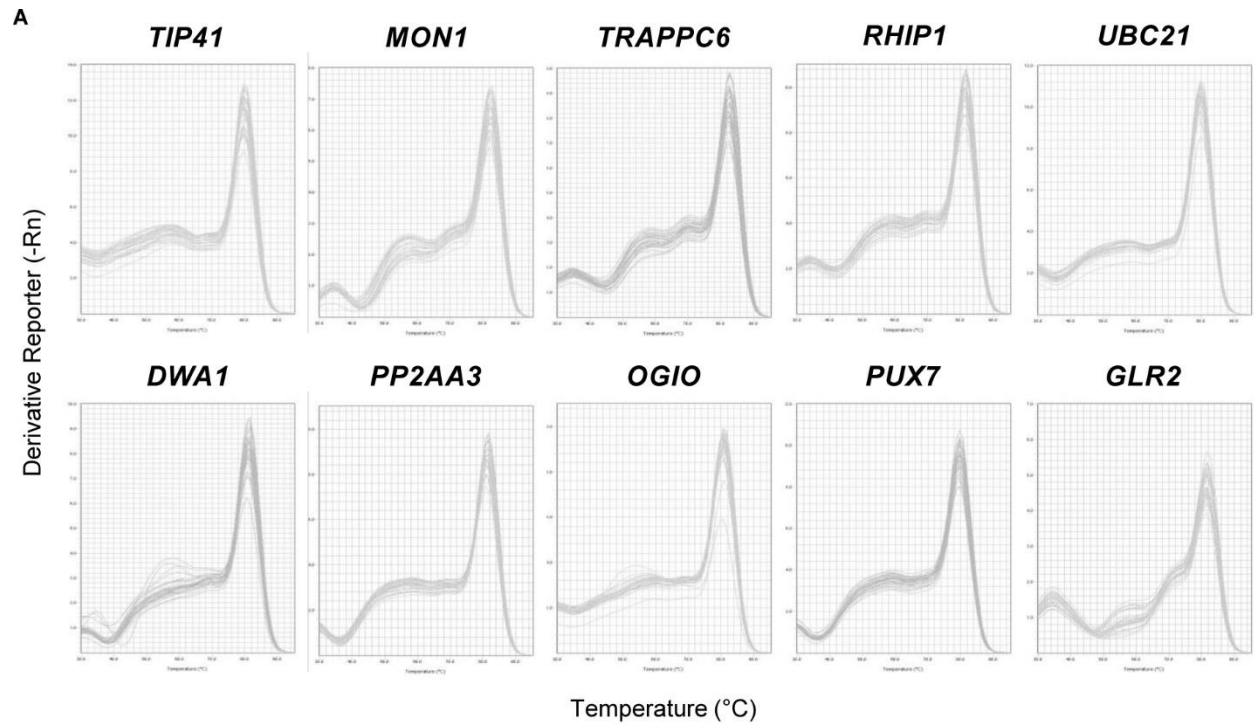
Appendix B3. Germination rate (percentage of seeds with radicle emergence) for wild type (COL) and lines with BPM1 overexpression (L104 and L003) one, two or four days after imbibition. Germination rates are shown as mean values \pm S.D.. Asterisks indicate statistically significant differences between means of control and tested samples (Student's T Test, $P < 0.01$).



Appendix B4. BPM1-GFP protein diffuses and translocates to root stele during prolonged dark exposure. Seedlings of BPM1 overexpression line L104 were incubated in the dark for 24 h and immediately analyzed by confocal microscopy. Fluorescent and merged (bright field and BPM1-GFP signal) images are shown in top and bottom panel, respectively. Scale bar = 50 μ m.



Appendix B5. Quality assessment of RNA extracted from *Arabidopsis* tissues exposed to elevated temperatures. Twelve-day-old seedlings, and rosette leaves and flower buds from 5-week-old plants were incubated for 3 h at different temperatures (22°C, 27°C, 32°C, 37°C and 42°C) followed by RNA extraction. Integrity of RNA was confirmed by agarose gel electrophoresis and RNA purity was assessed by determination of $A_{260/280}$ and $A_{260/230}$ ratios. Results of two independent experiments (R1 and R2) are shown in top and bottom panel, respectively.



Appendix B6. Specificity of RT-qPCR amplification. (A) Dissociation curves of ten candidate reference genes showing individual peaks, based on two technical replicates of 15 cDNAs from three different *Arabidopsis* tissues exposed to five different temperatures. (B) Agarose gel showing single qPCR products of ten candidate reference genes, with expected size (bp) denoted above bands.

Appendix B7. C_q values of ten candidate reference genes in *Arabidopsis* tissues exposed to elevated temperatures. Seedlings, leaves and flower buds of *Arabidopsis* were incubated for 3 h at different temperatures (22 °C, 27 °C, 32 °C, 37 °C and 42 °C) and RT-qPCR analysis was performed. Raw amplification data was analyzed in LinReg software and C_q values of two technical replicates per sample were averaged. Results of two independent experiments (biological replicates R1 and R2) are shown.

TISSUE	REPLICATE	TEMPERATURE TREATMENT	TRAPPC6	PUX7	OGIO	DWA1	GLR2	PP2AA3	RHIP1	TIP41	MON1	UBC21
SEEDLINGS	R1	22°C	23.15	22.68	22.46	24.02	26.41	21.82	22.29	23.14	22.32	22.03
		27°C	22.50	22.31	22.36	23.92	26.15	21.65	22.12	23.04	22.34	21.89
		32°C	23.00	22.41	22.49	24.10	26.92	22.01	22.36	23.19	23.18	22.21
		37°C	23.68	22.87	22.49	24.61	26.89	22.04	21.91	23.37	23.09	22.86
		42°C	23.38	22.92	22.74	24.35	26.72	21.61	22.07	23.26	23.18	22.41
	R2	22°C	22.43	22.16	22.44	23.96	26.29	23.27	22.31	22.91	22.46	21.13
		27°C	23.24	23.02	23.23	24.82	26.61	24.04	23.44	23.49	23.45	21.96
		32°C	24.24	23.30	23.50	25.45	27.85	23.30	23.91	24.07	24.71	22.58
		37°C	23.92	22.51	22.75	24.69	27.10	22.64	22.59	22.88	23.11	22.27
		42°C	23.46	23.33	23.25	24.93	27.18	23.67	23.45	23.37	24.19	22.30
LEAVES	R1	22°C	24.77	22.62	23.12	25.06	25.82	23.45	24.30	24.06	28.28	22.33
		27°C	24.32	22.69	23.08	24.63	25.26	23.13	23.40	23.61	28.17	22.04
		32°C	24.21	22.85	22.79	24.51	24.32	22.48	23.34	23.26	28.41	22.08
		37°C	24.94	23.11	22.72	25.23	24.44	22.54	23.13	23.30	28.46	22.38
		42°C	25.01	23.60	23.19	25.54	24.34	23.67	23.38	24.08	28.70	22.52
	R2	22°C	25.16	23.22	23.54	25.19	26.31	22.72	23.78	24.21	23.37	22.59
		27°C	24.69	22.95	22.90	24.80	26.48	22.76	23.38	23.67	23.16	22.28
		32°C	24.51	23.72	23.79	25.19	27.29	23.22	23.66	24.23	24.51	23.19
		37°C	23.95	22.78	22.49	25.38	26.50	22.43	22.49	24.21	23.50	22.42
		42°C	25.04	23.60	23.11	25.07	27.73	23.32	22.96	24.40	24.23	23.16
BUDS	R1	22°C	21.96	21.16	21.62	22.76	23.96	21.13	21.58	22.15	26.15	20.81
		27°C	23.81	23.53	22.50	24.74	25.68	21.89	23.39	23.70	28.72	22.29
		32°C	23.87	23.45	22.94	24.54	25.30	21.66	23.48	23.49	28.42	21.85
		37°C	22.45	21.54	21.33	23.27	23.68	20.77	21.38	21.94	26.23	20.71
		42°C	22.53	22.18	23.15	23.92	25.59	21.67	22.12	22.63	26.41	21.68
	R2	22°C	22.14	21.26	21.71	22.80	24.10	20.89	21.37	22.47	21.62	21.00
		27°C	22.14	21.35	21.36	22.98	24.41	20.78	21.17	22.00	21.28	20.70
		32°C	22.34	21.16	21.49	22.56	24.71	21.04	21.11	22.13	21.24	20.72
		37°C	22.64	21.17	21.15	22.76	24.27	21.24	21.36	22.03	21.36	20.87
		42°C	22.07	21.40	22.01	22.90	26.23	21.33	21.72	22.54	21.62	21.27

LIST OF ABBREVIATIONS

Amino acids

A, Ala – Alanine	I, Ile – Isoleucine	R, Arg – Arginine
C, Cys – Cysteine	K, Lys – Lysine	S, Ser – Serine
D, Asp – Aspartic acid	L, Leu – Leucine	T, Thr – Threonine
E, Glu – Glutamic acid	M, Met – Methionine	V, Val – Valine
F, Phe – Phenylalanine	N, Asn – Asparagine	W, Trp – Tryptophan
G, Gly – Glycine	P, Pro – Proline	Y, Tyr – Tyrosine
H, His – Histidine	Q, Gln – Glutamine	

Bioinformatics

BLAST – Basic Local Alignment Search Tool (search algorithm)
NCBI – National Center for Biotechnology Information
TAIR – The Arabidopsis Information Resource
TIGR – The International Rice Genome, Rice Genome Annotation Project
UniProt – Universal Protein, repository for protein data

Chemicals and solutions

DAPI – 4',6-diamidino-2-phenylindole
DO – Dropout, as in Dropout Supplement lacking specific amino acids for yeast selection based on prototrophy
EDTA – Ethylenediaminetetraacetic acid
LB – Luria Bertani medium, broth for cultivation of bacteria
SOC – Super Optimal Broth with Catabolic Repression, broth for cultivation of bacteria
SYBR - Synergy Brands, Inc. (stock symbol), a fluorescent dye specifically binding dsDNA
Tris – Trisaminomethane
YC – Yeast Complete, growth medium for cultivation of yeast
YPD – Yeast Peptone Dextrose, growth medium for cultivation of yeast

Genetics and molecular biology

BamHI – *Bacillus amyloliquefaciens* HI, a restriction endonuclease isolated from *B. amyloliquefaciens* strain H
cDNA – complementary DNA
Cq – quantitation cycle
DNA – deoxyribonucleic acid
dsDNA – double stranded DNA
EcoRI – *E. coli* RY13 I, a restriction endonuclease isolated from *E. coli* strain RY13
PCR – polymerase chain reaction
RNA – ribonucleic acid
UTR – untranslated region

Standard units of measurement

a.m. – *ante meridiem* (before noon)

p.m. – *post meridiem* (after noon)

°C – degree Celsius

cm – centimeter

g – gram

h – hour

L – liter

M – molar

mg – milligram

min – minute

mL – milliliter

mm – millimeter

mM – millimolar

ng – nanogram

nm – nanometer

nM – nanomolar

µg – microgram

µL – microliter

µm – micrometer

µM – micromolar

rpm – revolutions per minute

s – second

SD – standard deviation

U – unit (for enzymes)

w/v – weight to volume

CURRICULUM VITAE

Andreja Škiljaica was born on the 24th of October, 1992 in Koprivnica, Croatia. In 2016, she graduated in molecular biology from the Department of Biology, Faculty of Science, University of Zagreb. In December 2016, she began work as a research assistant in the group of Prof. Emer. Sibila Jelaska at the Division of Molecular Biology, Department of Biology, Faculty of Science, University of Zagreb. Since then, she worked as a laboratory practice assistant in four classes, Developmental Biology, Mechanisms of Plant Development, Animal and Plant Cell Culture, and Genetic Engineering in Biotechnology.

In 2017, she enrolled in the University postgraduate program of Biology at the Department of Biology, Faculty of Science, University of Zagreb. She carried out her PhD work under supervision of Dr. Nataša Bauer. Assoc. Prof.

Since 2020, she performed the role of a Managing Editor in *Acta Botanica Croatica*, an international journal published by the Faculty of Science, University of Zagreb.

Publications:

Škiljaica, A., Jagić, M., Vuk T., Leljak Levanić D., Bauer N., and Markulin L. (2022) Evaluation of reference genes for RT-qPCR gene expression analysis in *Arabidopsis thaliana* exposed to elevated temperatures. *Plant Biol. J.* 367–379. doi:10.1111/plb.13382.

Markulin, L., Škiljaica, A., Tokić, M., Jagić, M., Vuk, T., Bauer, N. and Leljak-Levanić, D. (2021). Taking the wheel – de novo DNA methylation as a driving force of plant embryonic development. *Front. Plant Sci.* 12, 764999. doi:10.3389/fpls.2021.764999.

Škiljaica, A., Lechner, E., Jagić, M., Majsec, K., Malenica, N., Genschik, P., et al. (2020). The protein turnover of *Arabidopsis* BPM1 is involved in regulation of flowering time and abiotic stress response. *Plant Mol. Biol.* 102, 359–372. doi:10.1007/s11103-019-00947-2.

Bauer, N., Škiljaica, A., Malenica, N., Razdorov, G., Klasić, M., Juranić, M., et al. (2019). The MATH-BTB protein TaMAB2 accumulates in ubiquitin-containing foci and interacts with the translation initiation machinery in *Arabidopsis*. *Front. Plant Sci.* 10, 1469. doi:10.3389/fpls.2019.01469.